SOUND PROPAGATION IN URBAN AREAS

Ph.D. Thesis
by R. Buller

Mr Stead/sf

16 May 1978

Mr R.B. Bullen
2 Oak Walk
Fair Oak
EASTLEIGH HANTS SO5 7JS
UNITED KINGDOM

Dear Mr Bullen,

Further to my letter of 24 January 1978 concerning your candidature for the degree of Doctor of Philosophy, I have now been advised by the Head of the Department of Architectural Science that the required amended copy of your thesis has been received and that the emendations have been made to the satisfaction of the Head of the Department.

I am pleased to confirm therefore that you have now been awarded the degree of Doctor of Philosophy.

Since you are at present overseas I assume that you would not be available to attend a conferring of degrees ceremony this month or next month. The next ceremony of conferring of degrees which you could attend would therefore not be until 1979. Alternatively your degree could be conferred 'in absentia' at the next appropriate meeting of the Senate of the University. I would be grateful if you could advise me of your wishes in this regard.

Yours sincerely,

Kenneth W. Knight
Registrar

cc
Professor Cowan
Dr Fricke
Mr Smart
Rare Book Librarian (undertaking re immediate availability
BPGS -signed)
File - 1. Mrs Gaffney
2. Ms Donaldson
3. Records

BULLEN, Robert Bruce

Ph. D. June 1978

SOUND PROPAGATION

IN URBAN AREAS

by Robert Bullen, B.Sc.

Thesis submitted to fulfil the requirements for the degree of Doctor of Philosophy at the Department of Architectural Science, University of Sydney.

May, 1977

SUMMARY

The effective control of noise levels in urban areas requires an understanding of the dynamics of sound propagation among large built-form structures. At present, no theory exists which adequately describes this propagation, and thus the approach to urban noise control has been rather piecemeal.

In this thesis, some of the important processes involved in urban sound progagation are studied and an attempt is made to discover the ways in which they interact. Although the theory developed is, in many respects, not rigorous, experimental results from both model and full-scale tests are in substantial agreement with its predictions. This suggests that the basic approach to the problem is sound.

In particular, the interaction between absorption and scattering processes, which have previously been studied only in isolation, is investigated and found to be important in describing long-distance propagation. Properties of the sound field which depend on the shape and nature of the source are also found to be important in some situations.

It is hoped that studies such as this, which attempt to take into account all relevant aspects of the environment of a noise source, can lead to an approach to urban noise control which operates on the level of urban planning, rather than of acoustic barriers, post construction insulation, etc., which attempt to cure small-scale problems as they arise.

ACKNOWLEDGEMENTS

The assistance and encouragement of my supervisor, Dr Ferg Fricke, has been invaluable throughout this work. His suggestions and evaluations, as well as his willingness to assist with experimental work, have been greatly appreciated.

Other members of staff and technicians from the Department of Architectural Science have also assisted this work in numerous ways.

ACI Fibreglass, Mr John Collis of the Sydney City Council, and Mr Lex Brown of the Department of Civil Engineering, University of Queensland, have all been most helpful in supplying data for use in this research.

I am grateful for the financial assistance which has been provided by a Commonwealth Postgraduate Scholarship and also by the Australian Road Research Board.

LIST OF MATHEMATICAL SYMBOLS

(These symbols may be re-defined in appendices)

$[x]$	indicates "the integer part of x"
r, z, ψ	cylindrical polar co-ordinates (figure 2·1)
c	speed of sound
ρ	density of air
λ	free-space wavelength
ω	angular frequency
d	distance between scatterers in a street
R	reflection co-efficient of scatterers
γ	measure of absorption (see equation 2·4)
d_1, d_2	separation of scatterers in two directions (figure 2·3)
θ_i	angle of incidence on scattering surface (figure 2·3)
h	height of buildings
a	width of (source) street
b	width of receiver street
a'	width of street in the presence of a scatterer
$k_n, \epsilon_n, k'_m, \epsilon'_m$	see equations 2·11, 2·13 and 4·5 ff.
P_n	modal co-efficients
ξ	arc sin (k_n/k_o) (see figure 4·1)
α_n	phase shift (see equation 4·9)
Q_n	see equation 4·9 ff.
Φ	phase of propagating wave
S	see equation 4·14
l	mean free path of sound ray
n	average line density of noise sources
k	perpendicular distance to a road
F	vehicle flow rate
v	average vehicle speed

TABLE OF CONTENTS

1. INTRODUCTION

1·1 General Outline of the Work

The problem of noise control, like many other problems, becomes, in an urban environment, both magnified in scale and complicated in detail. Such an environment contains large numbers of noise sources, such as automobiles, factories, airports, etc., in a relatively small area, and sound from these sources is acted upon by the environment in a complicated way before it reaches a listener. The effect of this environment (which for acoustic purposes consists of many large, irregularly-shaped built-form structures) on sound propagation has been shown to be very significant [1]. The possible benefits which could derive from careful control of this environment in terms of reduced noise exposure, have also been predicted to be great [2]. However, due to its complexity, few workers have attempted to describe this effect in detail.

In this thesis, some special and, in some ways, idealised cases of the interaction of sound with an urban environment will be studied. The work is descriptive rather than prescriptive, since it is an attempt to understand the basic factors which influence sound propagation. This understanding must be a prerequisite for the development of any overall noise control policy.

Three situations are studied:

(i) sound propagating directly down a well-defined street with tall buildings on either side

(ii) propagation at an intersection of two such streets and

(iii) propagation among essentially randomly-placed buildings, with no preferred direction of propagation, such as in a suburban area, seen on a large scale.

In each case, a number of idealisations and approximations are made. However, the level of agreement between theoretical and experimental studies suggests that at least some of the important processes operating in real situations have been isolated. In situation (iii) in particular, the agreement is such that the theoretical result could be used for prediction of sound levels in real situations.

In a number of places, applications of formulae or concepts used in this work to other fields, such as duct acoustics, are mentioned.

1·2 Previous Work

Much previous work on the effect of the environment on external sound propagation has been concerned with the solution of specific problems as they arise. For example, much analysis has been done on the acoustic properties of depressed roads [3] and of acoustic barriers [4,5]. This

work has as its aim the optimal attenuation of sound by the manipulation of an "artificial" environment. In contrast, the present study is an attempt to isolate factors in a "given" environment which are important for sound propagation – factors which are usually far more complex than in any "artificial" environment.

A number of studies have been made of sound propagation in an environment containing no large built-form structures [6-11]. These find that the major factors affecting sound propagation are

(i) absorption by the air, ground and vegetation and

(ii) meteorological conditions.

However, Weiner, Malme and Gogos [12] find that meteorological conditions have far less effect in urban than in non-urban areas, presumably due to the fact that large built-form structures create their own "micro-climate" which is relatively stable. Absorption by the ground is, of course, greatly reduced in the case of a street compared to open grassland [2]. Blumenfeld and Weiss [11] comment that in urban areas, scattering and shielding by structures would probably be important in describing propagation.

Most research on propagation in urban areas has concentrated on propagation in a single well-defined street, or around a single corner into a side-street [12-18]. A notable exception is a paper by Shaw and Olsen [19] which

considers noise propagation on a city-wide scale, assuming attenuation is by spherical spreading of the sound wave, atmospheric absorption, and an empirically-determined "shielding factor". Theoretical treatments of the single-street case almost invariably use ray acoustics techniques and ignore scattering from building surfaces. A computer program has been developed [13] which can take account of random scattering. However, the program demands knowledge of precise details of the environment, which may in some cases be extremely difficult to determine except by hindsight, and its use would not lead to a great deal of enlightenment as to the general principles operating in urban sound propagation. A paper by Davies [20] uses a somewhat different approach to a similar problem, considering propagating modes rather than rays. However, he does not consider scattering and his conclusions are similar to those reached by other methods.

Unfortunately, the rates of attenuation with distance predicted by these methods are much lower than those found in real streets (see below). Lyon [1] suggests that this discrepancy may be due to the effect of scattering, but does not suggest how this could be incorporated into a theoretical treatment. In Chapters 2 and 3, an attempt will be made to take account of scattering in this situation and to assess the validity of Lyon's suggestion, while in the remainder of the thesis, ideas derived from this work will be applied to other urban situations.

2. PROPAGATION IN A WELL-DEFINED STREET - THEORY

2·1 Absorption and Scattering Processes

An urban street may be taken to consist of a hard "floor" with long rows of tall buildings on either side, and small gaps (if any) between buildings. The simplest theoretical model of this situation is to consider two parallel planes which reflect sound perfectly (figure 2·1). The "floor" may be ignored, since a source above a perfectly-reflecting floor may be shown [21] to be equivalent to two sources placed symmetrically about the position of the floor, with the floor removed. Thus, we may simply add the pressure fields from these two sources. (In practice, the source-receiver distance is much larger than the height of the source above the ground, and in this situation the presence of the "image" source does not significantly affect attenuation rates.)

It is well known [13] that if a source is placed between two such planes, the sound intensity at a distance r from the source is proportional to $1/r$ (see equation (2·12)), i.e. the sound pressure level drops at a rate of 3 decibels per doubling of distance from the source (3 dB/d.d.) due to "cylindrical spreading" of the wave. Attenuation rates in real streets, however, are much higher than this – ranging from 6 to 12 dB/d.d. [1,12]. Two major processes could

account for this "excess attenuation" – absorption by the "walls" and scattering from irregularities on them. Absorption processes have been studied by a number of workers, as described above, but the predictions of these methods are not adequate to explain measured attenuations. For example, theoretical results in reference [12] imply that the rate of attenuation can never exceed 6 dB/d.d. Thus, the effect of scattering processes on attenuation rates will now be studied in detail.

2·2 Scattering from Large Protrusions

The sound field in a street will be described in this section as series of wave fronts moving in the r direction, rather than as rays. The basis for this approach is described in section 2·5.

If such a wave front meets a large protrusion or irregularity in the walls, it will be partially reflected by it. If the street contains a series of such protrusions, a distance d apart (figure 2·2), we may find the probability per unit distance, $f(r,t)$, that a "quantum" of sound energy emitted at time $t=0$ will be found at a distance r from the source at a time t. The total intensity due to a continuously-emitting source will then be given by

$$I = \int_0^\infty \frac{d}{ct}\, f(r,t)\, d(ct) \qquad (2\cdot1)$$

where the factor d/ct accounts for cylindrical spreading. (This formula assumes that the intensity at a distance d from the source is ½, in the absence of scattering.)

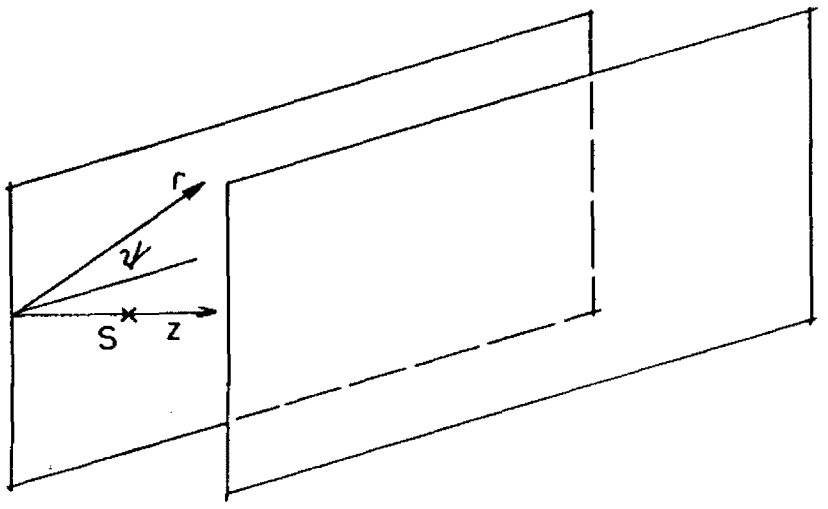

Figure 2·1: Simple model of a street. *S* represents the sound source.

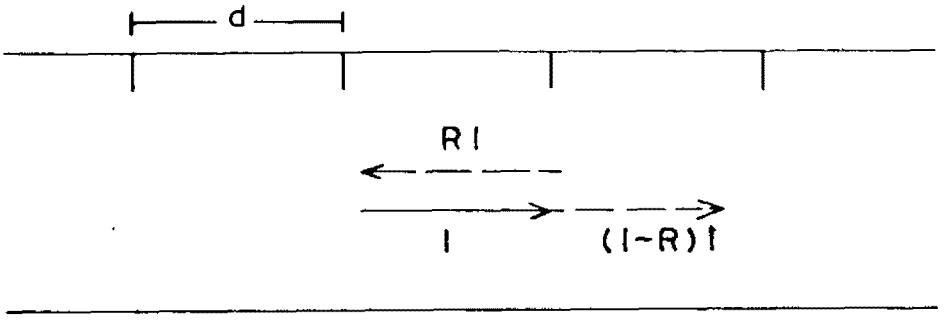

Figure 2·2: Scatterers on a street wall, with reflection co-efficient *R*.

It is shown in Appendix 3 that if R is the proportion of incident energy reflected at any protrusion, then for an infinitely long street, and for $r/d \gg 1/R$, we have

$$f(r,t) = \left\{ \frac{R}{2\pi(1-R)dct} \right\}^{\frac{1}{2}} e^{-\frac{Rr^2}{2(1-R)dct}} \qquad (2\cdot2).$$

For $R=\frac{1}{2}$ this reduces to the usual formula for particles undergoing a one-dimensional "random walk". If $r/d \lesssim 1/R$, $f(r,t)$ may be calculated from first principles, and the integral in (2·1) performed numerically on a computer.

Using (2·1) and (2·2), we have

$$I = \left\{ \frac{Rd}{2\pi(1-R)} \right\}^{\frac{1}{2}} \int_0^\infty (ct)^{-\frac{3}{2}} e^{-\frac{Rr^2}{2(1-R)dct}} d(ct)$$

$$= d/r \qquad (2\cdot3),$$

so that the attenuation rate is still 3 dB/d.d.

However, this prediction is significantly changed when a finite street is considered. Figure 2·3 shows computer calculations of attenuations for this situation, assuming that no sound is reflected back from beyond the end of the street. Significantly higher rates of attenuation are seen from approximately half-way to the end of the street.

The addition of small amounts of absorption also changes the prediction significantly, so (2·1) becomes

$$I = \int_0^\infty \frac{d}{ct} f(r,t) e^{-\gamma ct/d} d(ct) \qquad (2\cdot4)$$

(see Appendix 6), where $1-e^{-\gamma}$ is the proportion of energy absorbed in travelling a distance d.

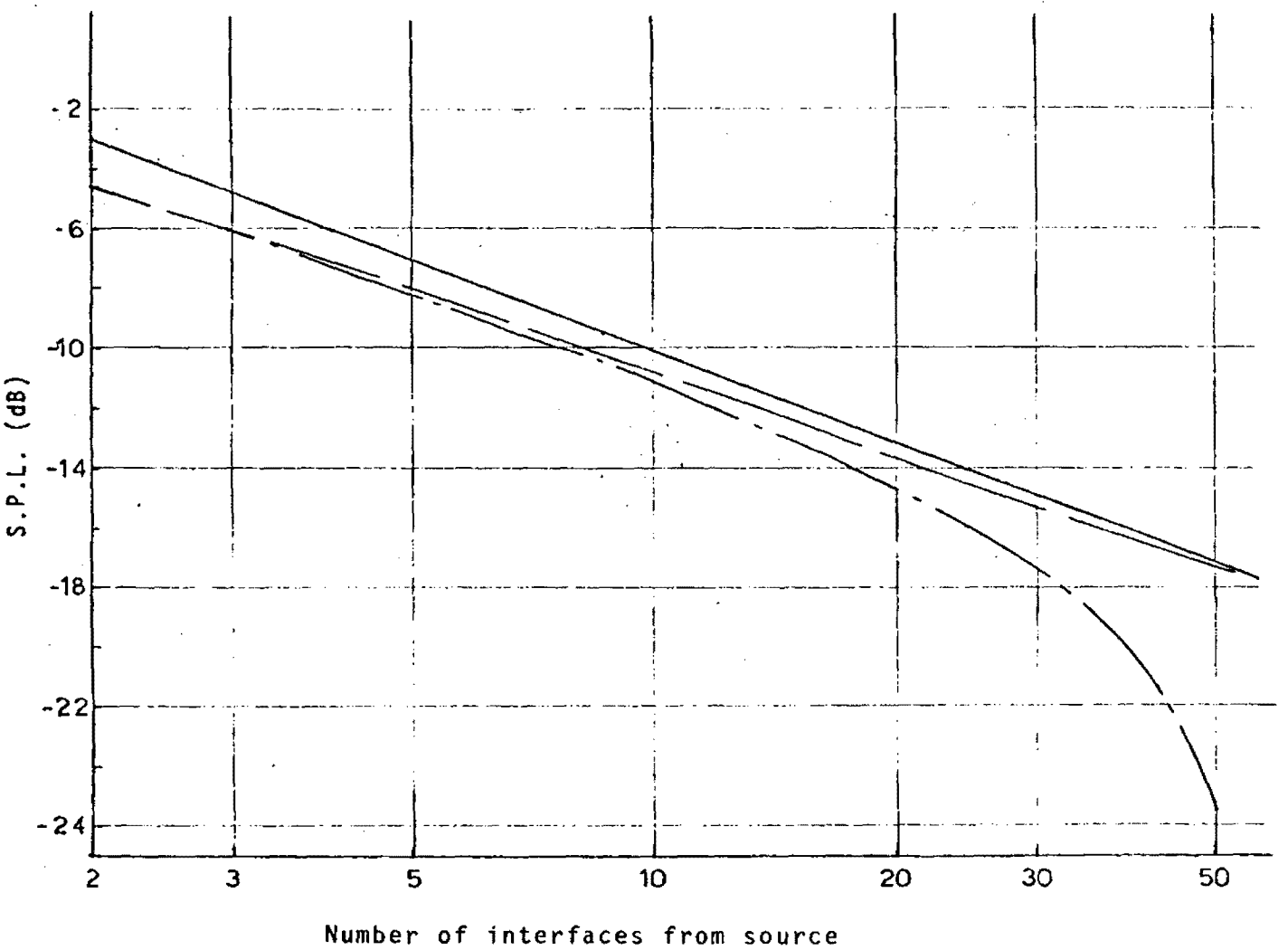

Figure 2·3: Computer calculations of relative intensities in a street, with scatterers having a reflection co-efficient $R = 0.1$. —— —— - infinite street; —— - —— - finite street with 50 interfaces; ———— - equation (2·3).

From (2·2), we then have

$$I = \left\{ \frac{Rd}{2\pi(1-R)} \right\}^{\frac{1}{2}} \int_0^{\infty} (ct)^{-\frac{3}{2}} \; e^{-\frac{Rr^2}{2(1-R)dct} - \gamma ct/d} \; d(ct)$$

$$= \frac{d}{r} \; e^{-\frac{r}{d}\left(\frac{2R\gamma}{1-R}\right)^{\frac{1}{2}}} \qquad (2\cdot5)$$

(see Appendix 2). If $2R/(1-R) > \gamma$, this gives a higher rate of attenuation than would result simply from absorption. Once again, if the finite length of the street is taken into account, the attenuation rate is even greater (see figures 3·7-3·13).

It would thus appear that rates of attenuation in streets may be controlled by the interplay between the scattering and absorption of sound. Experimental verification of the above formulae is discussed in section 3·3. A similar method may be used to calculate attenuations in ducts where scattering may be important, such as corridors (see Appendix 4).

2·3 Scattering in a Real Street

Although equation (2·5) makes clear the general effects of the processes of absorption and scattering as they operate in a street, its direct application in a real situation is difficult for two major reasons:

(i) R will usually be small, so that the condition $r/d \gg 1/R$ will not be satisfied except in the case of very long streets. Although computer calculations may be used for small values of r/d, these calculations would be rather time-consuming, both in terms of computer-time and of programmer-time.

(ii) More importantly, the effective value of γ is, in a real situation, extremely difficult to determine. In theory, γ could be calculated from the impedance of the building materials, as measured in an impedance tube. However, the value determined in this way does not take into account "excess" absorption of a wave not meeting the surface normally, which is due to surface roughness, and which may be quite considerable (see note under table 3·1).

In real situations, therefore, it is necessary to make further approximations.

It is reasonable to assume that in most streets, R, although small (usually of the order of 0.1), will be larger than γ, since most building materials have very low absorption co-efficients (lower, for instance, than 0.05 - the absorption co-efficient of plywood at 8 kHz, for which this approximation appears adequate [see sections 3·2 and 3·3]). It may also be assumed for most purposes that $r/d \lesssim 1/R$, since over longer distances, street intersections will almost certainly be encountered. In these circumstances, it is reasonable to make the approximation that in calculating $f(r,t)$, only wave-fronts which have not been reflected, or which have been reflected only once, be considered, and that these be assumed to have propagated without absorption. These wave-fronts will, in general, have a lower value of t for a given r than others, and thus

have suffered less absorption. They will also be less likely to have travelled past the end of the street. For $\gamma < R$ and $r/d \lesssim 1/R$, absorption of the waves which are taken into account in this approximation will be small.

Making this assumption, we have

$$2f(r,t) = (1-R)^{ct/d}\ \delta_{[r/d],[ct/d]} + R(1-R)^{(ct/d)-1}\ \varepsilon_{[r/d],[ct/d]} \qquad (2\cdot6),$$

where $\delta_{n,m} = \begin{cases} 1 & \text{for } n=m \\ 0 & \text{for } n\neq m \end{cases}$

and $\varepsilon_{n,m} = \begin{cases} 1 & \text{for } n<m \text{ and } m-n \text{ even} \\ 0 & \text{for } n<m \text{ and } m-n \text{ odd} \\ 0 & \text{for } n\geq m \end{cases}$

The same normalisation has been used as for equation (2·2).

From (2·1), approximating $r/d = [r/d]$, etc., where necessary, we have

$$I = \frac{d}{2r}(1-R)^{r/d} + \frac{R}{4(1-R)}\ E_1\{-(r/d)\ln(1-R)\} \qquad (2\cdot7)$$

where $E_1(x) = \int_x^\infty \frac{1}{t}\ e^{-t}\ dt$

The accuracy of this approximation is illustrated in figures 3·7-3·13.

2·4 Scattering in Two Dimensions

In a real street, sound may be scattered not only from points further down the street, but also from points higher on the "walls" and from "image scatterers" below the ground level (taking into account wave-fronts which have been reflected from the ground). For the case of small scatterers placed randomly on the walls, addition of this second dimension to the problem requires a change from the concept of "reflection co-efficient" to that of "scattering cross-section". The resulting formulae are derived in Appendix 5.

However, the situation in most streets is better approximated by considering scatterers to be long surfaces oriented either horizontally or vertically (see figure 2·4). We now have d_1, the average distance between scattering surfaces when moving horizontally, and d_2, the average distance when moving vertically. In general, R will be a function of the angle of incidence on the scattering surface, θ (figure 2·4). It will be seen from figure 2·4 that the extra intensity at r resulting from scattering from horizontal surfaces will be given by

$$I_{hor} = 2 \sum_{i=1}^{[h/d_2]} \frac{R(\theta_i)(1-R(\theta_i))^{2i-1}(1 - R(\pi/2 - \theta_i))^{[r/d_1]}}{\sqrt{r^2+(2id_2)^2}} \quad (2\cdot8),$$

where h is the height of the buildings, and $tan\theta_i = r/2id_2$, for a source and receiver at a height less than that of the first horizontal interface. This term may be added to equation (2·7), with d in this equation replaced by d_1, to give the total intensity.

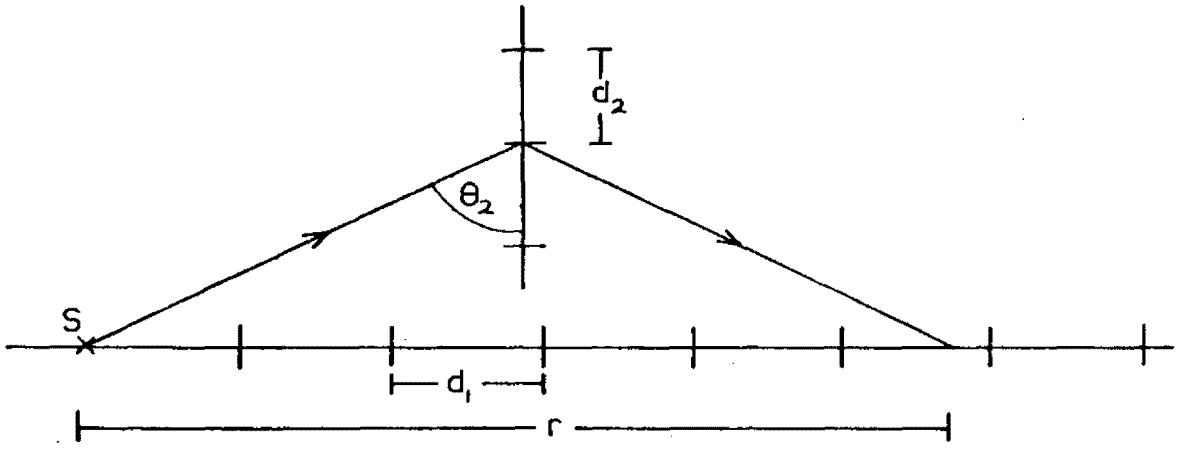

Figure 2·4: Scattering from a horizontal surface.

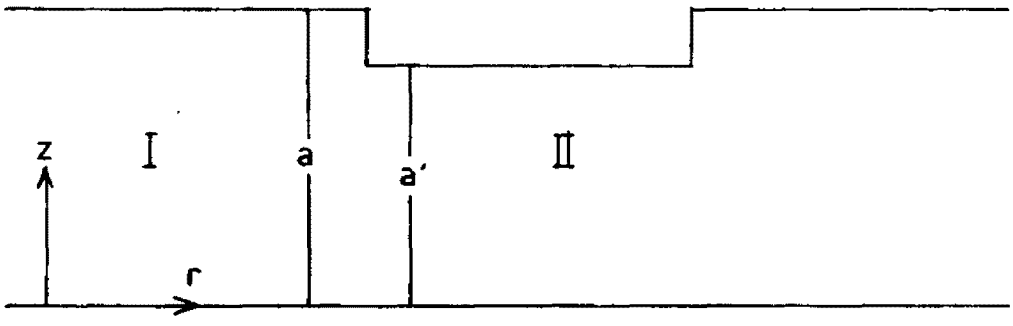

Figure 2·5: Simple representation of a scatterer on a street wall.

2·5 Determination of R

In order to estimate R, some assumption must be made as to the form of the scatterers in a street. The simplest possible assumption is to regard a scattering surface as producing a sudden change in the width of the street from a to a', as represented in figure 2·5. A simple picture of the sound-field in the street which represents it in terms of parallel rays moving down the street would then predict

$$R = \begin{cases} (a - a')/a & \text{for } a>a' \\ 0 & \text{for } a<a' \end{cases} \qquad (2\cdot9)$$

(In this approximation, R is independent of the angle of incidence.)

In many cases, this expression is adequate. However, a more accurate description of the sound field leads to the conclusion that even in the region $z<a'$ (figure 2·5), some sound energy is reflected. Since this energy is in some cases not inconsiderable, a more exact expression for the reflection co-efficient will be derived.

For plane, perfectly-reflecting walls, the acoustic pressure field in the street for a spherically-symmetric source may be written in cylindrical polar co-ordinates [23]

$$p = \sum_{n=0}^{\infty} P_n H_0^{(1)} (k_n r) \cos \varepsilon_n z \qquad (2\cdot10)$$

where $H_0^{(1)}$, the zero-order Hankel function of the first kind, has been chosen to represent an outgoing wave. For simplicity, all sources will be assumed to radiate in a spherically symmetric way.

$k_n^2 = (2\pi/\lambda)^2 \{1-(n\lambda/2a)^2\}$, where λ is the free-space wavelength, and $\varepsilon_n = n\pi/a$. The values of the co-efficients P_n depend on the nature and position of the source. (For instance, if the source is symmetrical about the centre of the street, we will have $P_n=0$ for all odd values of n.)

At distances from the source greater than the order of a few wavelengths, (2·10) becomes

$$p = \sum_{n=0}^{[2a/\lambda]} P_n (k_n r)^{-\frac{1}{2}} \; e^{ik_n r} \cos \varepsilon_n z \qquad (2\cdot11).$$

Thus, the pressure field is represented as a sum over propagating modes.

The intensity is given by

$$I = \sum_n |P_n|^2 \; (\rho c k_0 r)^{-1} \cos^2 \varepsilon_n z \qquad (2\cdot12).$$

If the walls are absorbing, k_n becomes complex, giving an extra attenuation of $e^{-Im(k_n)r}$ (see Appendix 6).

If a wave approaching an interface is in the nth mode of propagation, this mode must, on passing the interface, be represented by a sum of modes in a street of width a'. It is shown in Appendix 7 that, in this process, a proportion R_n of the incident energy is reflected, where for normal incidence,

$$R_n \sim \left(\frac{k_n - k'_m}{k_n + k'_m}\right)^2 \qquad (2\cdot13).$$

Here, $k'^2_m = (2\pi/\lambda)^2 \{1-(m\lambda/a')^2\}$ and m is the nearest integer to na'/a.

If the angle of incidence is θ, the corresponding expression is

$$R_n(\theta) \begin{cases} \sim \left(\dfrac{\cos\theta - ((k'_m/k_n)^2 - \sin^2\theta)^{\frac{1}{2}}}{\cos\theta + ((k'_m/k_n)^2 - \sin^2\theta)^{\frac{1}{2}}} \right)^2 & \text{for } \sin\theta < k'_m/k_n \\ = 1 \qquad \text{for } \sin\theta > k'_m/k_n \end{cases} \tag{2·14}$$

(see Appendix 7).

The total reflection co-efficient will then be

$$R = (a-a')/a + \frac{a'}{a} \sum_n R_n P_n^2 \Big/ \sum_n P_n^2 \quad \text{for } a' < a \tag{2·15}.$$

and $$R = \sum_n R_n P_n^2 \Big/ \sum_n P_n^2 \quad \text{for } a' > a$$

In cases where protrusions, etc., cause an alternation in street width between a and a' (as in figure 3·6), the average reflection co-efficient for a single interface, $\bar{R}$, must be chosen so that

$$(1-\bar{R})^2 = (1-R(a,a'))\ (1-R(a',a)) \tag{2·16}.$$

3. PROPAGATION IN A WELL-DEFINED STREET — EXPERIMENT

3·1 Description of Models Used

All model studies in this work were carried out in a small (5m x 5m x 2.5m) anechoic room. A street was modelled by two plywood boards, 2000 x 1000 x 10 mm, with bases attached so that they stood vertically and parallel, with the longer sides horizontal. Between these boards a microphone on a carriage could be moved by the mechanism shown in figure 3·1. A sound source was placed at the centre of the street near one end of the boards and sound level readings were taken with the microphone at various distances from the source. In order to prevent spurious reflections from the ends and top of the street, it was found to be necessary to place fibreglass absorbing material all around the model.

Two sound sources were used:

(i) a Phillips tweeter, approximately 5 cm in diameter, driven by a white noise generator with an octave-band filter, or else by a function generator when a single-frequency source was required. (See Appendix 1 for details of the equipment.)

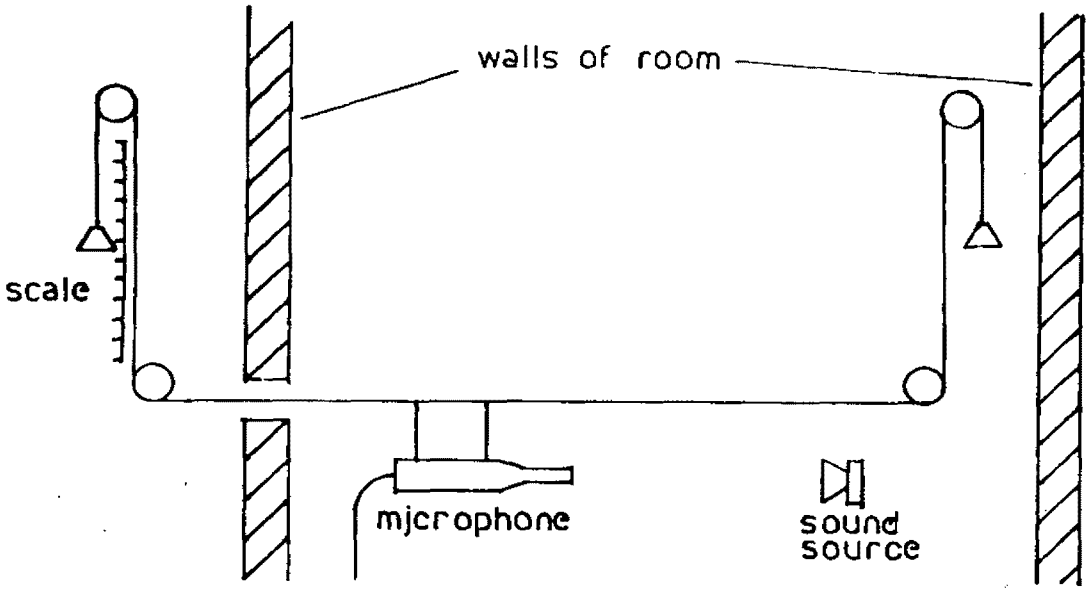

Figure 3·1: Mechanism for remotely moving a microphone.

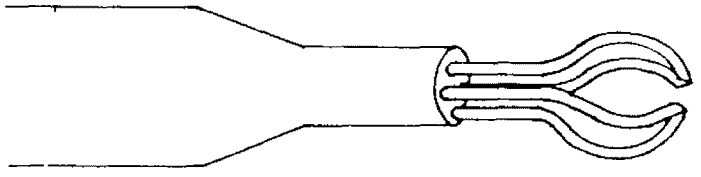

Figure 3·2: Nozzle of air-driven sound source.

(ii) a nozzle having four impinging air-jets (figure 3·2), driven from a compressor, whose output in $\frac{1}{3}$-octave bands is shown in figure 3·3. This output was omnidirectional to within 2 dB.

A ¼" microphone was used, connected to a signal amplifier and filter.

3·2 Determination of γ

In order to estimate the value of γ for the plywood boards, readings of the SPL were taken at 5 cm intervals down the street, using both sources. These were then corrected for attenuation due to cylindrical spreading, and a linear regression was used to find the value and standard error of the residual attenuation in dB's per metre, from which γ may be easily found, if d is known. Other variations in SPL were probably caused largely by interference between various modes which move in and out of phase as one moves down the street. Some results are shown in figures 3·4 and 3·5.

Both sources were tested because rates of absorption are, in general, different for different modes and, therefore, will depend on the particular combination of modes produced by the source. However, in the case of the speaker, interference effects largely masked the absorption and a linear regression gave only attenuations (in a 20 cm -wide street) of 0.7 ± 0.7 dB's/m at 8 kHz and 1.2 ± 1.4 dB's/m

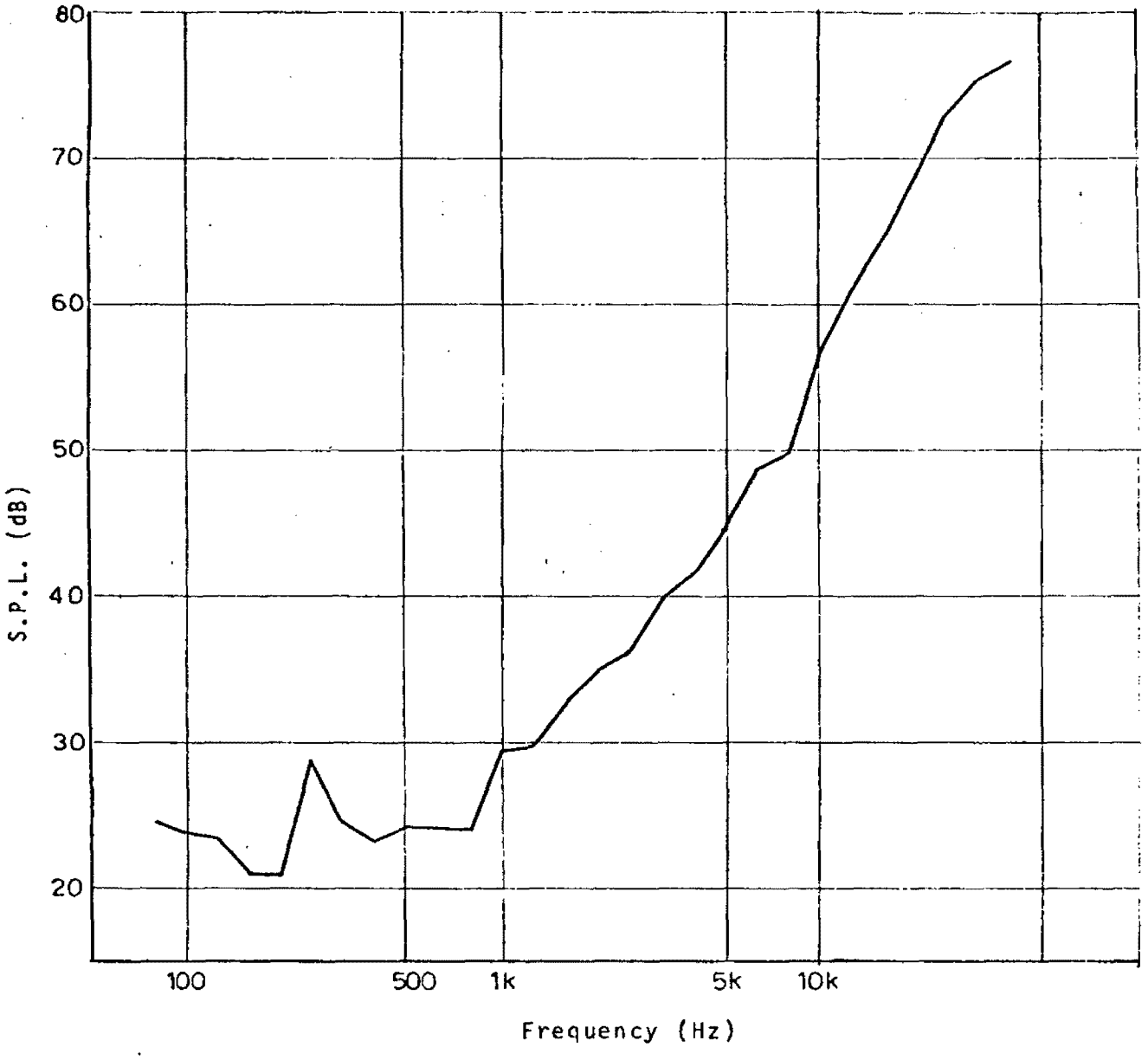

Figure 3·3: Output of air-driven source in ⅓ -octave bands, at driving pressure 50 p.s.i.

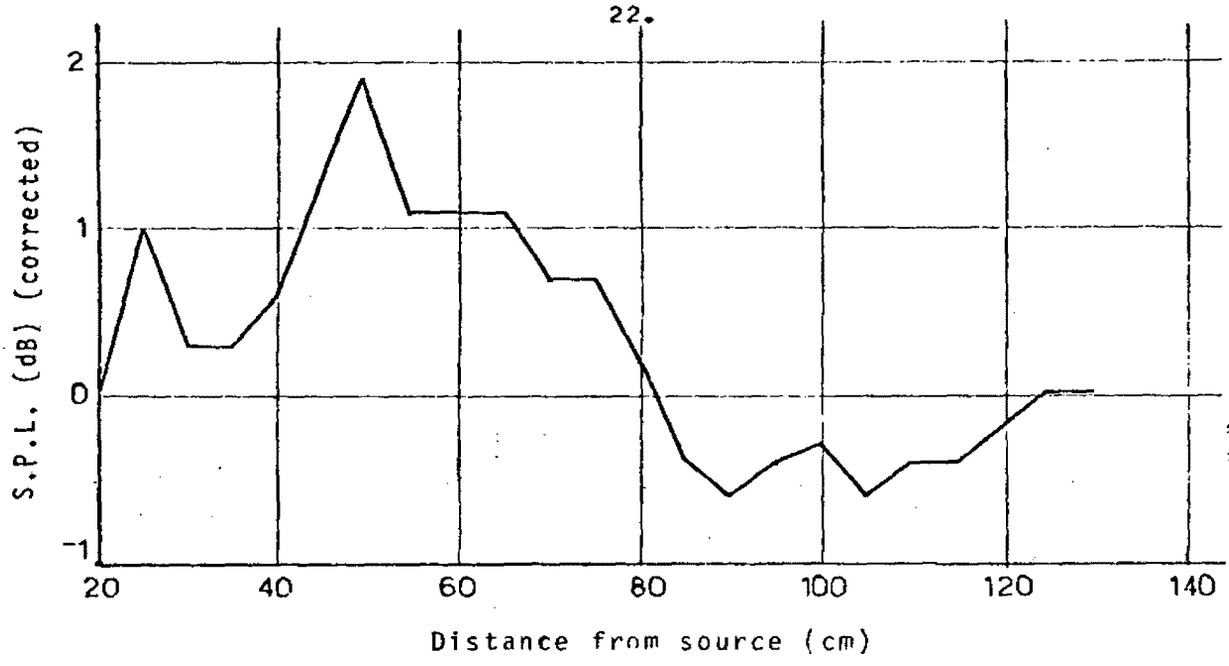

Figure 3·4: Absorption in a 20 cm-wide plywood street at 8 kHz, using the air source. S.P.L. is corrected for cylindrical spreading and arbitrarily normalised.

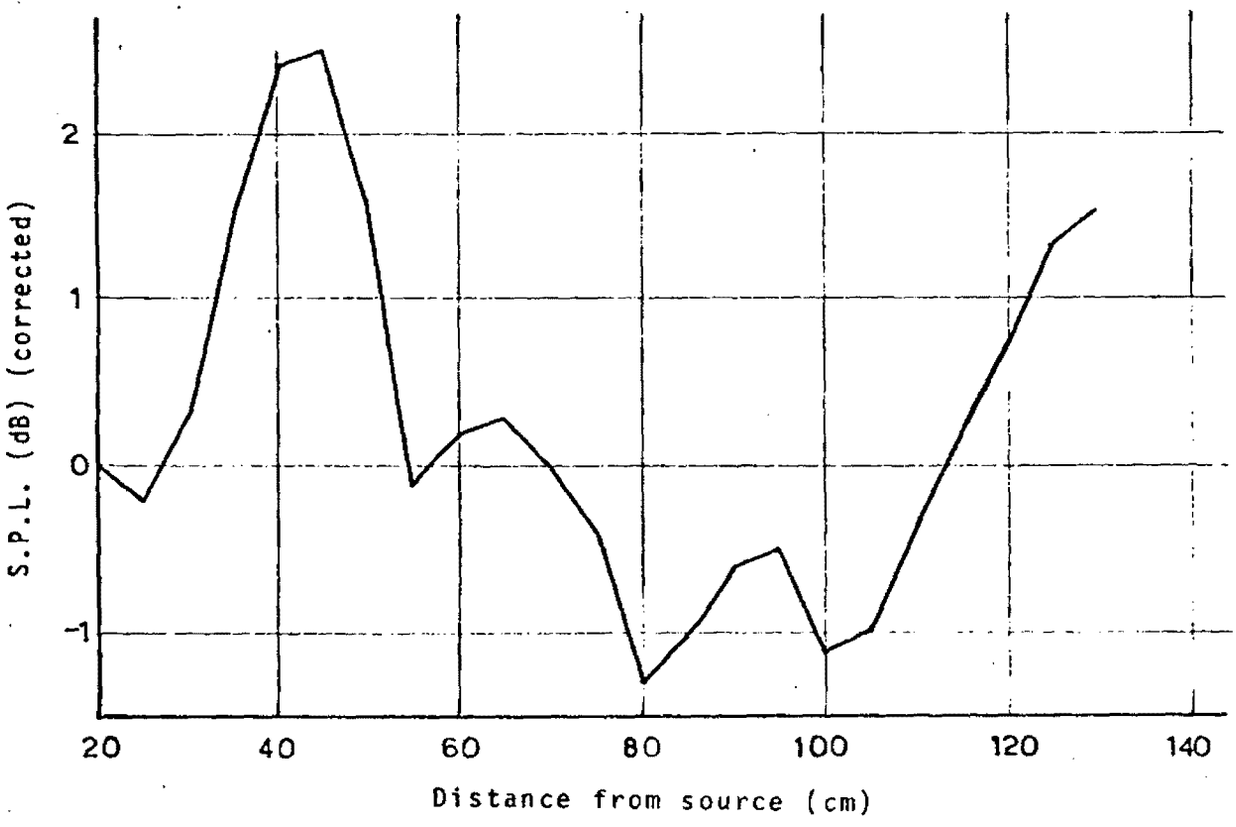

Figure 3·5: Absorption in a 20 cm-wide plywood street at 8 kHz, using the speaker. S.P.L. is corrected for cylindrical spreading and arbitrarily normalised.

at 16 kHz. Thus, values found for the air source were assumed to apply also to the speaker. These values are shown in table 3·1.

Street width	Octave-band centre-frequency	Absorption (dB's/m)
20 cm	8 kHz	1.3 ± 0.4
	16 kHz	1.7 ± 0.2
	31.5 kHz	2.9 ± 0.2
40 cm	8 kHz	0.8 ± 0.2
	16 kHz	1.1 ± 0.2
	31.5 kHz	2.0 ± 0.2

Table 3·1: Attenuations due to absorption by plywood street walls.

Note: From measurements on plywood in an impedance tube, the absorption at 8 kHz in a 20 cm-wide street would have been predicted to be less than 0.01 dB/m.!

3·3 Modelling of Scattering Processes

Vertical plywood strips 1 cm thick and 3 cm wide were attached to the boards representing the street walls, as shown in figure 3·6. Taking R from equation (2·9) and using equation (2·16) gives $\overline{R}$ = 0.051 if a =20cm, and $\overline{R}$ = 0.025 if a =40 cm. R_n may be calculated for each n by integrating equation (2·13) with respect to frequency, since all the interfaces are normal to the direction of propagation. This shows that R_n is negligible except in

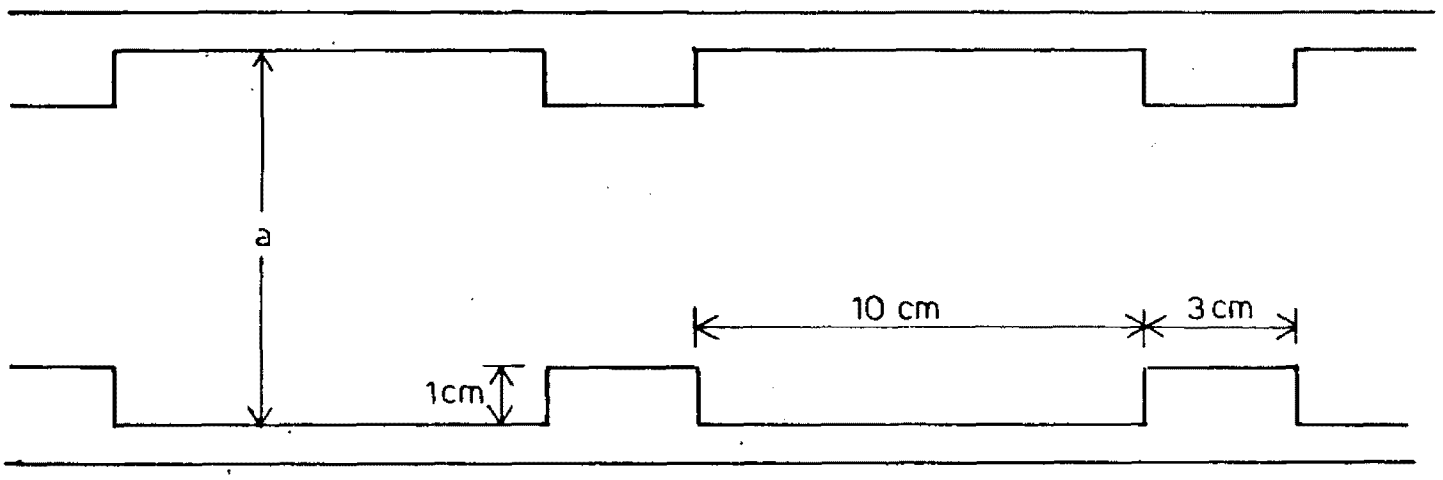

Figure 3·6: Modelling scatterers in a street.

the case of propagation in the mode of highest possible order, in which case $\bar{R} \sim 0.1$ for $a = 20$ cm, and $\bar{R} \sim 0.05$ for $a = 40$ cm. (These values are the same, ± 0.005, for the 8 kHz, 16 kHz and 31.5 kHz octave-bands.)

Using a technique described in sections 4·3 and 5·1, it was possible to determine the "average" mode of propagation (defined more precisely in section 4·1) when using the speaker as the source. (This was not possible in the case of the air source, since this cannot produce a pure tone.) At 8 kHz in a 20 cm street, the average mode number was 3, from a possible 4, while at 16 kHz it was less than 3 from a possible 9. It was found that smaller sources tended to emit higher-order modes, and that increasing the street width for a given source decreased the average mode number in relation to the total number of possible modes (see section 5·1). Thus, considering that the source area of the air source is much smaller than that of the speaker, it would seem reasonable to assume that propagation was in the mode of highest possible order in the case of the air source at 8 kHz in a 20 cm street, but at no other time.

Making this assumption, and using the above values of γ, predictions of the expected attenuation were made by numerically integrating equation (2·1) on a computer, both for the case of an infinite street and for a street the length of the experimental street (i.e. 26 interfaces).

These were compared with experimental results, and with the predictions of equations (2·5) and (2·7) (figures 3·7 – 3·13). Equation (2·7) is seen to be a good approximation if R is low, and γ even lower. For R relatively high, (2·7) still gives a fair approximation to the slope of the curve, if not to its absolute value. (Absolute values of sets of experimental points were arbitrarily fixed.)

It should be noted that attenuation rates within approximately one street width of the source may be expected to be higher than those predicted by the above theory, since near this point all modes begin to come into phase. This explains the drift of experimental points away from the predicted line at less than approximately 6 interfaces from the source in the results for the 40 cm-wide street. The attenuation rate at 8kHz in the 40 cm street appears to be greater than was predicted, possibly indicating that a considerable proportion of the sound energy is still in the highest-order mode.

Model tests of scattering from horizontal interfaces were not performed due to the limited size of the anechoic room available at Sydney University.

3·4 Full-Scale Tests

James Lane in Sydney was chosen for the site of a full-scale experiment. This is a lane 6.3 m wide, with buildings approximately 7 m high lining each side, and having no gaps between them. At one end of the lane is James Street, which is approximately 20 m wide, and at approximately 75 m from this corner, the lane is partially

Figures 3·7 - 3·13: Attenuation in a model street with scatterers.

——— - predictions derived numerically from equation (2·1), for an infinite street.

---- - predictions derived numerically from equation (2·1), for a street of 26 interfaces.

—+—+— - predictions of equation (2·5).

—·— - predictions of equation (2·7).

o - experimental results.

Octave-band centre-frequency, street width and source are given under each figure.

Figure 3.7

8KHz, 20 cm street, air source. (R=0.1, γ=0.019)

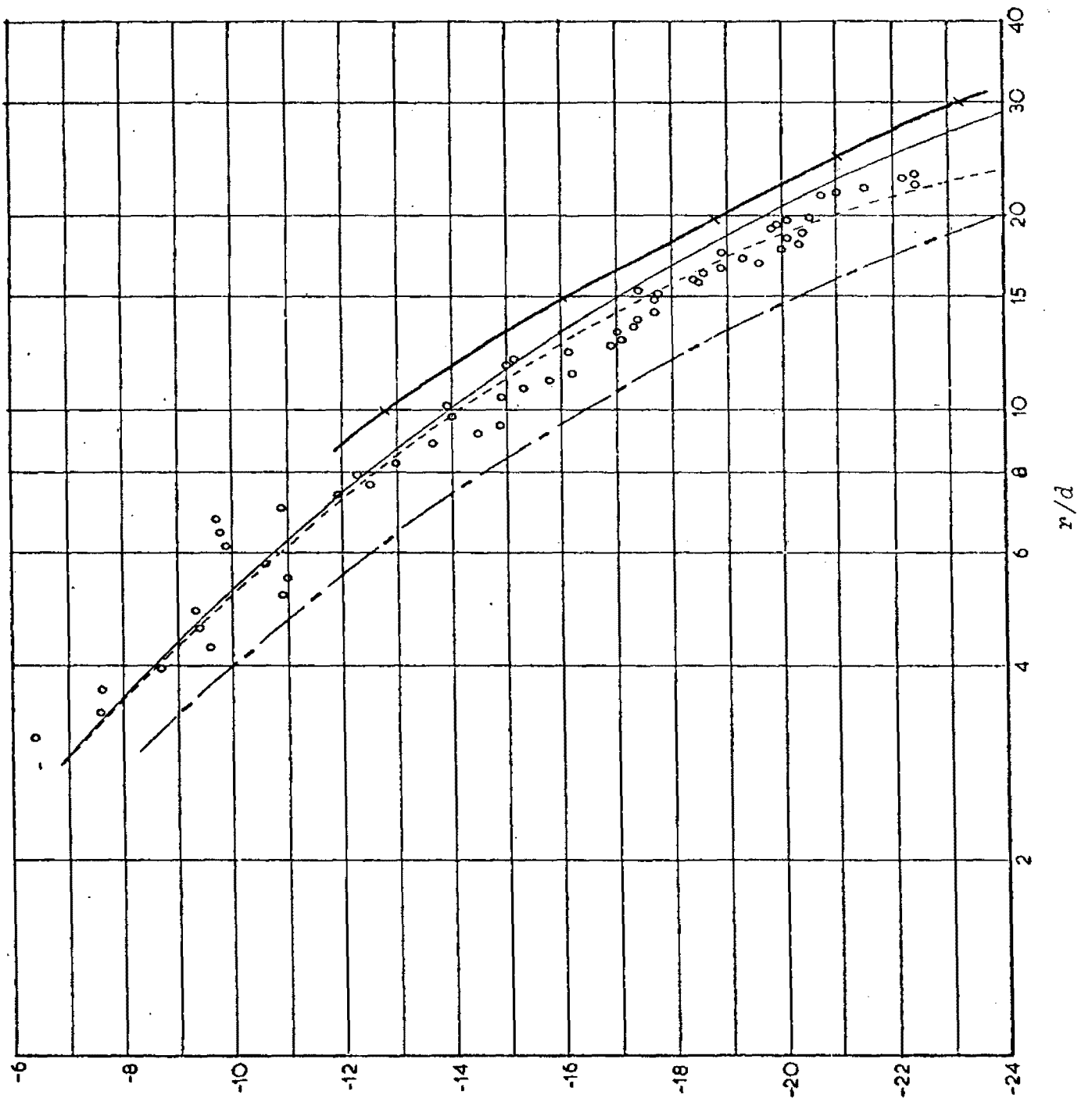

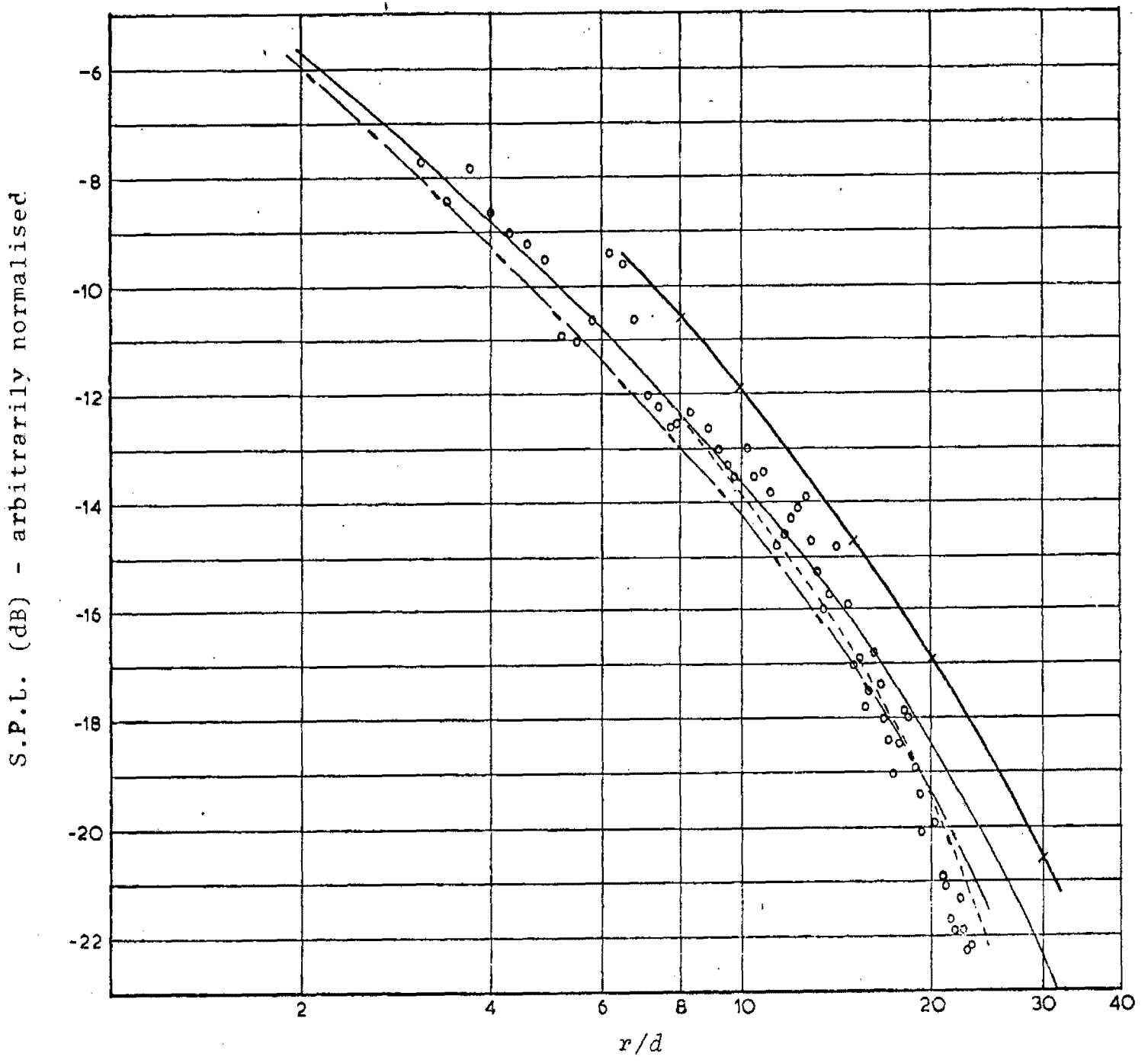

Figure 3·8

8 KHz, 20 cm street, speaker source. (R=0.05, γ= 0.019)

Figure 3·9

16 KHz, 20 cm
street, x - air
source, o - speaker
source. (R=0.05,
γ=0.025)

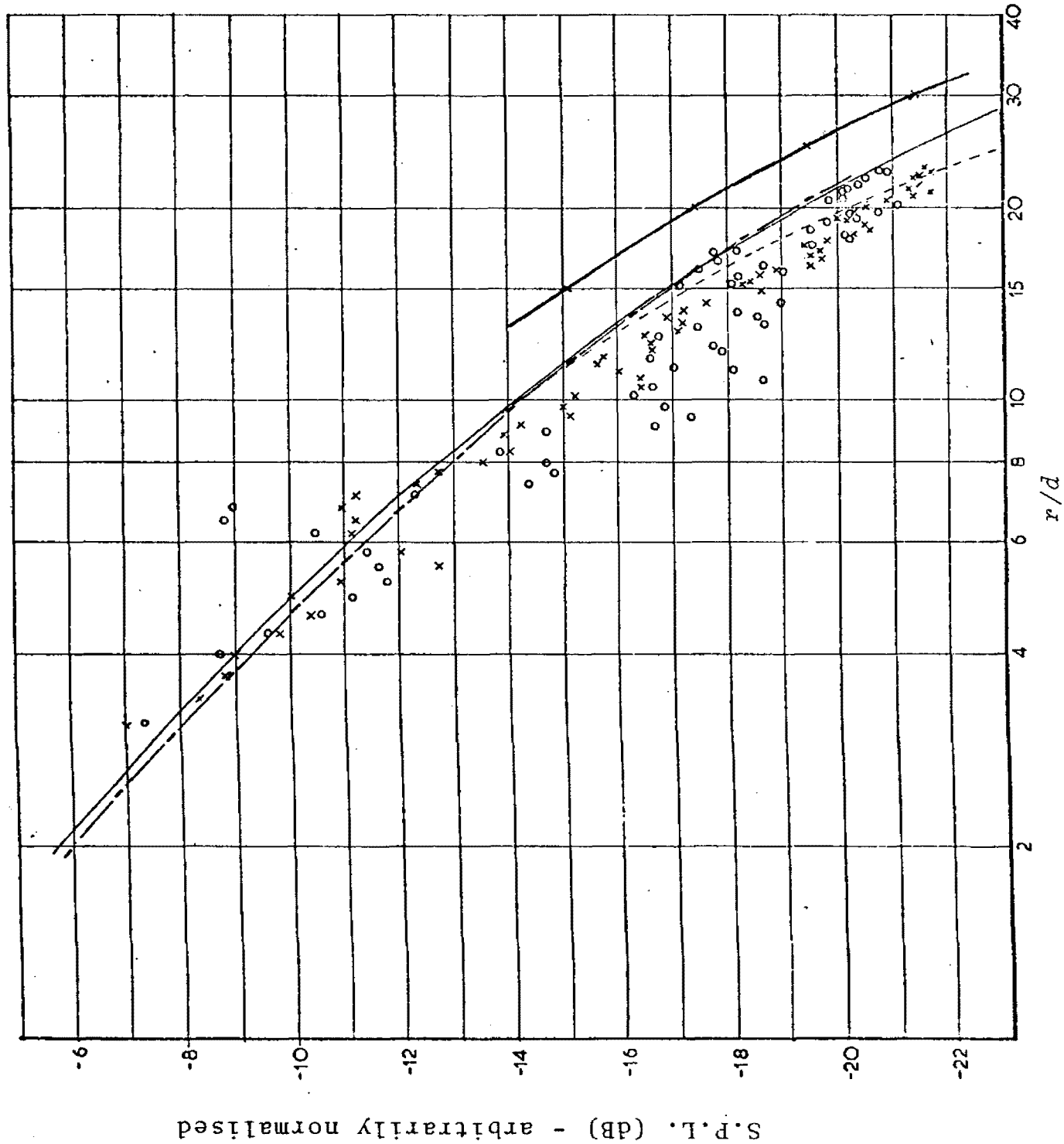

Figure 3.10

31.5 KHz, 20 cm
street, air source.
(R=0.05, γ=0.043)

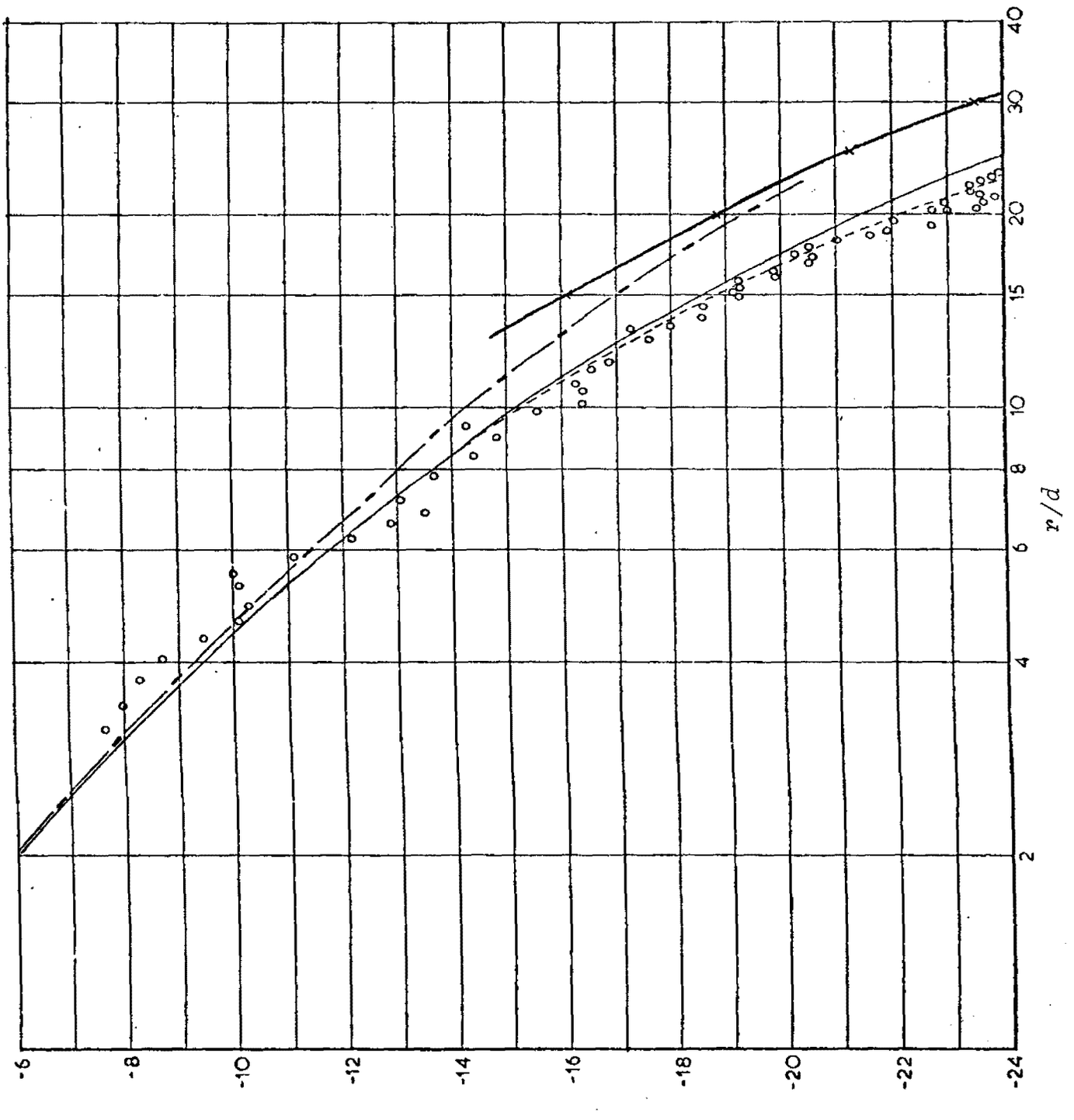

Figure 3·11

8KHz, 40 cm street, air source. (R=0.025, γ=0.012).

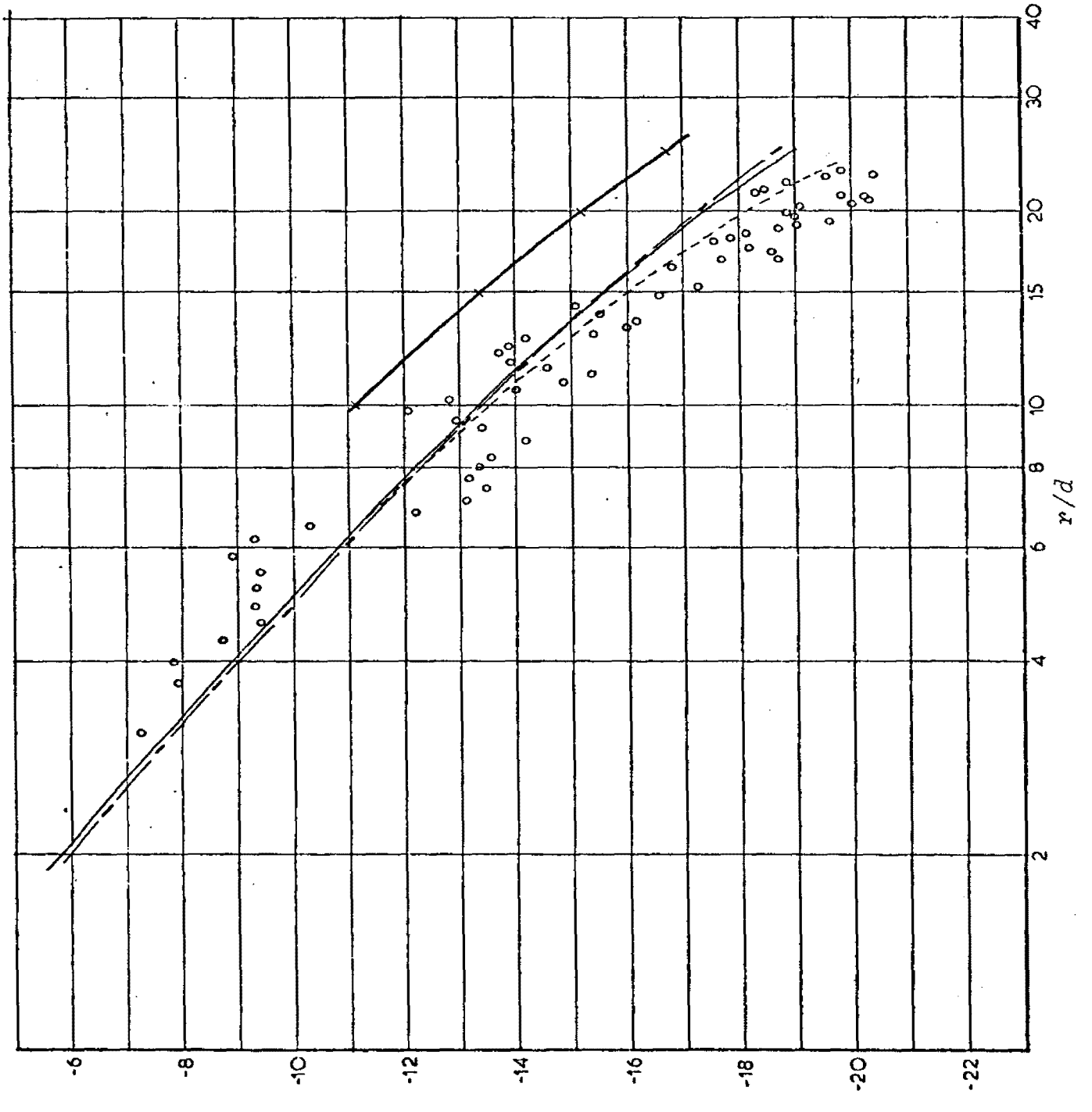

Figure 3.12

16 KHz, 40 cm street, air source. (R=0.025, γ=0.016)

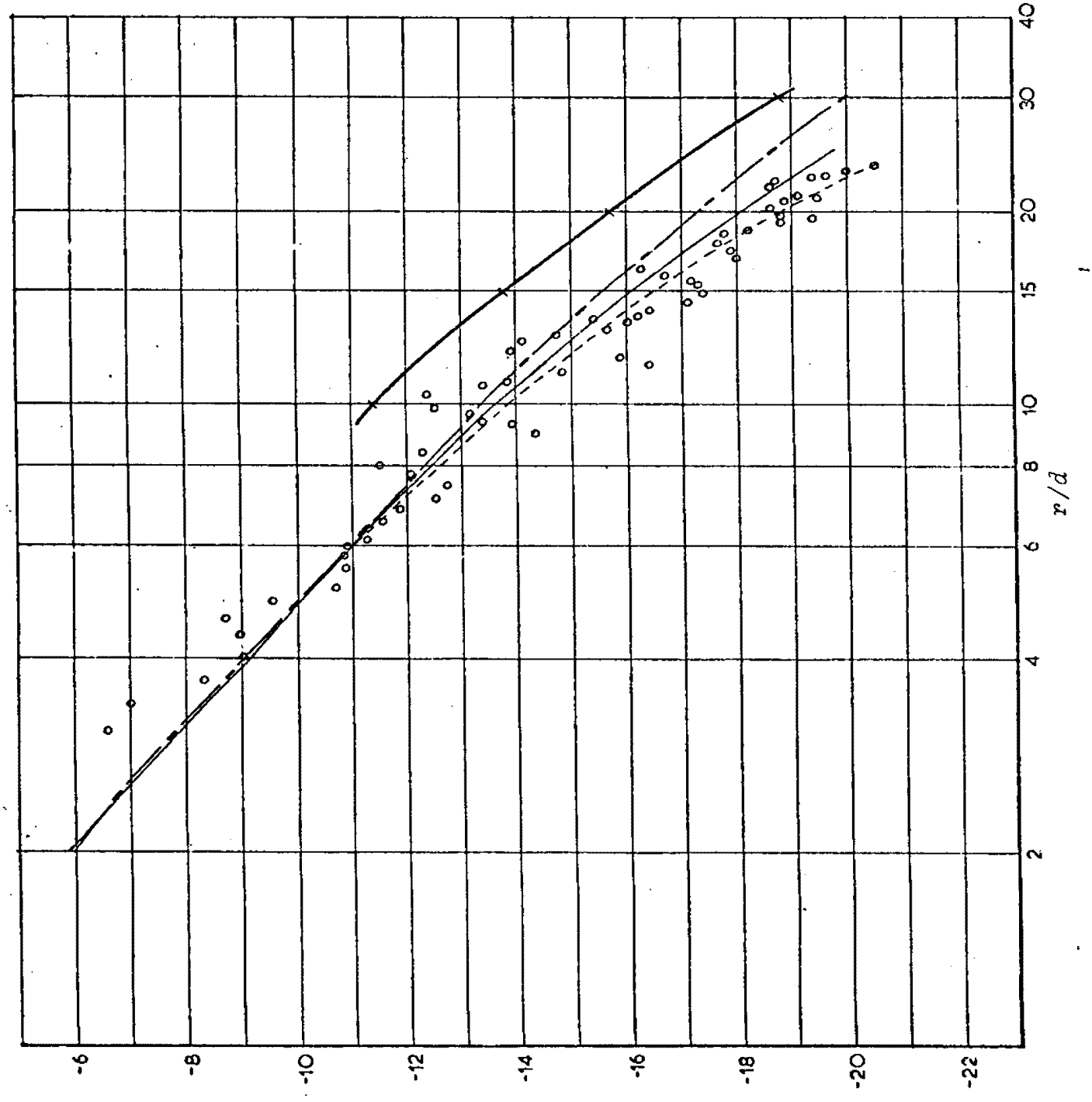

Figure 3.13

31.5 KHz, 40 cm street, air source. (R=0.025, γ=0.03)

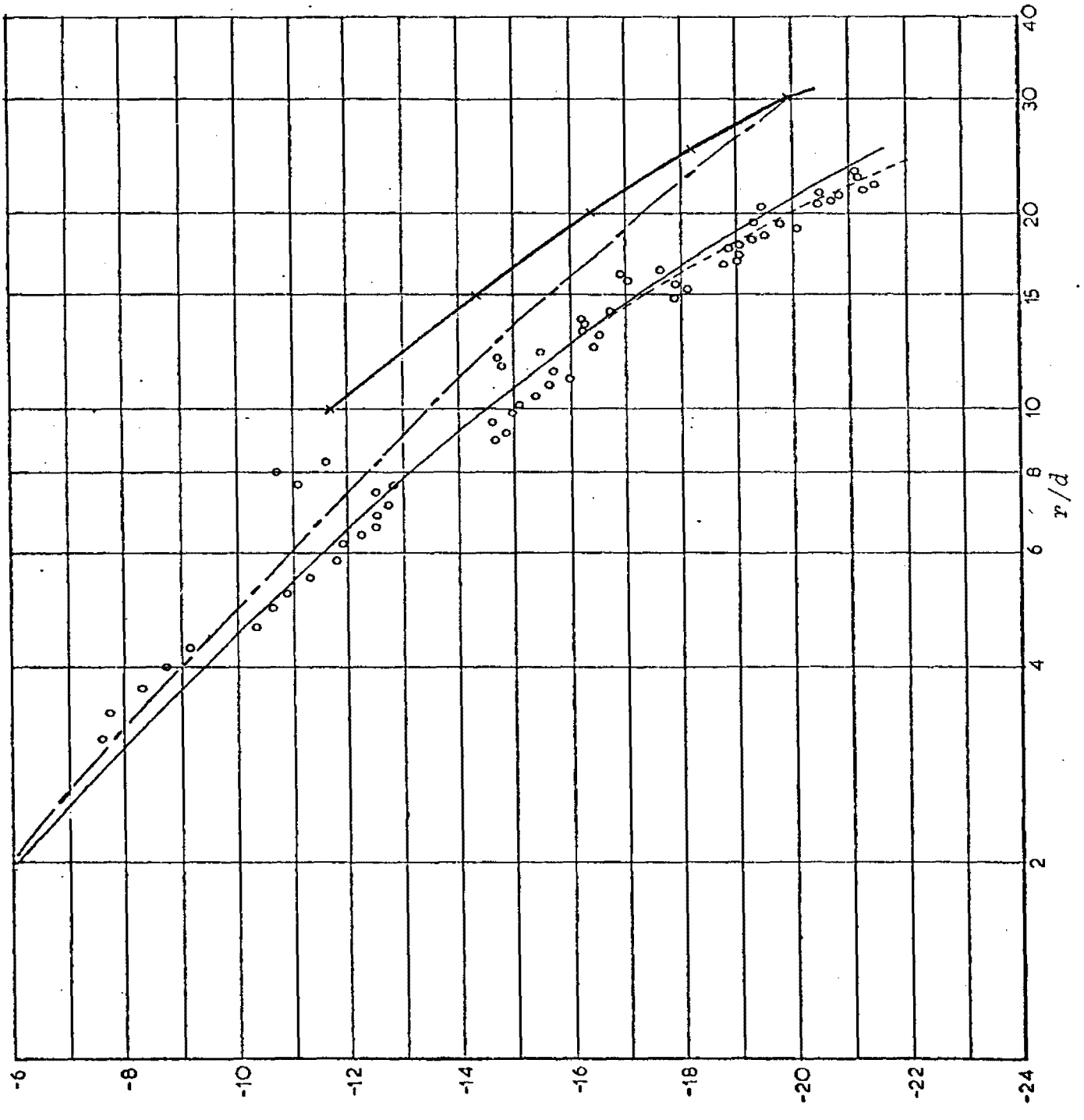

Figure 3·14: James Lane, Sydney, seen from James Street. The car was not present while experiments were being carried out.

blocked by buildings (figure 3·14). On one side, scattering surfaces consisted of the edges of entrances and windows, with the following parameters:

d_1 = 2.3 ± 0.1 m

d_2 = 1.5 ± 0.1 m

$|a-a'|$ = 60 ± 5 cm

On the other side, the surfaces consisted of the edges of windows, and these surfaces had the following parameters:

d_1 = 1.2 ± 0.1 m

d_2 = 1.5 ± 0.1 m

$|a-a'|$ = 15 ± 3 cm

Errors in the above figures are estimated, and result from difficulties in determining parameters for the "average" scatterer. Ambient noise was low (always at least 10 dB below the signal) since the test was conducted in the early morning. (This also ensured that entrances, windows, etc., were closed.)

The sound source used was an omnidirectional speaker placed near James Street through which pre-recorded white sound was played. The sound field at points down the street was recorded via a sound level meter and subsequently analysed using an octave-band filter and signal amplifier.

The results are shown in figures 3·15 and 3·16 and and compared with the predictions of equations 2·7 and 2·8. Since the speaker is 35 cm wide, it was assumed that low-

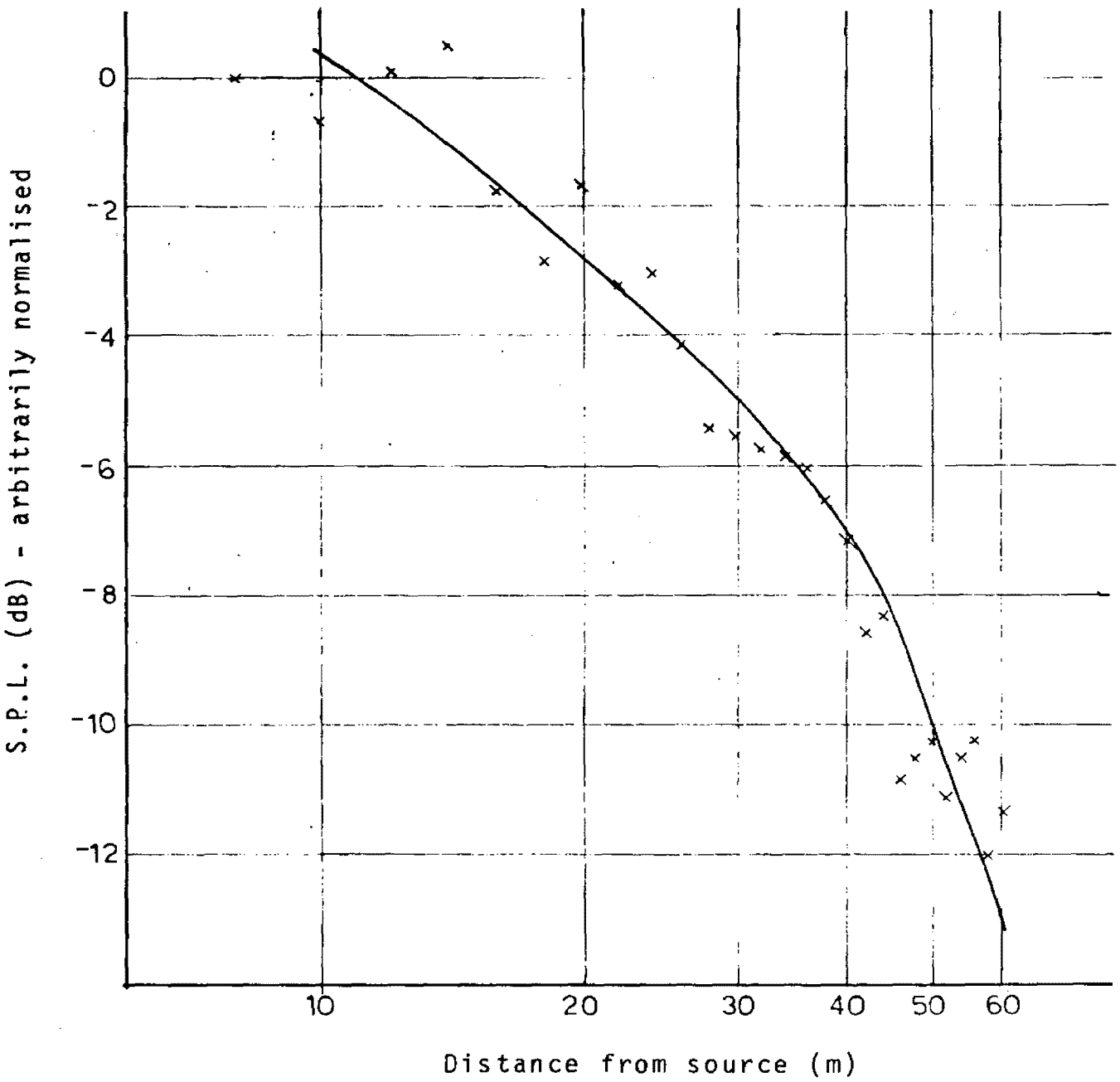

Figure 3·15: Attenuation in James Lane in the octave-band centred on 500 Hz. ——— - predictions of equation (2·7); x - experimental results.

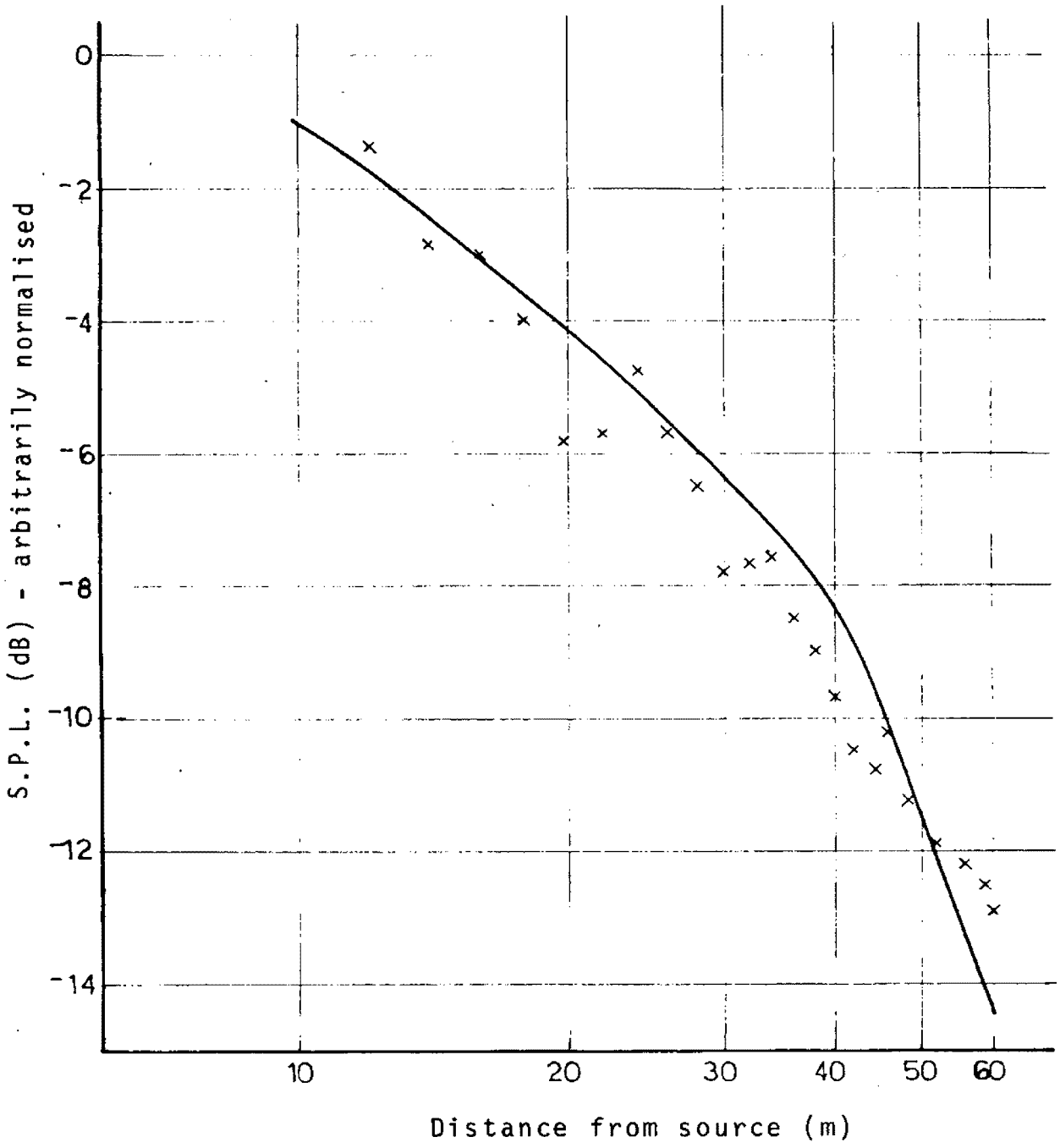

Figure 3·16: Attenuation in James Lane in the octave-band centred on 1 kHz. ——— - predictions of equation (2·7); x - experimental results.

order modes were propagated. However, in this case, even the assumption that the highest-order mode was propagated changed the predictions by less than 1 dB. Similar uncertainty arose from errors in d_1, d_2 and $|a-a'|$. Despite this uncertainty, it would appear from figures 3·15 and 3·16 that equations 2·7 and 2·8 give a useful prediction of the rate of attenuation in some urban streets - those whose walls are high, have few gaps, and have low absorption. For high absorption, equation (2·1) must be integrated numerically, or for large distances, equation (2·5) used (if γ is known).

It has been seen that rates of attenuation in the kind of streets studied are governed by the interaction of absorption and scattering processes. In Chapters 6 and 7, this will be seen to be true for a much more general class of sound propagation problems.

4. PROPAGATION AT AN INTERSECTION - THEORY

4·1 The Sound Field Near an Intersection

In this section of the work a study was made of a situation in which two or more of the kind of streets described in the previous section, meet. In particular, a description was sought of the sound field generated in one street by a source in another street. This knowledge is, of course, necessary in order to formulate a description of propagation in a network of such streets, and, together with results in the previous section, it gives, in principle, a complete description of this propagation. (In practice, the results derived here appear to be useful only on a small scale – i.e. within approximately a block of the source – for reasons explained in following chapters.)

For the sake of simplicity, only four-way intersections where all streets meet at right angles, as in figure 4·1, will be considered. It is believed that the work described here could be extended to other types of intersections with few major changes. Attention was concentrated on the problem of predicting the drop in intensity arising from moving around a corner at such an intersection (from the "source street" to the "receiver street"). However, other properties of the resulting sound field were also found to be important.

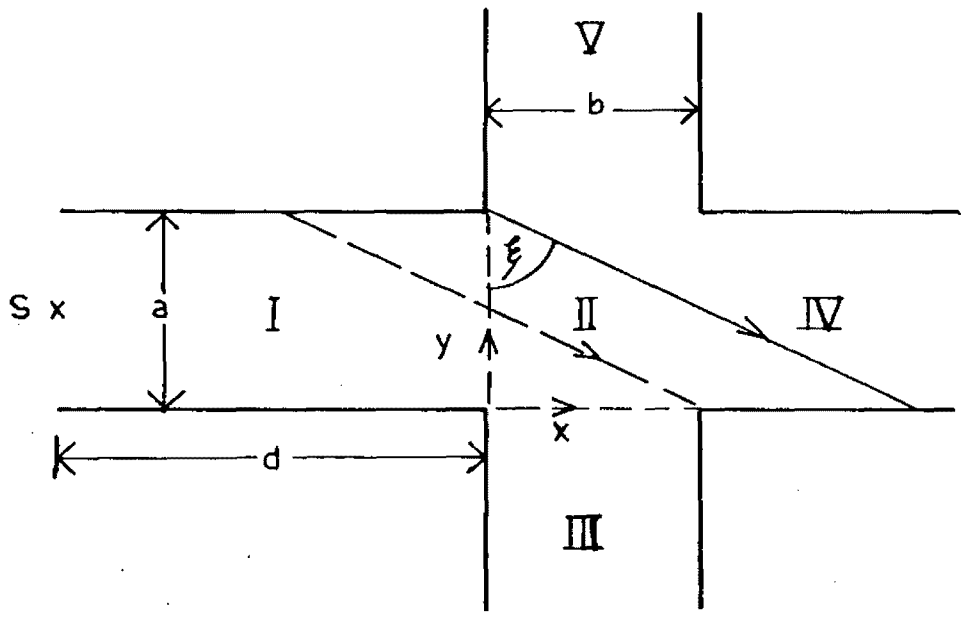

Figure 4·1: A four-way intersection, showing modal propagation at an angle of incidence ξ.

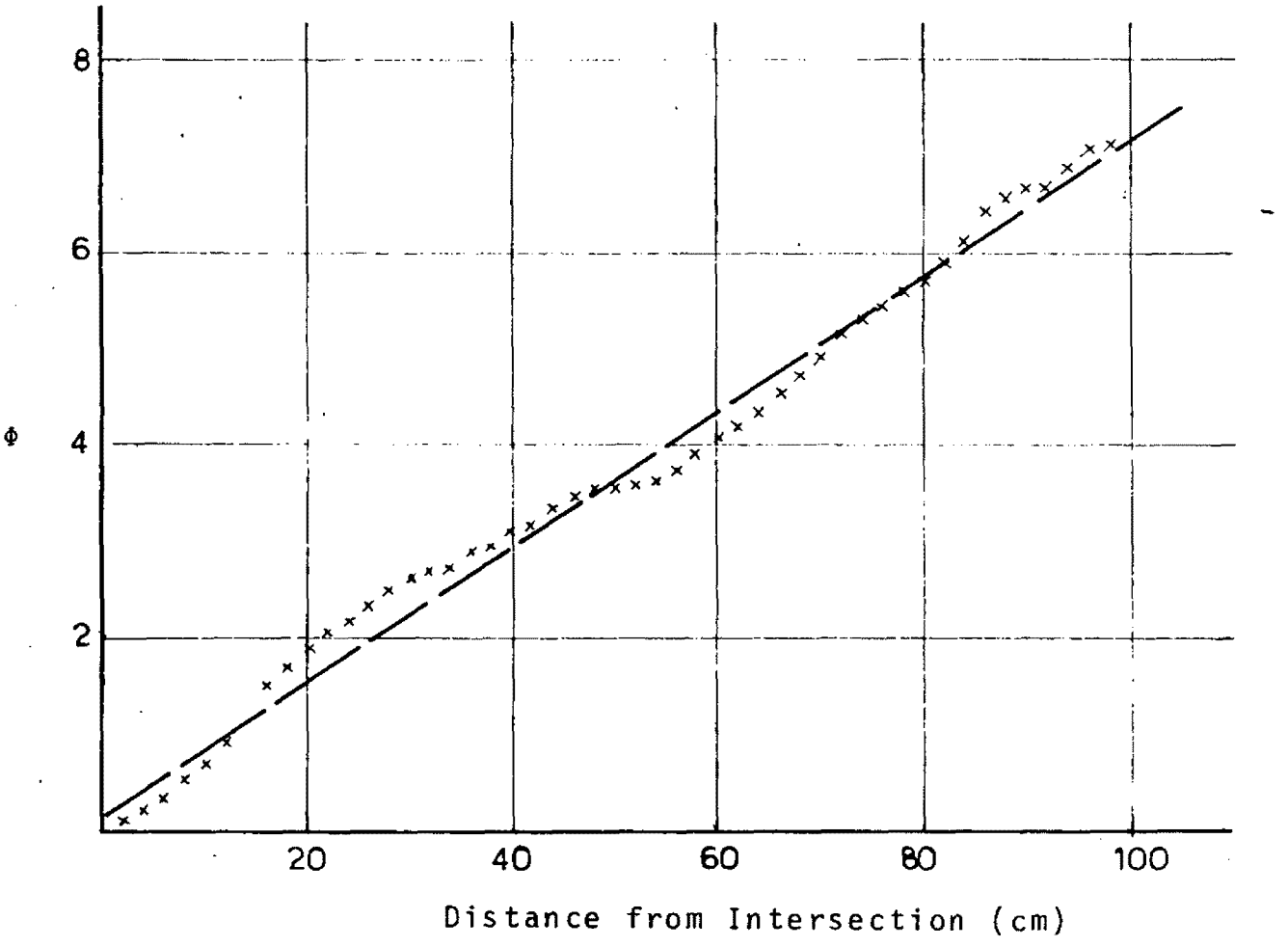

Figure 4·2: Φ *vs* r in a 40 cm-wide receiver street, with a 40 cm-wide source street, at 4 kHz, showing that variations in $\frac{d\Phi}{dr}$ are small.

The sound fields in streets near an intersection (regions I, III, IV and V of figure 4·1) may be described by equation 2·11, with suitable choices of P_n; r and z in equation 2·11 become x and y in figure 4·1, with r becoming x in region I, r becoming $-y$ in region III, etc. For region I, equation 2·11 may be written

$$p = \tfrac{1}{2} \sum_n P_n (k_n x)^{-\frac{1}{2}} \{ e^{i(k_n x + \varepsilon_n y)} + e^{i(k_n x - \varepsilon_n y)} \} \qquad (4\cdot1).$$

Thus, each propagating mode in the source street may be considered to consist of two cylindrical waves, with intensities proportional to $\frac{1}{4}|P_n|^2/x$, travelling such as to make an angle of incidence ξ with the street walls, where $\sin \xi = k_n/k_o$ (see figure 4·1).

It will be assumed that the behaviour of the sound field may be described by the behaviour of a single "average" mode, which may be defined as the mode for which $1/k_n$ is nearest to $(\sum |P_n|^2/k_n)/(\sum |P_n|^2)$. This assumption will be valid only if most sound energy is concentrated in a single mode. That this was the case in the experimental situations studied is demonstrated in section 4·3.

A detailed description of the sound pressure field in an intersection would be extremely difficult to find. However, in order to determine the resulting attenuation, it is only necessary to find the intensity of sound propagated into the receiver street. An approximate expression for this will now be found.

4·2 Attenuation Across an Intersection

When the plane waves described above encounter an intersection, their path will be as shown in figure 4·1.

Since the street width is assumed to be large compared to λ, diffraction effects will be ignored [21]. Figure 4·1 assumes that $\tan \xi > b/a$, which is generally true in a real situation. In this case, the average intensity at the edge of the intersection in region III of figure 4·1 will be

$$I_{III} = \frac{1}{b} \int_0^{b \cot \xi} \frac{|P_n|^2 \, dy}{4(r + y \tan \xi)}$$

$$= (1/4b) |P_n|^2 \cot \xi \ln(1 + b/r) \qquad (4·2)$$

where r is the distance from the source to the intersection and n is the average mode number.

Since the average intensity at the edge of the intersection in region I is

$$I_I = \tfrac{1}{2} |P_n|^2 / r \qquad (4·3),$$

the resulting attenuation will be

$$I_{III}/I_I = (r/2b) \cot \xi \ln(1 + b/r) \qquad (4·4).$$

$$\to \tfrac{1}{2} \cot \xi \quad \text{as} \quad b/r \to 0$$

When $\tan \xi < b/a$, we have

$$I_{III} = \frac{1}{b} \int_0^{a} \frac{|P_n|^2 \, dy}{4(r + y \tan \xi)}$$

$$= (1/4b) |P_n|^2 \cot \xi \ln(1 + (a/r) \tan \xi) \qquad (4·5)$$

and $$I_{III}/I_I = (r/2b) \cot \xi \ln(1 + (a/r) \tan \xi) \qquad (4·6).$$

$$\to a/2b \quad \text{as} \quad b/r \to 0$$

In region III, the angle of incidence, ξ', will be given by $\sin \xi' = \cos \xi$, i.e. if m is the mode number in this region and $\varepsilon'_m = m\pi/b$, then

$$\varepsilon'_m = k_n$$

$$\text{or} \quad k'_m = \varepsilon_n \qquad (4·7).$$

Of course, there will not, in general, be a mode of propagation in region III for which equation (4·7) will be satisfied exactly. However, where there is a large number of modes, some will have $\varepsilon'_m \sim k_n$, and in this case it will be assumed that the sound energy will be concentrated in the mode with ε'_m nearest to k_n, and that attenuation due to this "mismatch" will be negligible.

4·3 Determination of the Average Mode

In confirming the above theory, it was necessary that some means be devised of determining the average mode of propagation in a simple street. The method used was to measure the rate of change of phase of the wave with distance along the street.

The average value of the acoustic pressure across the street may be written

$$\bar{p} = \sum_n Q_n \sin (k_n r + \alpha_n - \omega t) \qquad (4\cdot9)$$

where $Q_n = \frac{|P_n|}{\sqrt{4k_n}}$ (the factor $r^{-\frac{1}{2}}$ being ignored for distances which are small compared with the source-receiver distance), and α_n is a phase shift between modes. Then, the phase $\Phi(r)$ may be defined as the value of $\omega t/2\pi$ when $\bar{p}(r) = 0$. Although this gives a multi-valued function, one value may be specified by the requirement that $\Phi(r)$ is continuous, and $\Phi(0) = 0$.

Thus,

$$\sum_n Q_n \sin (k_n r + \alpha_n - 2\pi\Phi) = 0 \qquad (4\cdot10)$$

leading to

$$\tan 2\pi\Phi = \frac{\sum Q_n \sin (k_n r + \alpha_n)}{\sum Q_n \cos (k_n r + \alpha_n)} \qquad (4\cdot11).$$

This gives

$$\frac{d}{dr}(2\pi\Phi) = \frac{\sum k_n Q_n^2 + \sum_{m\neq n} k_n Q_n Q_m \cos ((k_n - k_m) r + \alpha_n - \alpha_m)}{\sum Q_n^2 + \sum_{m\neq n} Q_n Q_m \cos ((k_n - k_m) r + \alpha_n - \alpha_m)} \qquad (4\cdot12).$$

For large r, the values of $\cos ((k_n - k_m) r + \alpha_n - \alpha_m)$ will be approximately randomly distributed between -1 and 1, so that the second terms of the numerator and denominator will generally be much smaller than the first. To first order in these quantities, we have

$$\frac{d}{dr}(2\pi\Phi) = \frac{\sum k_n Q_n^2}{\sum Q_n^2} + \frac{\sum_{m\neq n} k_n Q_n Q_m \cos ((k_n - k_m) r + \alpha_n - \alpha_m)}{\sum Q_n^2}$$

$$- \frac{\{\sum k_n Q_n^2\}\{\sum_{m\neq n} Q_n Q_m \cos ((k_n - k_m) r + \alpha_n - \alpha_m)\}}{\{\sum Q_n^2\}^2} \qquad (4\cdot13).$$

By averaging over a range of values of r, the sinusoidally varying terms may be removed, leaving

$$\frac{d}{dr}(2\pi\Phi) \sim \sum k_n Q_n^2 / \sum Q_n^2$$

$$= \frac{\{\sum |P_n|^2\}}{\{\sum |P_n|^2 / k_n\}}$$

$$= S \qquad (4\cdot14).$$

Thus, the "average" mode, as defined above, will be the mode having $1/k_n$ nearest to $1/\frac{d}{dr}(2\pi\Phi)$.

If we assume that for large r the phases of the sinusoidally varying terms in (4·13) are incoherent, then the mean-square variation of $\frac{d}{dr}(2\pi\Phi)$ from its average value S will, from (4·13), be

$$D = \frac{\sum_n \left(\sum_{m \neq n} Q_m^2 \right) Q_n^2 (S - k_n)^2}{\left(\sum Q_n^2 \right)^2} \qquad (4\cdot15).$$

If for some n it is not true that $\sum_{m \neq n} Q_m^2 \sim \sum_m Q_m^2$, then the energy of the sound field must be concentrated in that mode. If this is true for all n, then we may say

$$D \sim \frac{\sum Q_n^2 (S - k_n)^2}{\sum Q_n^2} \qquad (4\cdot16),$$

which is the mean-square deviation of k_n from its "average" value, S.

Figure 4·2 shows a typical graph of Φ *vs* r. In this case, as in all other cases tested, the mean-square variation in $\frac{d}{dr}(2\pi\Phi)$ was small compared to its mean value, indicating concentration of energy in a small range of values of k_n, as assumed above.

The most convenient measure of the modal properties of the sound field was found to be the "modal ratio" -- the ratio of the average mode number to the highest possible mode number.

5. PROPAGATION AT AN INTERSECTION – EXPERIMENT

5·1 Studies of Average Mode Numbers

Plywood was used to model street walls, as described in section 3·1. For this section of the work, all walls used were flat. It was decided to investigate the average mode numbers of the sound fields produced by various sources in an 80 cm-wide street. The source was placed in the middle of the street, emitting a pure tone, and a ¼" microphone moved along the street by the mechanism shown in figure 3·1. The output of the microphone was connected via a signal amplifier to an oscilloscope, which was triggered by the output of the signal generator that fed the source. In this way, the relative phase of the wave could be measured at various points down the street. The results gave graphs similar to figure 4·3, and a linear regression on these points gave a value of $\frac{d\Phi}{dr}$, from which the average mode number was determined as described in section 4·3. It was found that average values of $\frac{d\Phi}{dr}$ did not change significantly when measurements were made at different points across the street, so that averaging in this dimension was unnecessary.

The sources used were

(i) a Magnavox 17 cm-diameter speaker

(ii) a Phillips 5 cm-diameter tweeter

(iii) a PEAK 5 cm-diameter horn tweeter

and (iv) source (ii) at the end of two parallel boards, 80 cm long and 2 cm apart. In this case, the

end of the street was blocked by plywood boards, except for the 2 cm "source" region.

The results of these tests are shown in figure 5·1.

A number of trends are obvious from this figure. The intuitively reasonable idea that a smaller source will tend to produce higher-order modes at a given frequency is born out. However, the results from sources (ii) and (iii), which are of the same size, but with different geometries, indicate that more complex factors are also involved. It would appear that the pressure distribution in the source region must be known in some detail before confident predictions of the average mode number of the sound field may be made.

Another clear trend is that modal ratios for the same source are lower at higher frequencies. Measurements are also made using source (ii) in a 40 cm-wide street. This gave modal ratios of 0.56 at 4 kHz and 0.44 at 8 kHz, suggesting that modal ratios are lower in a wider street.

These considerations may be relevant to work in duct acoustics, as well as to propagation in streets (see Appendix 8).

5·2 Model Studies of Intersections

An intersection was modelled as shown in figure 5·2. (Figure 5·3 shows a photograph of the model.) Only

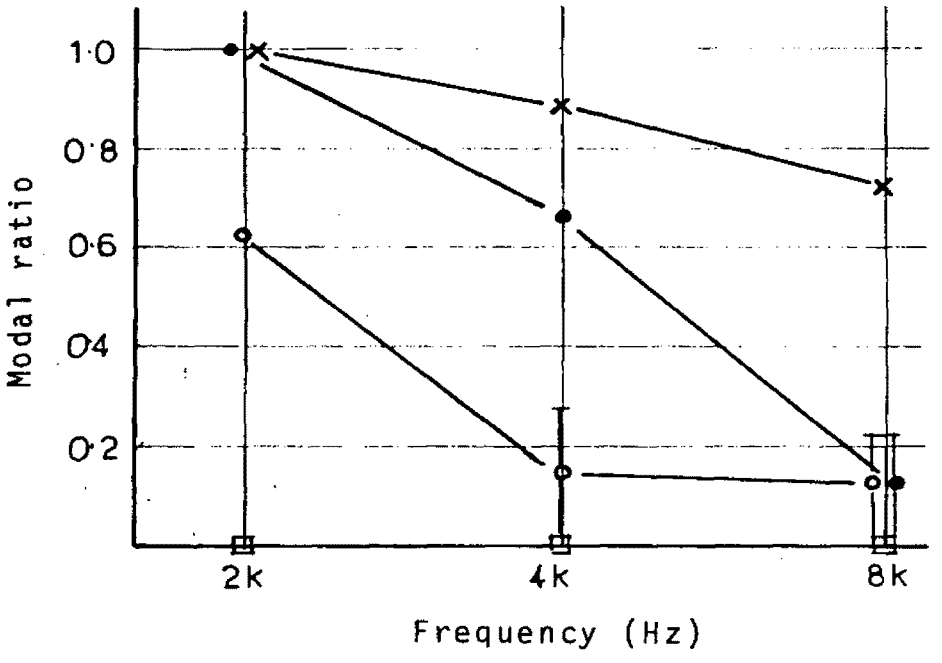

Figure 5·1: Modal ratios in an 80 cm street for various sources (see text). □ - source (i); o - source (ii); ● - source (iii); x - source (iv).

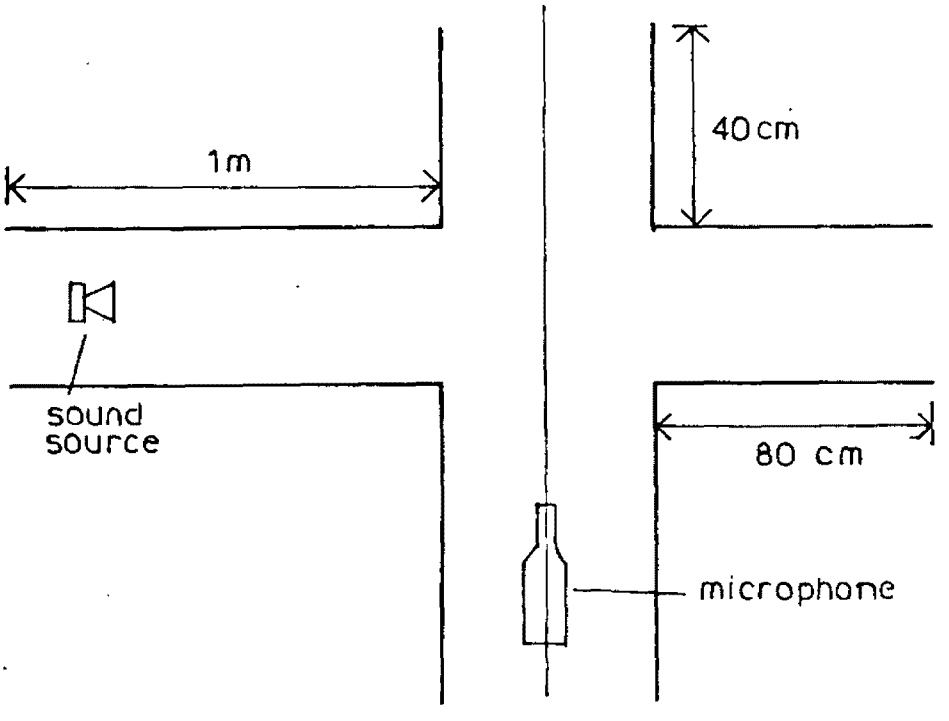

Figure 5·2: Modelling a four-way intersection.

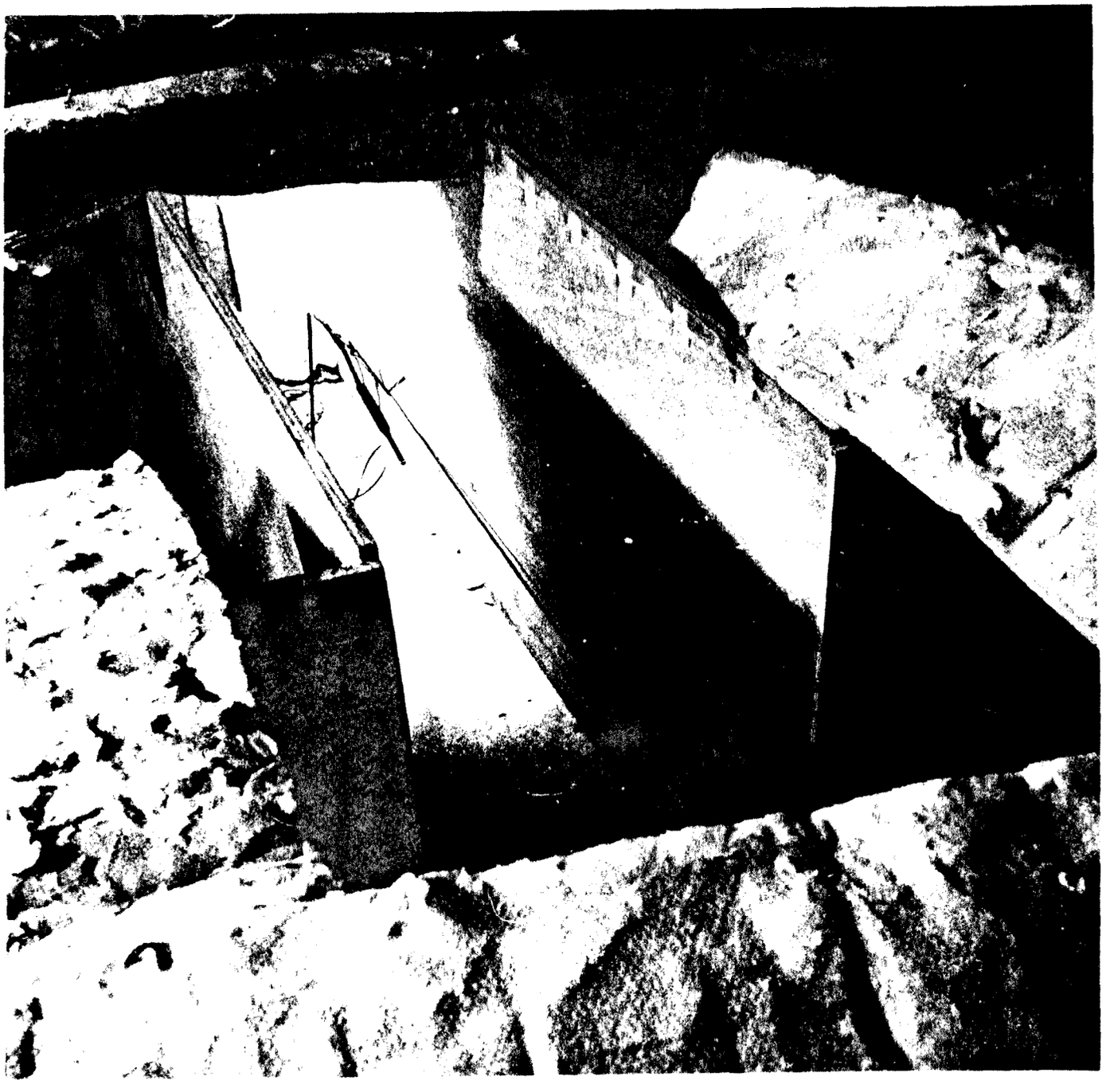

Figure 5·3: Experimental model of an intersection.

propagation around a corner was studied, since the total length of source and receiver streets required to study direct propagation was greater than the dimensions of the anechoic room. Source (ii) was used in a 40 cm-wide source street, and modal ratios in the receiver street measured at 4 kHz and 8 kHz.

White sound, filtered in octave-bands centred on these frequencies, was then played through the speaker. The intensity of this sound in the source street was determined by averaging 20 readings across the end of the street. In the receiver street, a series of intensity readings was taken along the street. It was assumed that all attenuation, other than cylindrical spreading, was linear with distance along the street. Thus, after correcting for cylindrical spreading, a linear regression gave the value of the intensity at the intersection. The results of this study are shown in table 5·1.

Modal ratios produced by source (ii) in 40 cm- and 80 cm-wide streets without intersections are given in table 5·1 as M_S. However, these were probably altered by the presence of the intersection. Thus, measured values of k'_m, rather than k_n, were used in predictions of attenuation.

Although the standard errors of measured attenuations are large, they show trends similar to the predicted values, and are consistent with them, with the exception of one point. Here, there are only four propagating modes in the

Frequency	M_S	Width of receiver street (cm)	Predicted M_R	Measured M_R	"Average" k_m'/k_o	Predicted attenuation (dB)	Measured attenuation (dB)
4 kHz	0.56	20	1.00	1.00	0.41	7.0	5.4 ± 1.2
		40	0.89	0.78	0.62	5.0	5.3 ± 1.2
		80	0.89	0.94	0.43	7.8	7.8 ± 0.7
8 kHz	0.44	20	0.89	0.78	0.64	4.3	4.7 ± 0.8
		40	0.94	0.94	0.43	7.1	7.4 ± 1.0
		80	0.89	0.95	0.29	9.7	9.5 ± 0.9

Table 5·1 Attenuations at model intersections. M_S represents the modal ratio in the source street, and M_R, that in the receiver street. The source street was 40 cm wide and the source was 83 cm from the intersection.

receiver street, and it is probable that the averaging processes described above begin to break down for this small number of modes. These attenuations are significantly smaller than those found by other workers [12,1], whose results indicate attenuations of 10 dB or more. However, this may be explained by an effect to be described in the following section.

5·3 Large-Scale Study

A group of large (80 m x 40 m) weatherboard wool-sheds was used to test the above theory on a larger scale (figure 5·4). The buildings were approximately 5 m high, and source and receiver streets were both 9.2 m wide.

Pre-recorded white sound was fed via an amplifier to the omnidirectional source. This was recorded through a sound level meter at various distances from the source in both the source and receiver streets and later analysed using an octave-band filter. Extraneous noise was always at least 10 dB below the signal. However, when an attempt was made to turn a second corner and record levels in a third street, this criterion was not satisfied. These results were therefore discarded.

A pure tone of 300 Hz was also played and recorded simultaneously on the two tracks of the recorder through two sound level meters. One SLM was kept stationary, while the

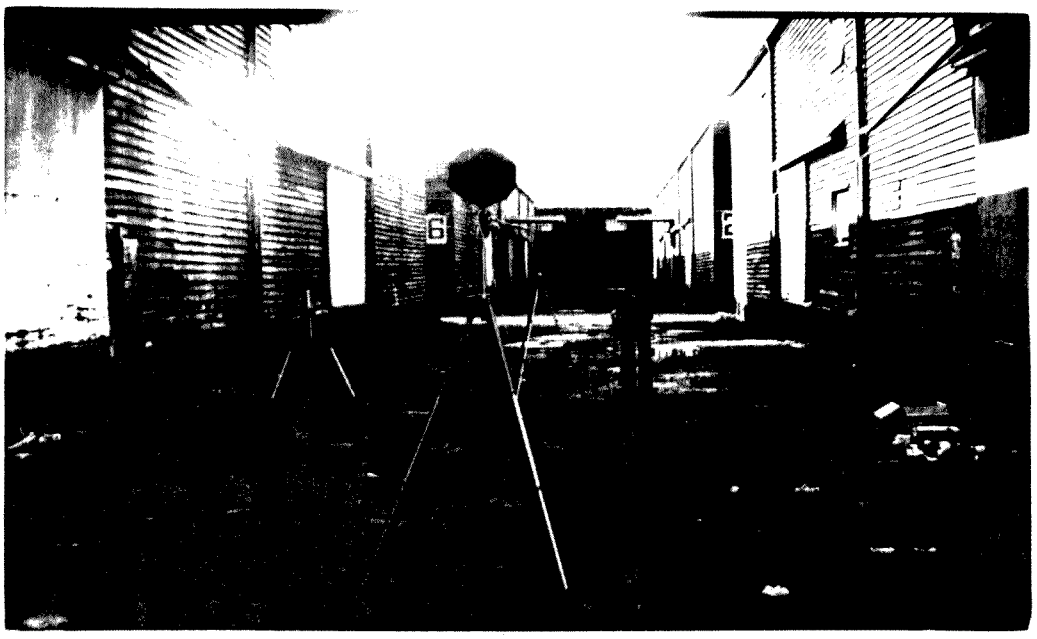

Figure 5·4: Site of large-scale tests, showing omnidirectional source and two sound level meters.

other was moved in 50 cm intervals. The recording on one track was later played into an oscilloscope, which was triggered by the recording on the other track. In this way, the average mode number in the source and receiver streets was determined at 300 Hz. (This average mode number was used in predicting attenuations for the 250 Hz octave-band.)

Results of intensity measurements at 250 Hz are shown in figure 5·5. The modal ratio in the source street was 0.67 (=10/15) and in the receiver street 0.87 (=13/15). The predicted value in the receiver street was 0.80 (=12/15). Since there were few important scattering interfaces on the walls, it was assumed that attenuation was due entirely to absorption, after correction for cylindrical spreading. This is born out by the linearity of the observed attenuation with distance (figure 5·5). Linear regressions in the source and receiver streets gave a drop of 6 ± 2 dB's across the intersection. The predicted value was 4.1 dB's using k_n, or 5.2 dB's using k_m'.

Figure 5·6 shows the results of intensity measurements at 4 kHz. The fast initial rate of attenuation in the receiver street may be explained as follows. Since high-frequency sound has, in general, a low modal ratio (see section 5·1), we may assume that the modal ratio in the source street was very low at 4 kHz, which, in turn, implies

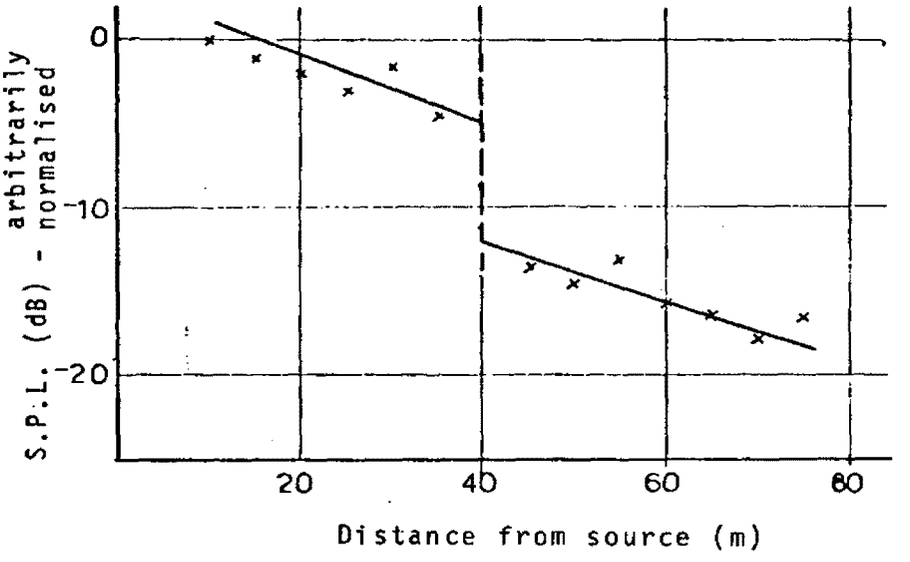

Figure 5·5: Attenuation at a large-scale intersection - 250 Hz octave-band.

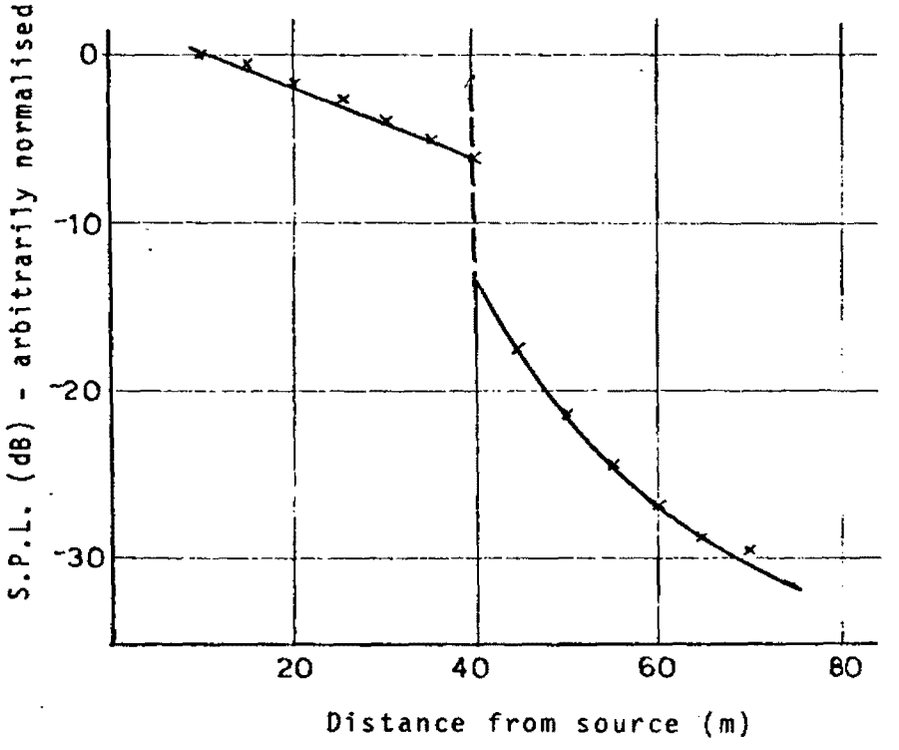

Figure 5·6: Attenuation at a large-scale intersection - - 4 kHz octave band.

a high modal ratio in the receiver street. Now, high-order modes are absorbed much more quickly than low-order modes [21], and thus the fast initial attenuation rate in the receiver street could represent the absorption of these high-order modes.

A quantitative prediction of this effect would be very difficult indeed, requiring detailed knowledge of the modal structure of the sound field in the source street. However, it may explain the large attenuations reported by other workers. (Weiner, Malme and Gogos [12] comment on the fact that the initial rate of attenuation in the receiver street is faster than that in the source street.) A similar effect occurs in lined ducts, where the modal structure of the propagating sound, though rarely taken into account, appears to have a large effect on the absorption properties of the lining (see Appendix 8).

6. PROPAGATION AMONG RANDOMLY-PLACED BUILDINGS — THEORY

6·1 Propagation as a "Random Walk"

While the discussion above appears to be adequate for sound propagation in a well-defined street on a relatively small scale (i.e. within approximately a block of the source) the situation is more complex in other cases. If the receiver is a number of blocks from the source, sound may reach it by many different routes. Also, streets are rarely arranged in a regular pattern, complicating the problem of predicting attenuations at intersections. More seriously, buildings often have significant spaces between them and may not be oriented parallel to the road. (They may, in fact, have curved facades, making any discussion of propagating modes impossibly complex.) In a suburban, rather than an urban, area the presence of large open spaces makes the above analysis totally inapplicable.

In situations such as this, where building surfaces are not closely enough aligned to form coherent modes, the use of geometrical acoustics suggests itself. The path of a "ray" of sound may be followed as it is reflected from

various surfaces, its intensity being taken to be inversely proportional to the distance travelled from the source, due to spreading in the vertical direction. The sound intensity would then be proportional to the sum of the intensities of all rays passing though a unit of area.

A computer program to trace rays in this way has been developed by Lyon, Holmes, Donovan and Kursmark [13]. However, the use of this program would demand relatively detailed knowledge of the positions of building facades, scattering surfaces, etc., in the area, which may not always be available. For propagation over a large distance (defined more precisely below), it would seem reasonable to assume that the orientation of building facades was random with respect to the direction of propagation of the ray, and that the distances travelled between reflections were randomly distributed about a "mean free path" (m.f.p.), l.

Thus, the ray will undergo a two-dimensional "random walk", and the probability per unit area, $g(r,t)$, that it will be at a distance r from the source at a time t is, from well-known theory [22],

$$g(r,t) = \frac{1}{\pi l c t}\, e^{-r^2/lct} \qquad (6\cdot1)$$

for $r \gg l$.

Thus, the total intensity due to a continuously-emitting source (for unit intensity of the wave at a distance l

from the source, in the absence of scattering) will be

$$I = \int_0^\infty \frac{2\pi l^2}{ct}\, g(r,t)\; d(ct)$$

$$= 2(l/r)^2 \qquad (6\cdot2).$$

That is, the rate of attenuation will be exactly as it would have been in the absence of any buildings.

6·2 Effects of Absorption

As in the situation discussed in Chapter 2, the presence of small amounts of absorption changes the above prediction substantially. If the proportion of the energy absorbed per m.f.p. is $1 - e^{-\gamma}$, then equation (6·2) becomes

$$I = \int_0^\infty \frac{2\pi l^2}{ct}\, g(r,t)\; e^{-\gamma ct/l}\; d(ct)$$

$$= (4\gamma^{\frac{1}{2}} l/r)\; K_1(2\gamma^{\frac{1}{2}} r/l) \qquad (6\cdot3)$$

(see Appendix 2), where K_1 is the first-order modified Bessel function of the second kind. The absorption parameter, γ, must take into account absorption resulting from a single reflection from a facade, absorption by grass, trees, etc., and air absorption resulting from propagation over a distance l.

Expression (6·3), multiplied by $(r/l)^2$, is shown in figure 6·1 and compared to the simple expression

$$(r/l)^2 I = e^{-\gamma r/l} \qquad (6\cdot4)$$

which ignores scattering. (This is the expression used by Blumenfeld and Weiss [11] and others.) It would appear that

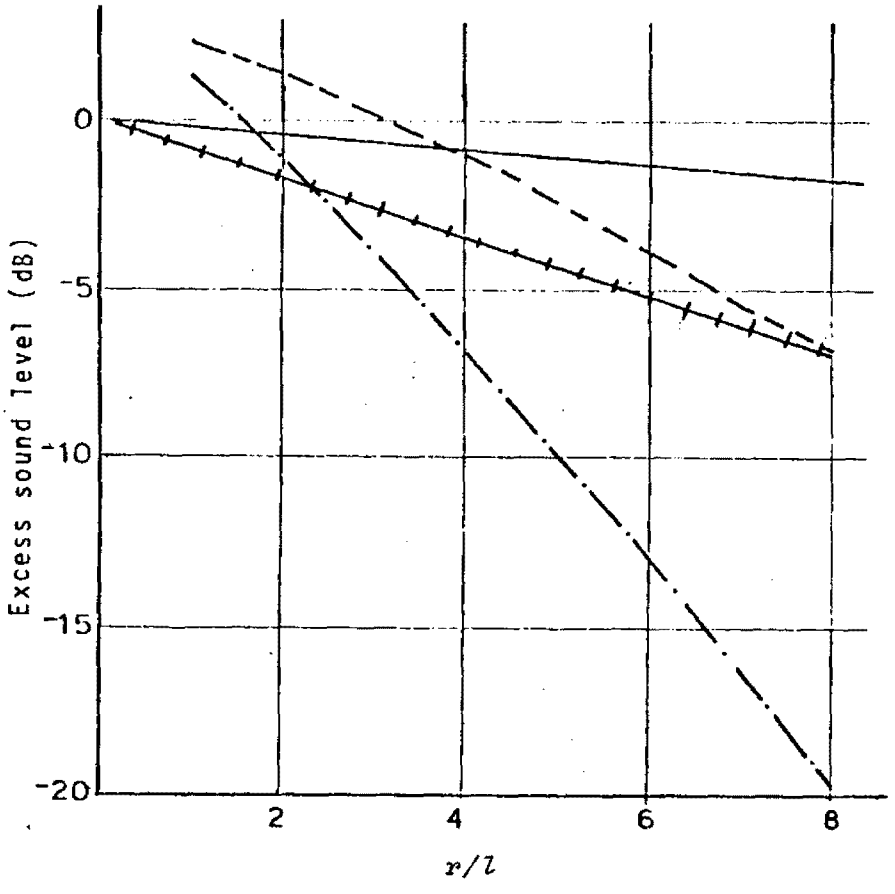

Figure 6·1: Predictions of excess attenuation above that due to spherical spreading. ——— - equation (6·4), $\gamma = 0.04$, —+—+— - equation (6·4), $\gamma = 0.16$; - - - - equation (6·3), $\gamma = 0.04$; —·— - equation (6·3), $\gamma = 0.16$.

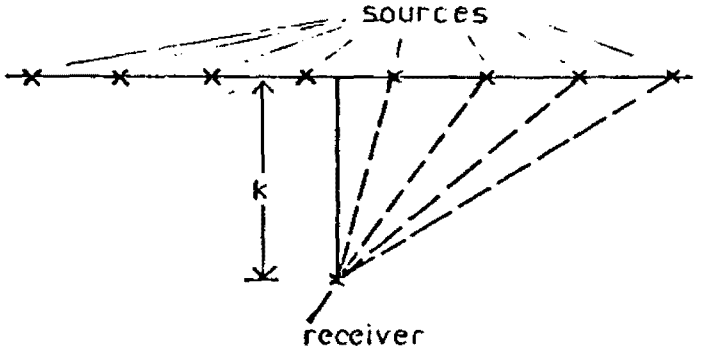

Figure 6·2: Radiation from a "line source".

in this situation, as well as in that discussed in Chapters 2 and 3, attenuation rates are controlled by the interaction of scattering and absorption processes.

6·3 Results for Distributed Sources

Since the most common noise source in urban and suburban areas is traffic noise which involves a number of spatially-distributed sources, equation (6·3) must be spatially integrated over this distribution. The most important application of this approach would appear to be the case of a line source, such as a major road, at some distance from the receiver (figure 6·2).

A number of workers [24,11] have shown that the movement of traffic along such a road may be regarded as a generalised shot noise process, where the gap between cars is taken to be a random variable with probability density ne^{-nx}. Here, x represents distance along the road and n is the average line density of the sources. If the perpendicular distance to the road is k, it can be shown [11] that in this case the mean intensity will be

$$\bar{I} = nI_r(R_r/l)^2 \int_{-\infty}^{\infty} I((k^2 + t^2)^{\frac{1}{2}})\, dt$$

$$= 2\pi I_r R_r^2 (n/k)\ e^{-2\gamma^{\frac{1}{2}}k/l} \qquad (6\cdot5)$$

(see Appendix 2), where I_r is the intensity of a source at the reference distance R_r (under free-field conditions). Where the sound field varies with time, the decibel equivalent of $\bar{I}$ will give L_{eq}.

It is clear that equation (6·3) will be valid only for values of r significantly larger than l, since otherwise small-scale environmental factors (eg. local shielding, elevation or depression of roads, geometry of individual facades, etc.) will have an overpowering effect on the sound level. Thus, equation (6·5) is valid only when k is significantly larger than l. The equation represents the "diffusion" of sound from a line source through houses, etc., over distances of the order of the length of a block, or more.

Appendix 9 gives the result of integrating equation (6·3) for sources evenly distributed over a plane, thus representing the effect of sources distributed over (for instance) an entire city, if the receiver is not placed near any important line source. Although this result may be compared in form to that of Shaw and Olsen [19], who attempt to represent the same situation by a simpler theory, no attempt was made to estimate l or γ over an area of this extent, and thus no quantitative evaluation can be given.

This analysis, of course, is valid only when the height of buildings is significantly greater than the wave length, in order to prevent diffraction over the top of the building. For a typical suburban house, say 3 to 4 m high, this condition excludes frequencies below about 150 Hz. However, since most sound-level measurements of interest are A-weighted, these frequencies are usually not significant. The analysis will also break down for large distances, of the order of 1 km or more due to atmospheric refraction caused by wind and temperature gradients.

7. PROPAGATION AMONG RANDOMLY-PLACED BUILDINGS — EXPERIMENT

7·1 Measurements in Copenhagen

Data was available for testing the theory set out in Chapter 6 from studies conducted in a number of locations. One such study was a traffic noise survey conducted in Copenhagen by Kragh and Astrup [30]. Noise levels were recorded at several sites (figure 7·1) over half-hourly intervals throughout the day and average traffic counts on major roads are given for each period.

Only two sites, sites 21 and 23, gave results which were appropriate for analysis using the above theory, the other sites being situated on major roads or near industrial works, or other noise sources. It was assumed that all noise at the chosen sites was due to traffic from the two nearest major roads.

In order to estimate l, an area was marked off on a large-scale map and cross-sections of all buildings within the area were measured in two pre-determined perpendicular directions. If the average value of these cross-sections is c, then l may be estimated by

$$l = A/Nc \qquad (7\cdot1)$$

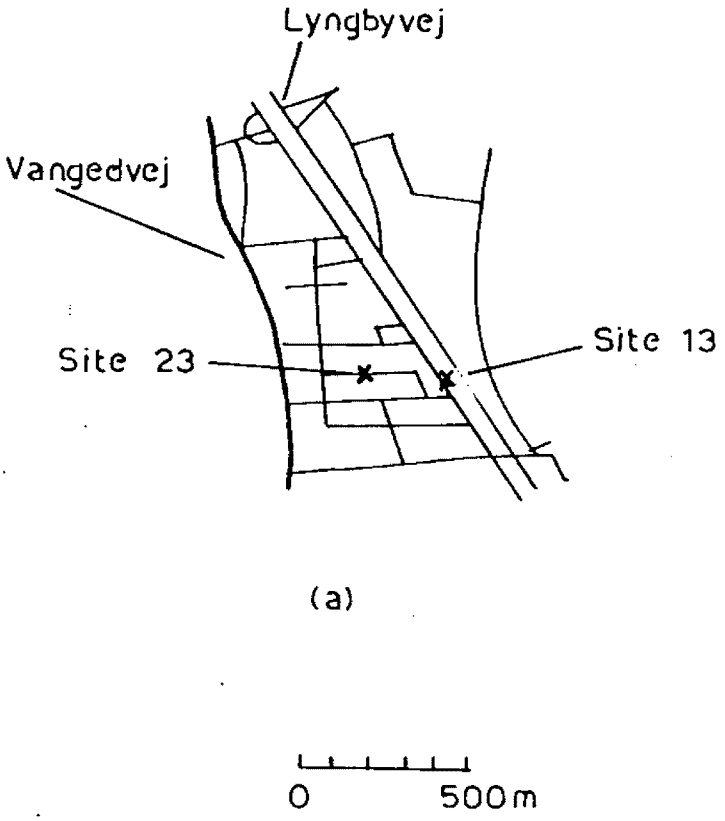

Figure 7·1: Measurement sites in Copenhagen.

where A is the area marked off and N, the number of buildings it contains. This technique gave a value for l of 62 m at site 21 and 68 m at site 23.

Emission levels of individual cars at R_r = 15.2 m were taken to be those used in the NCHRP 3 - 7/3 Revised Design Guide for Highway Noise Prediction and Control, as given in reference [29]. This may be approximated by

$$L_{emiss} = 12 + 30 \log v \qquad (7\cdot2)$$

where v is the speed of the car in km/h. A number of sources [2,19,25] are in substantial agreement with these figures.

For heavy vehicles, the Revised Desing Guide requires a breakdown into "heavy" and "medium" trucks. As this was not available, the figure given by Alfredson [25]of 79 dB(A) for heavy vehicles on Melbourne freeways was assumed to be the average over all heavy vehicles. As in most predictive methods, this value was assumed to apply independently of vehicle speed [29]. The value of n was taken to be F/v, where F is the vehicle flow rate and v, the estimated average speed.

In calculating γ, it was necessary to know the frequency distribution of the noise from an individual vehicle. Measurements of this distribution made in Ottowa [19] were assumed to apply. Reflecting surfaces were taken to be 90% brick or concrete and 10% glass, since the areas around the sites are residential. (In studies in industrial areas,

surfaces were taken to be composed only of brick or concrete.) Absorption co-efficients for these materials at various frequencies are given in reference [26]. Values of air absorption at various frequencies were taken from reference [19]. From photographs of the areas near the sites, it appeared that each wall was surrounded by an average of 2.5 m of garden and shrubbery, giving 5 m of such ground covering per m.f.p. The absorption resulting from propagation through shrubbery or thick grass is given by Beranek [6] as (0.18 *log* f - 0.31) dB's per meter, where f is the frequency.

In order to calculate γ, the noise levels at each frequency were first corrected for A-weighting and then added to give a "base" value. The original levels were then corrected for absorption over one m.f.p., corrected for A-weighting and added again. The new value was compared to the "base" value to give γ. This process gave $\gamma^{\frac{1}{2}} = 0.46$ for cars and $\gamma^{\frac{1}{2}} = 0.58$ for heavy vehicles.

The sound intensities resulting from cars and from heavy vehicles in the two major roads nearest to each site were calculated and added to give a total sound level. The results are shown in figures 7·2 and 7·3 and given in detail in Appendix 10. It should be remembered that the traffic counts used in these calculations are averages and may not be exactly the same as those on the day on which

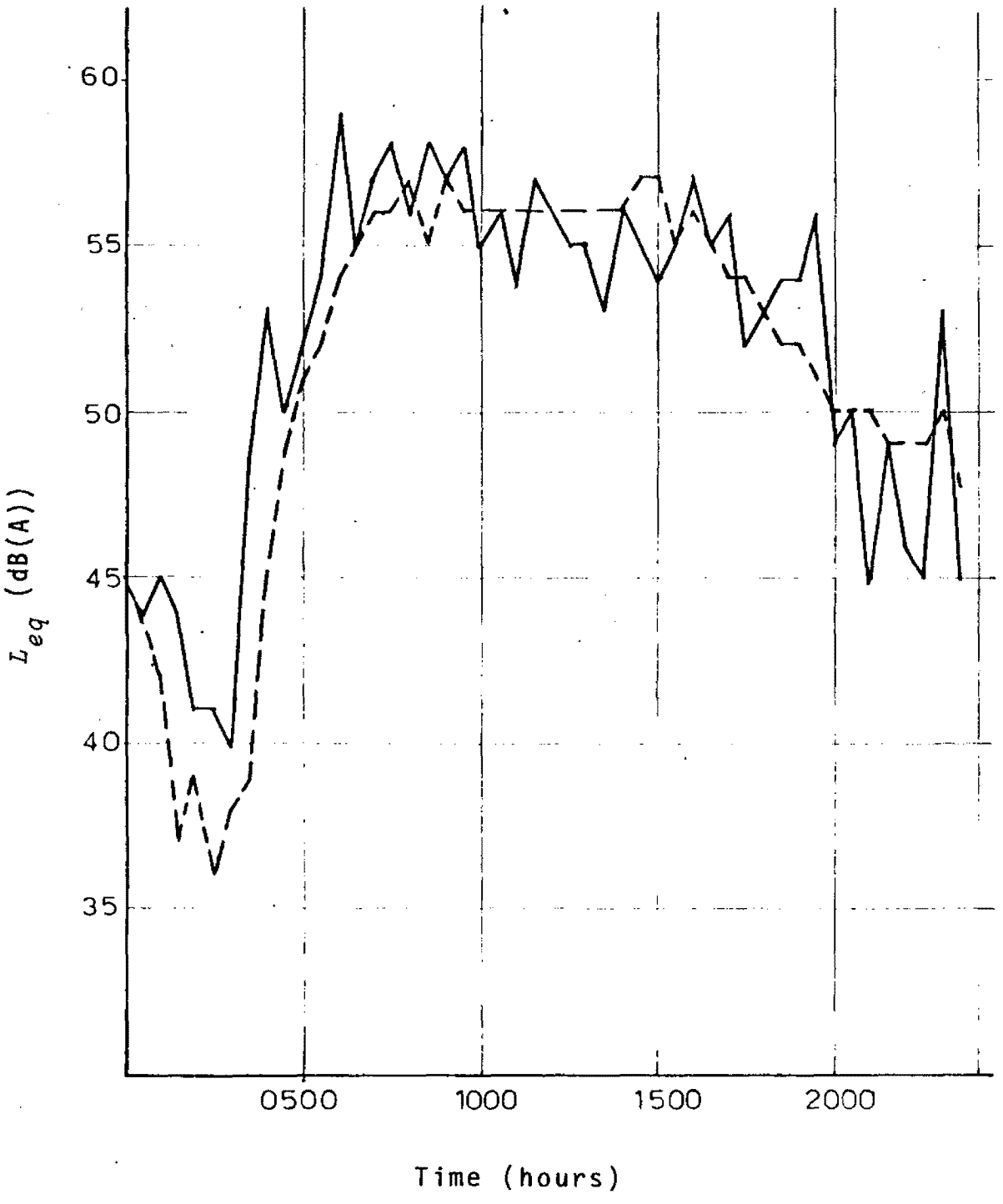

Figure 7·2: L_{eq} levels at site 21, Copenhagen.
- - - - predicted; ——— measured.

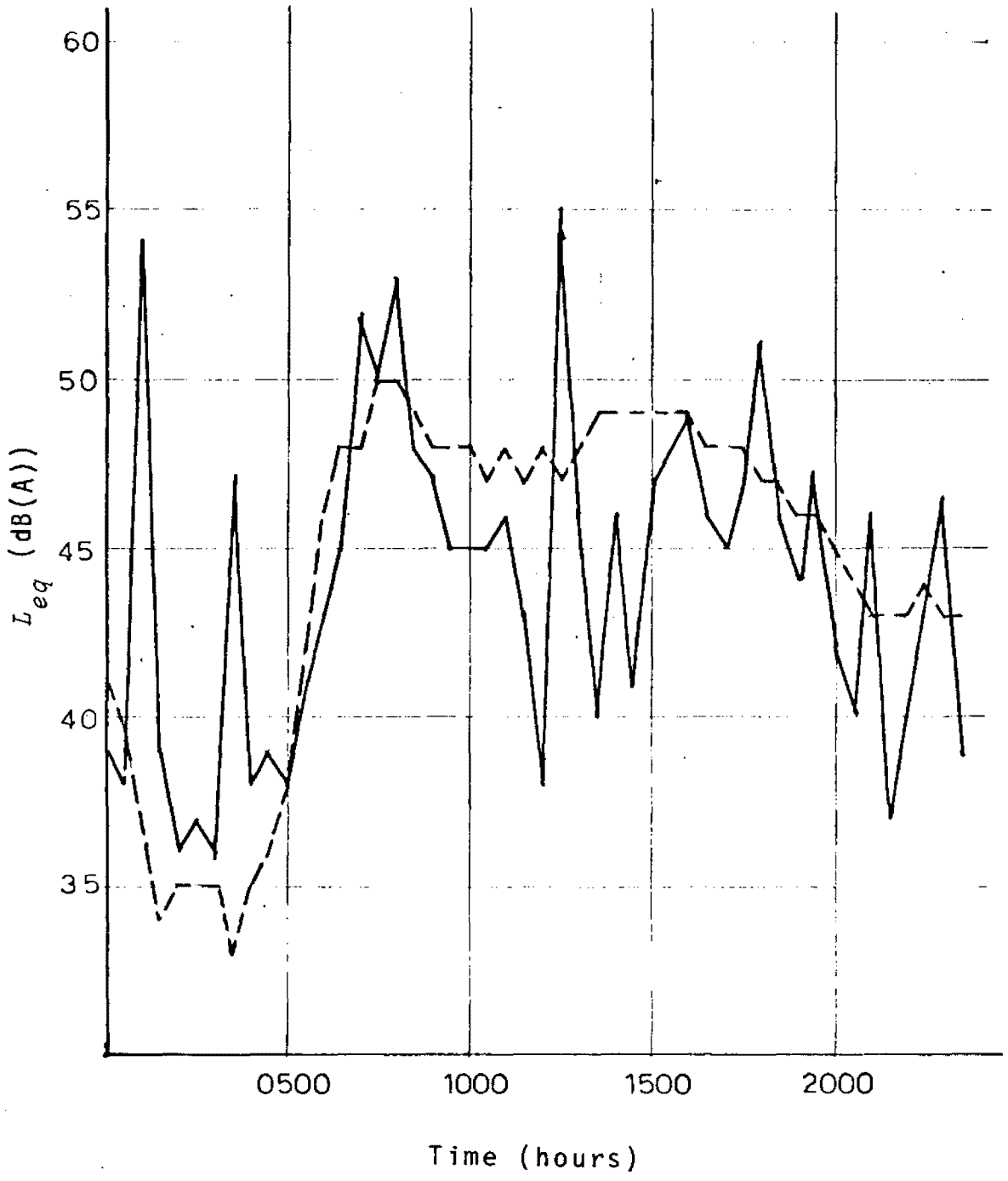

Figure 7·3: L_{eq} levels at site 23, Copenhagen.
- - - - predicted; ——— measured.

the sound level measurements were taken. Kragh and Astrup estimate that uncertainties of this kind could give rise to errors of ±5 dB(A) in L_{eq}.

7·2 Measurements in Sydney

Data from a noise survey conducted by the Sydney City Council in Newtown, Sydney, was also used in testing the theory given in Chapter 6. Traffic counts and noise levels were recorded at several sites (figure 7·4) at various times in the week (see Appendix 11). Only sites 4 and 9 were suitable for the application of the above theory, but results from site 3, with $k/l = 1.4$, were also analysed to gain some idea of the effect of a small value of k/l. It was assumed that all noise at these sites was due to traffic on King Street and Missenden Road, as measured at sites 2 and 1 respectively. (Traffic counts at sites 3, 4 and 9 were always lower than 40 veh./h.)

Parameters were determined as described in the previous section and the values found were l = 42 m, $\gamma^{\frac{1}{2}}$ = 0.33 for cars and $\gamma^{\frac{1}{2}}$ = 0.45 for heavy vehicles. (There was no shrubbery in the area.) Details of predicted and measured sound levels are given in Appendix 11. These values, for sites 4 and 9, are shown in figure 7·5, while figure 7·6 shows these results for site 3. Once again, traffic counts were not taken on the same day as sound level readings. Also,

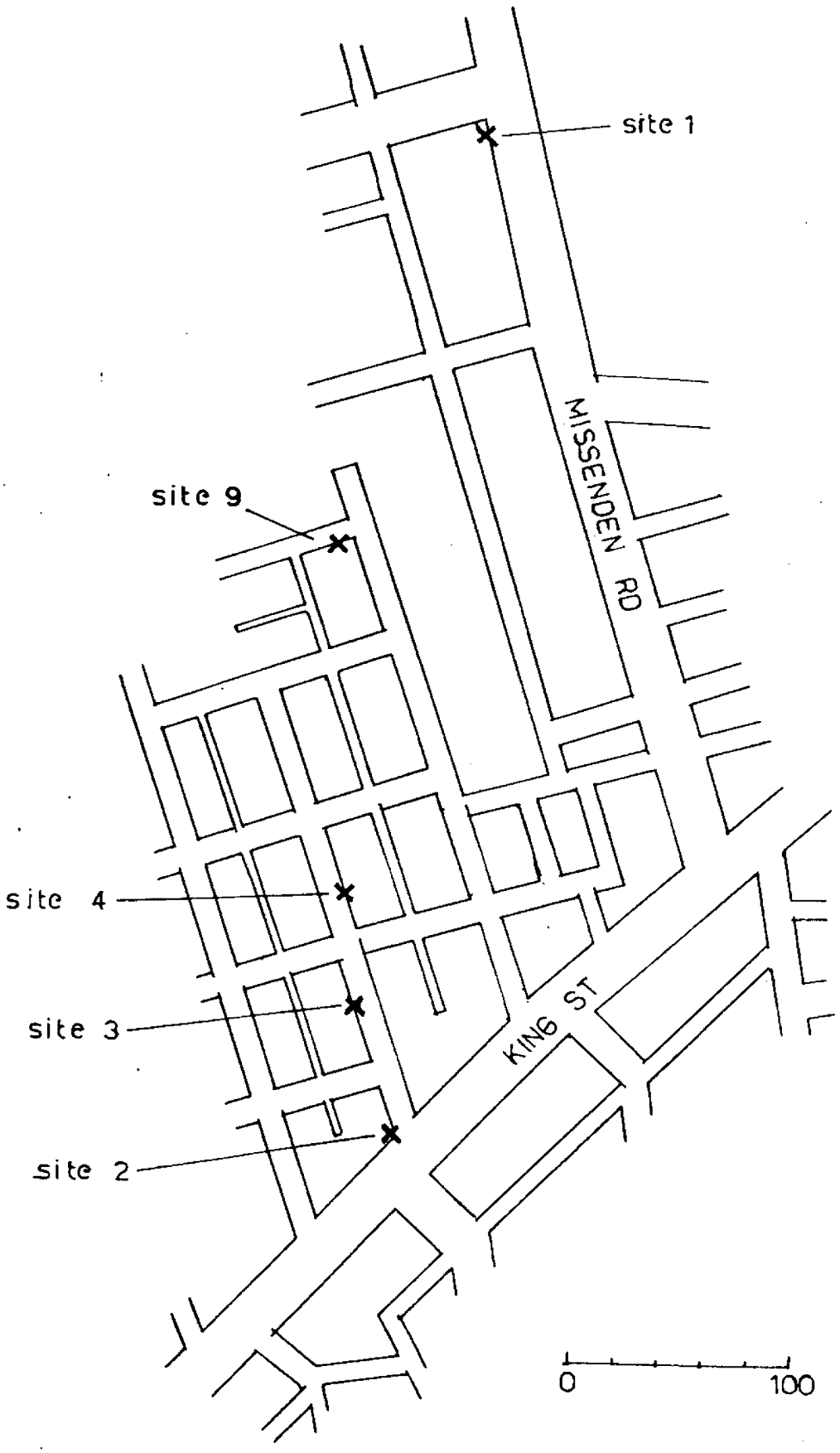

Figure 7·4: Measurement sites in Sydney.

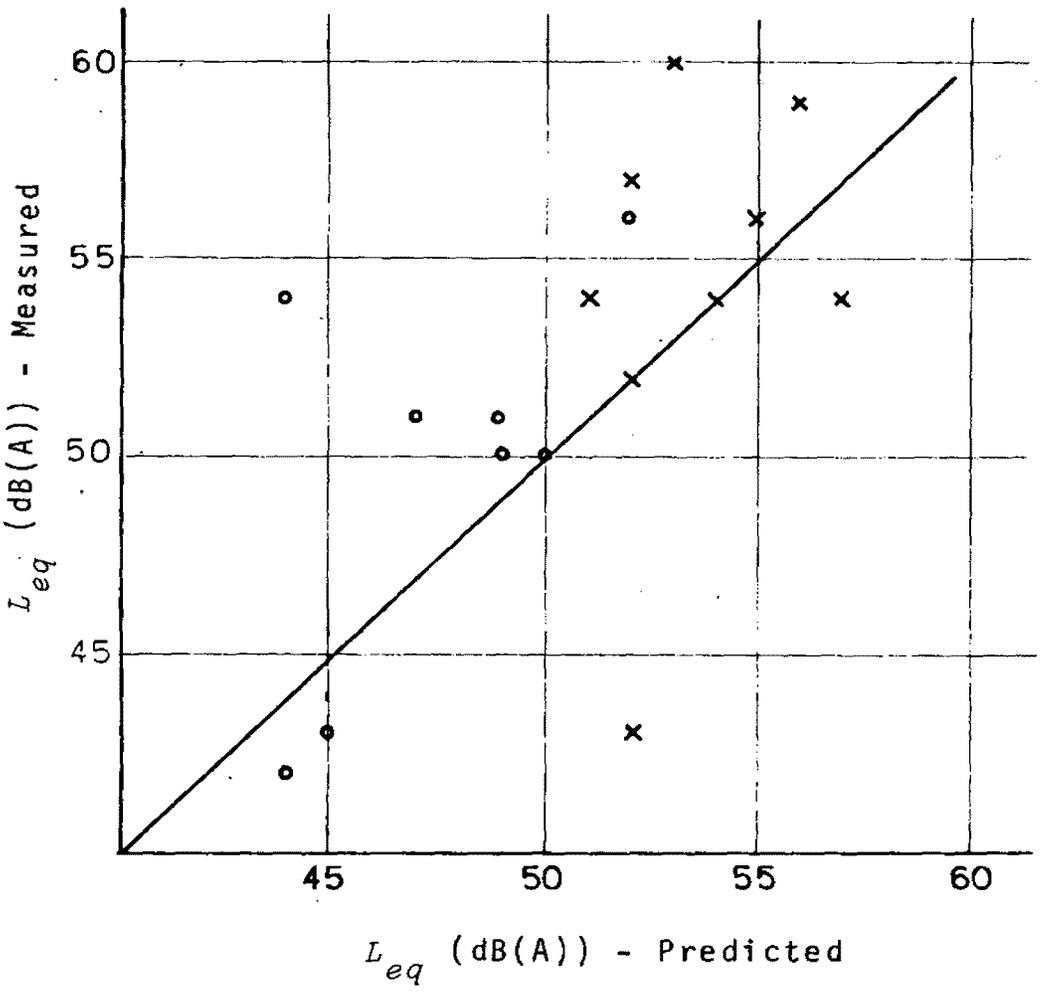

Figure 7·5: Accuracy of Leq predictions in Sydney.
- site 4; - site 9.

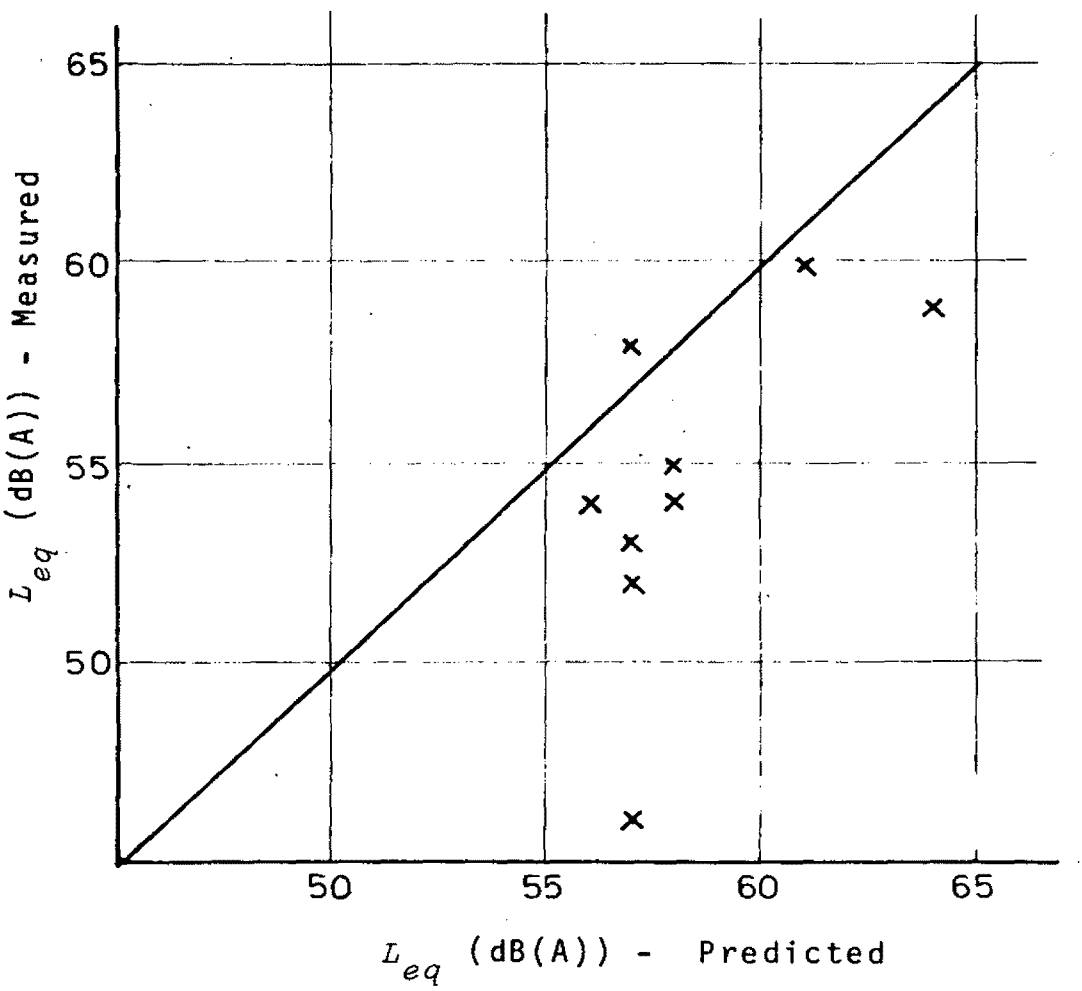

Figure 7·6: Accuracy of L_{eq} predictions in Sydney - site 3.

traffic on Missenden Road at site 1 is not necessarily the same as traffic on this road at points nearer to the measurement sites.

An attempt was made to compare these predictions with predictions made on the basis of methods developed by other workers. The method which appeared most applicable to this situation (and which gave most accurate results) was that of Alfredson [25], developed for estimation of noise levels arising from freeways in Melbourne. In his calculations, he allows for an "excess attenuation" over spherical spreading of 4 dB(A) per 100 m – i.e. his distance correction has the form of equation 6·4, with absorption set at 60% per 100 m. (The values of γ above are equivalent to approximately 25-30% per 100 m.)

Alfredson's predictive equation is

$$L_{50} = 5.2 + 16.4 \log F - 14.3 \log k + 17.4 \log v + 0.16p \quad (7\cdot3),$$

where p is the percentage of heavy vehicles. This value was increased by an amount equal to the measured difference between L_{eq} and L_{50}. The resulting predictions are given in Appendix 11 and graphed in figure 7·7. It should be noted that the values of F, k and v used here are well beyond the constraints on these parameters given by Alfredson and these results do not invalidate his method. However, these values give the closest fit to the observed data of all predictive methods tested. (The others are given in references [27-29].)

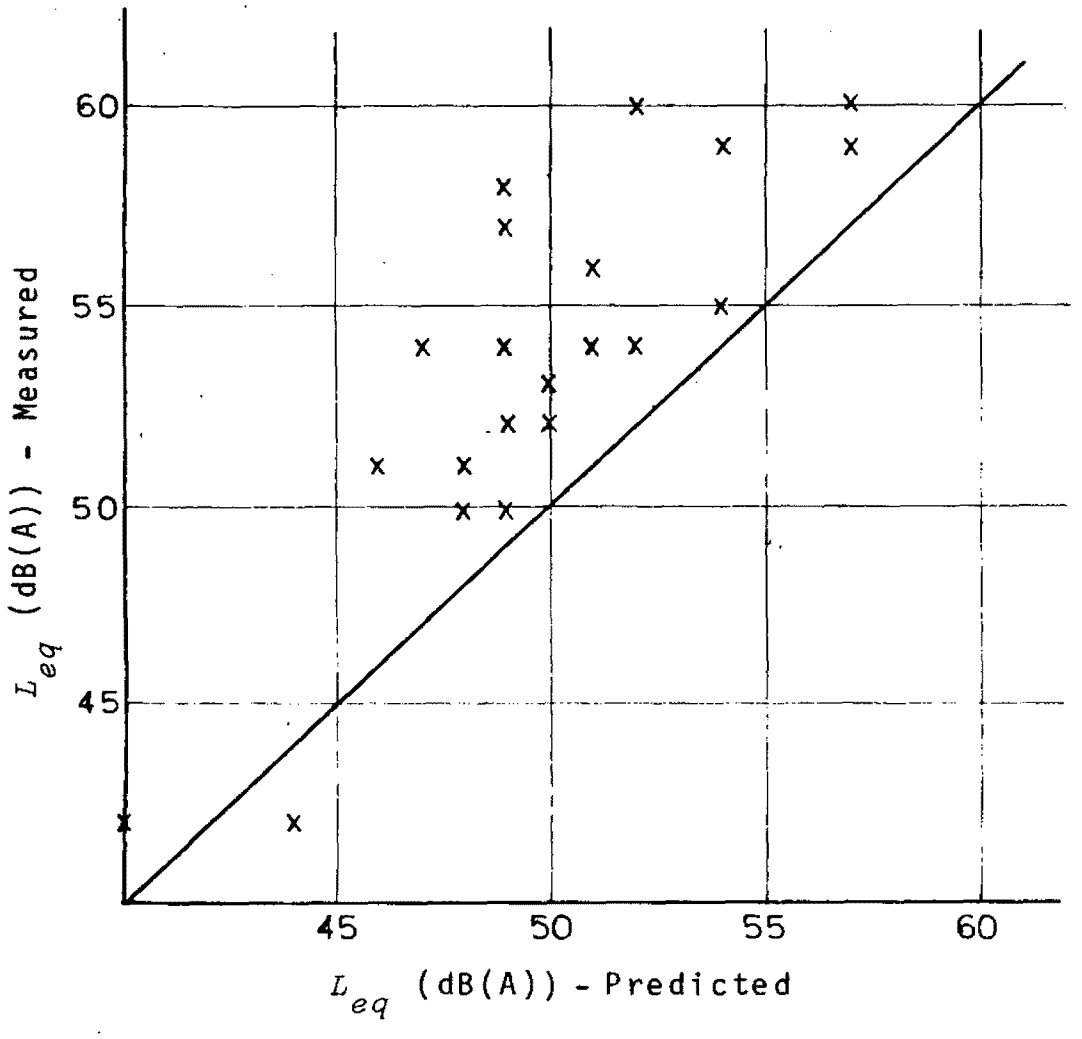

Figure 7·7: Accuracy of L_{eq} predictions from equation (7·3) in Sydney - sites 3,4 and 9.

7·3 Measurements in Brisbane

Data from a noise survey in Brisbane [31] was also analysed in the above way. The survey was intended to assess the impact of a new freeway on noise in the area but the data used here are the results of traffic counts on major roads and sound level readings at various sites before the freeway was opened (figure 7·8). Measurements were made during the morning peak hour, 0730 – 0830.

Since average traffic speeds are not given, an average speed of 50 km/h was assumed in all cases. An average of 5 m of shrubbery per m.f.p. was also assumed. Since L_{eq} is not given, the equation

$$L_{eq} = L_{50} + 0.07(L_{10} - L_{50})^2 \qquad (7·4)$$

was used [2]. Once again, traffic counts are average figures which may show daily variation.

Making the above assumptions, the values of the necessary parameters were found to be l = 56 m, $\gamma^{\frac{1}{2}}$ = 0.44 for cars and $\gamma^{\frac{1}{2}}$ = 0.56 for heavy vehicles. Details of results at each site are given in Appendix 11, and these results are shown in figure 7·9, with predictions based on Alfredson's equation in figure 7·10.

At all sites, there was at least one major road at a distance of less than $2l$, so that local factors probably had a large influence on sound levels, explaining the inaccuracy of both sets of predictions. In particular, almost every site was shielded from the nearest major road by a row of houses.

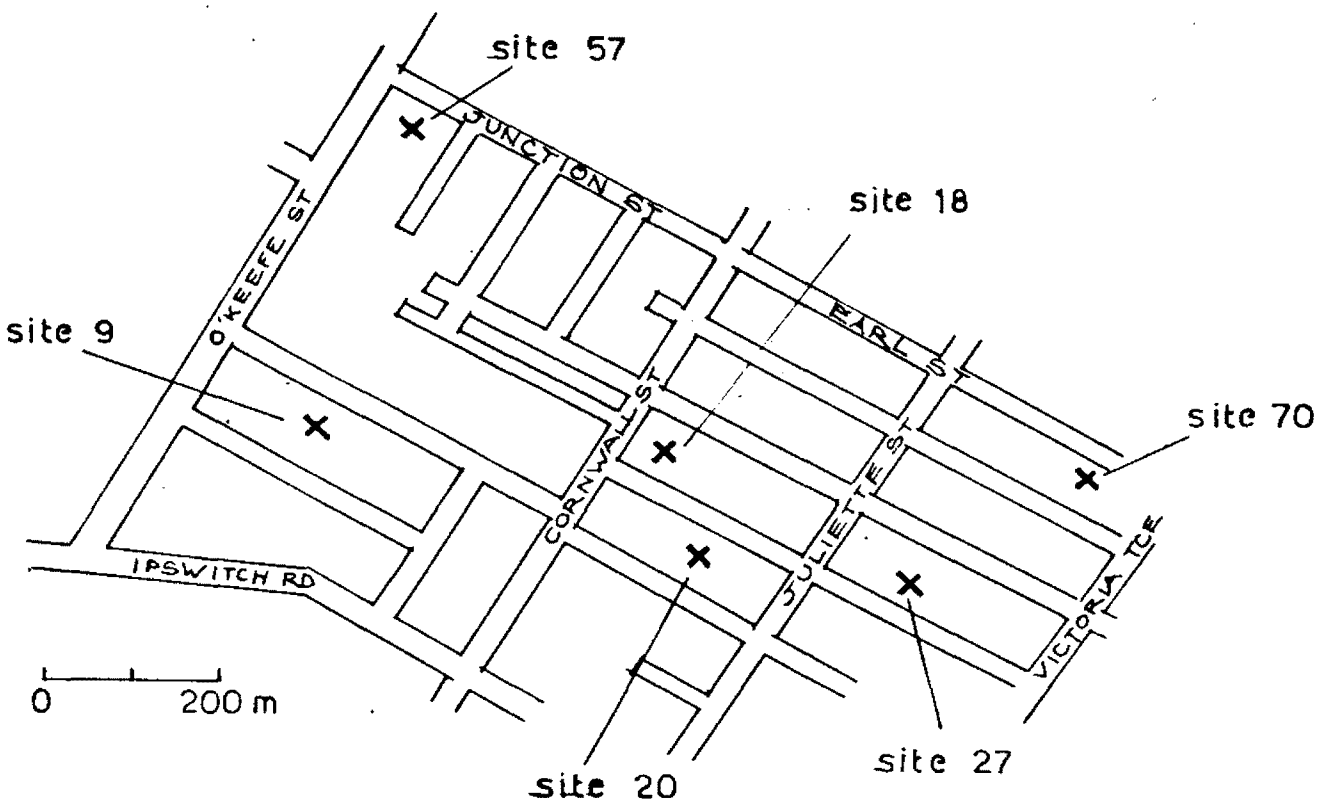

Figure 7·8: Measurements sites in Brisbane.

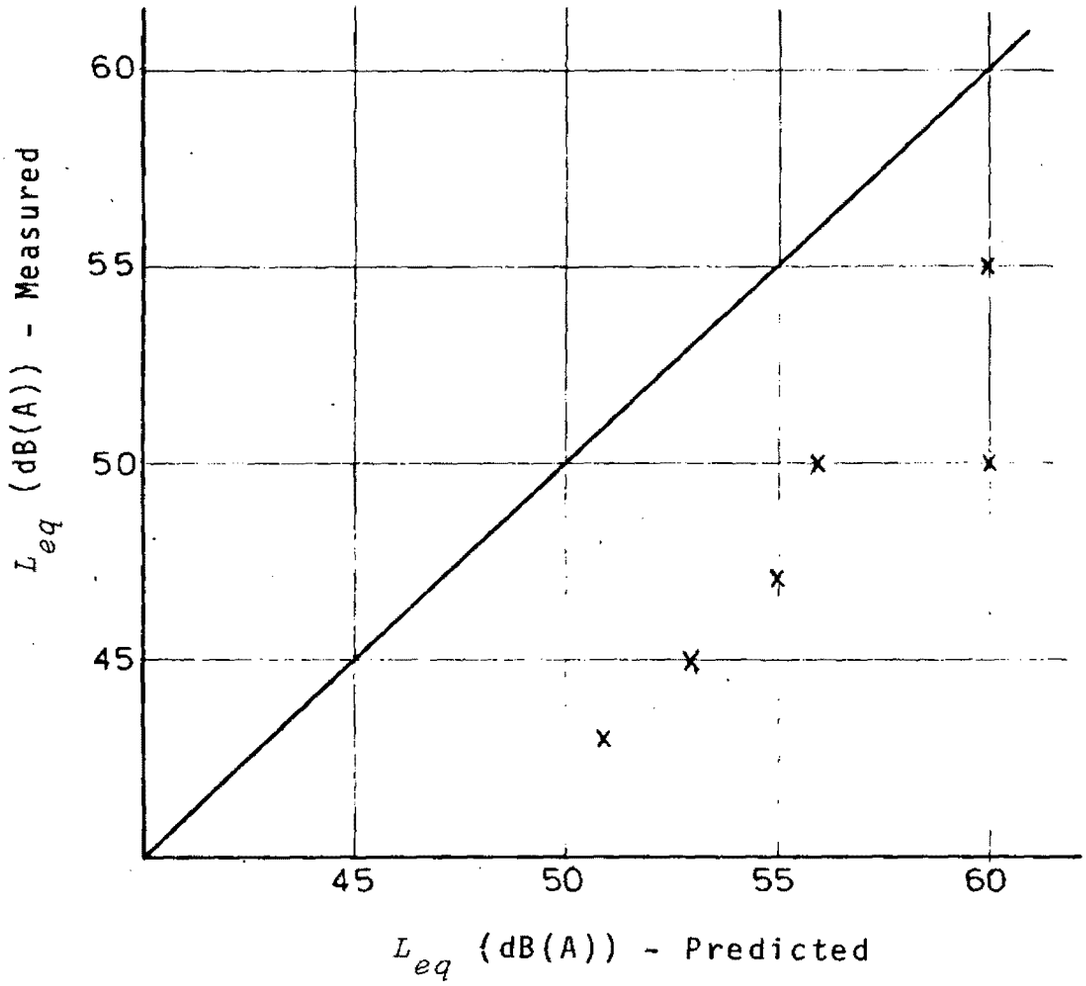

Figure 7·9: Accuracy of L_{eq} predictions in Brisbane.

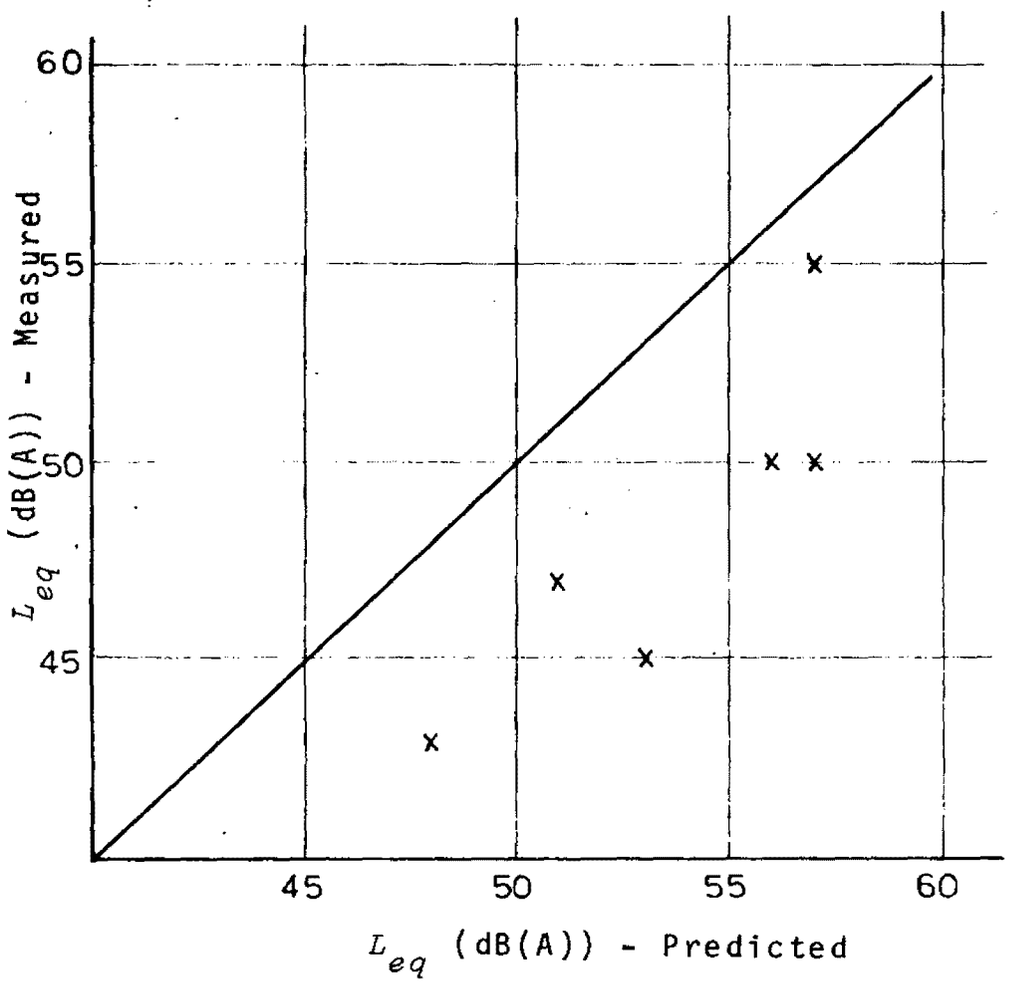

Figure 7·10: Accuracy of predictions from equation (7·3) in Brisbane.

7·4 General Remarks

Differences between predicted and measured sound levels from all three studies are summarised in table 7·1.

Measurements	Mean Δ	Standard Deviation Δ	Mean ΔA	Standard Deviation ΔA
Copenhagen	-0.2	4.0	-	-
Sydney (sites 4 & 9)	-1.4	4.9	-3.7	2.6
Sydney (site 3)	3.8	3.4	-4.0	3.0
Brisbane	9.5	1.8	6.3	2.2

Table 7·1: Accuracy of sound level predictions. Δ is the predicted value of L_{eq} minus its measured value, in dB(A). ΔA is the equivalent difference using equation (7·3).

Predictions on the basis of equation (7·3) were not made in the case of the Copenhagen results, since here the values of k were far beyond the limits set by Alfredson on the validity of his equation.

The theory of Chapter 6 appears to give good estimates of sound levels at sites where the distance to the nearest major road is greater than about $2l$.

It is interesting to note that equation (6·5), becuase it contains $\gamma^{\frac{1}{2}}$ and not γ in the exponent, implies that relatively small changes in γ can produce large changes in sound level. As an example of this effect, absorption co-efficients for ivy-covered walls were taken from reference [32] and used instead of those for plain brick walls in the calculation of γ for cars, assuming an m.f.p. of approximately 65 m. The results indicated that the ivy-covered walls would give an extra attenuation of approximately 1.5 dB(A) per 100 m away from the line source -- an attenuation which in some cases would not be insignificant. Attenuation due to large amounts of vegetation would, of course, be much greater. This result is contrary to the predictions of other workers, who, considering absorption alone, predict that changes in absorption co-efficients of street walls will have an insignificant effect on sound levels [15].

It is also worthy of note that the different frequency distributions of the sound produced by cars and by trucks gives rise to markedly different attenuation rates. For an m.f.p. of approximately 65 m, the figures given above indicate that noise from heavy vehicles is attenuated at approximately 1.5 dB(A) per 100 m faster than that from cars. This means that although heavy vehicle noise is known to be important in roadside noise measurements [2,29], this may not be the case for measurements at some distance from the road.

8. CONCLUSIONS

A number of firm general conclusions may be derived from the work described above:

(i) In order to adequately explain the structure of the urban sound field, account must be taken of the effect of scattering processes. It was seen both in the case of a well-defined street and in that of "random" buildings that theories which take only absorption into account fail to predict attenuation rates in these situations to an acceptable degree of accuracy, unless unrealistic and non-predictable values of absorption are used. Predictions based on such theories must therefore be regarded as extremely tentative, at best.

(ii) Scattering processes, considered alone, give rise to an even less realistic picture of the urban sound field than absorption processes. It is the interaction of these two processes which determines attenuation rates and thereby determines the distribution of sound in an urban area. It follows from this that changes to one of these parameters may have effects which are impossible to predict without knowledge of the other parameters of the system. An analogy may be made with

an ecological system, where small changes to one component may produce dramatic changes in the working of the system as a whole.

Although adequate experimental work has not been performed in this area, it would appear likely that similar comments would apply in the case of sound propagation in ducts where scattering is important (such as corridors).

(iii) In considering propagation in a well-defined street, account must be taken of the mode of propagation of the sound, which is determined largely by the street width and the nature of the source. This is particularly true in the case of propagation at an intersection where effects due to modal propagation may be quite pronounced.

A number of other more specific conclusions may also be drawn from this work. These must be regarded as tentative, since experimental confirmation has, of necessity, been obtained in only a limited number of model and full-scale studies. More research is required in order to ascertain more exactly the range of validity of these conclusions.

(iv) Equation (2·4), with $f(r,t)$ calculated and integrated numerically, leads to a good approximation to the rate of attenuation of sound in a well-defined street with one-dimensional scattering if γ, R and d are known to sufficient accuracy. If R is small, γ even smaller,

and $r/d \leq 1/R$, equations (2·7) and (2·8) give a good approximation to this rate for the case of two-dimensional scattering.

(v) The reflection co-efficient of an interface in a street is approximately that given by equation (2·15).

(vi) Techniques described in sections 4·3 and 5·1 enable the average mode of a sound field in a street (model or real) to be determined.

(vii) Equation (4·4) or (4·6), together with equation (4·7), gives a good approximation to the attenuation occuring when moving around a corner at an intersection.

(viii) Equation (6·5) gives the sound level arising from a line source at some distance from it, in the presence of "random" buildings, in most cases to within ± 5 dB(A).

In continuing this work, the next step would appear to be the building of a large-scale model of an environment consisting of "random" buildings, in order to test more fully the predictions of equation (6·5) with regard to changes in ℓ and γ. Unfortunately, facilities for such modelling are not available at this University.

REFERENCES

1. R.H. LYON 1974 Journal of the Acoustical Society of America 55, 493-503. Role of multiple reflection and reverberation in urban noise propagation.

2. A. ALEXANDRE, J.-Ph. BARDE, C. LAMURE and F.J. LANGDON 1975 Road Traffic Noise. London: Applied Science Publishers.

3. H.G. JONASSON 1972 Journal of Sound and Vibration 25, 577-585. Diffraction by wedges of finite acoustical impedance with applications to depressed roads.

4. W.E. SCHOLES, A.C. SALVIDGE and J.W. SARGENT 1971 Journal of Sound and Vibration 16, 627-642. Field performance of a noise barrier.

5. H.G. JONASSON 1972 Journal of Sound and Vibration 22, 113-126. Sound reduction by barriers on the ground.

6. L.L. BERANEK 1971 Noise and Vibration Control. New York: McGraw-Hill.

7. F.M. WIENER 1958 Noise Control 4, 224 ff. Sound propagation outdoors.

8. E.J. RATHE 1969 Journal of Sound and Vibration 10, 472-479. Note on two common problems of sound propagation.

9. U. INGARD 1969 Journal of the Acoustical Society of America 25, 405-411. A review of the influence of meteorological conditions on sound propagation.

10. U. INGARD, 1969 Journal of the Acoustical Society of America 45, 1038-1039. On sound-transmission anomalies in the atmosphere.

11. D.E. BLUMENFELD and G.H. WEISS 1975 Transport Research 9, 103-106. Attenuation effects in the propagation of traffic noise.

12. F.M. WIENER, C.I. MALME and C.M. GOGOS 1965 Journal of the Acoustical Society of America 37, 738-747. Sound propagation in urban areas.

13. R.H. LYON, D.G. HOLMES, P.R. DONOVAN and R. KURSMARK 1974 Final Report, Department of Transport Contract DOT/TSC 93, M.I.T. Sound propagation in city streets.

14. K. LEE, H.G. DAVIES and R.H. LYON 1974. Acoustics and Vibration Labaratory, M.I.T., Report. Prediction of propagation in a network of sound channels, with application to noise transmission in city streets.

15. K.P. LEE and H.G. DAVIES 1975 Journal of the Acoustical Society of America 57, 1477-1480. Nomogram for estimating noise propagation in urban areas.

16. J.V. MESTRE SANCHO 1975 Master of Science Thesis, Southampton University. Design and development of a scale model testing facility for architectural acoustics and outdoor urban noise problems.

17. W.A. KINNEY, A.D. PIERCE and E.J. RICKLEY 1974 Journal of the Acoustical Society of America 56, 332-337. Helicopter noise experiments in an urban environment.

18. T.S. KORN 1960 Noise Control 6, 5-6. Measurements of street noise on models.

19. E.A.G. SHAW and N. OLSEN 1972 Journal of the Acoustical Society of America 51, 1781-1793. Theory of steady-state urban noise for an ideal homogeneous city.

20. H.G. DAVIES 1973 Journal of the Acoustical Society of America 53, 1253-1262. Noise propagation in corridors.

21. P.M. MORSE and K.U. INGARD 1968. Theorteical Acoustics. New York: McGraw-Hill.

22. A. ISIHARA 1971 Statistical Physics. New York: Academic Press.

23. L.M. BREKHOVSKIKH 1960 Waves in Layered Media. New York: Academic Press.

24. G.H. WEISS 1970 Transport Research 4, 229-233. On the noise generated by a stream of vehicles.

25. R.J. ALFREDSON 1974 Proceedings of Noise Shock and Vibration Conference, Monash, 1974. pp.71-75. The prediction of noise levels from Australian freeways.

26. A.B. LAWRENCE 1970 Architectural Acoustics. London: Applied Science Publishers.

27. R.G. STAFFORD 1975 Department of Public Health, South Australia, Technical Report 3. Prediction of noise levels from road traffic.

28. D.R. JOHNSON and E.G. SAUNDERS 1968. Journal of Sound and Vibration 7, 287-309. The evaluation of noise from freely-flowing traffic.

29. Transport Research Circular No.175.(1976) Highway Traffic Noise Prediction Methods. Proceedings of a workshop sponsored by the Transport Research Board.

30. J. KRAGH and T. ASTRUP 1974 Acoustical Laboratory, Danish Academy of Technical Science, Report. Traffic noise measurements, Copenhagen 1972.

31. A.L. BROWN 1975 Proceedings of Conference on Metropolitan Transport - The Way Ahead? The effect of a freeway on community traffic noise levels.

32. D. AYLOR, J.-Y. PARLANGE and C. CHAPMAN 1973 Journal of the Acoustical Society of America 54, 1754-1757. Reverberation in a city street.

33. I.S. GRADSHTEYN and I.M. RYZHIK 1965 Tables of Integrals, Series and Products. New York: Academic Press (4th ed.)

APPENDIX 1

Equipment Used in Experimental Work

Microphones: B. & K. type 4135 ¼" microphones were used in model studies. Although these are not omnidirectional at high frequencies, they were used only in situations where angles of incidence were constant, and where relative sound levels only were required.

In large-scale tests, sound level meters with 1" B. & K. type 4144 microphones were used.

Sound Sources: (a) Air-driven source. See section 3·1.

(b) Magnavox speaker, approx. 17 cm diameter.

(c) Phillips tweeter, approx. 5 cm diameter.

(d) PEAK horn tweeter, approx. 5 cm diameter.

(e) For large-scale tests, an omnidirectional source consisting of a sphere 35 cm in diameter, containing 12 Phillips tweeters, each 8 cm in diameter.

Signal Generator:

Exact, Model 128 LOG/LIN Sweep Generator.

White Noise Generator:

B. & K. type 1402.

Filters: (a) B. & K. types 1612 and 1615 octave-band filters.

(b) B. & K. type 2107 narrow-band analyser. This was used when single-frequency propagation was studied, to remove extraneous noise.

Signal Amplifier: B. & K. type 2606

Sound Level Meters: B. & K. type 2205

Oscilloscope: Telequipment, Model DM 63

Tape Recorders: UHER 4200

APPENDIX 2

MATHEMATICAL FORMULAE

Some of the more important formulae used in mathematical derivations are listed below. These are found in reference [33].

(i) $$\int_0^\infty x^{\nu-1}\, e^{-\beta/x-\gamma x}\, dx = 2(\beta/\gamma)^{\nu/2}\, K_\nu(2(\beta\gamma)^{\frac{1}{2}})$$

$(\beta > 0, \gamma > 0)$, where K_ν is a modified Bessel function of the second kind.

(ii) $$K_{-\nu}(z) = K_\nu(z)$$

(iii) $$K_{\frac{1}{2}}(z) = (\pi/2z)^{\frac{1}{2}}\, e^{-z}$$

(iv) $$H_\nu^{(1)}(z) \sim (2/\pi z)^{\frac{1}{2}}\, e^{i(z\, -\, \pi/4\, -\, \nu\pi/2)}$$

for large $|z|$, where $H_\nu^{(1)}$ is a Hankel function of the first kind.

(v) $$\int_0^\infty K_\nu(\alpha(x^2 + z^2)^{\frac{1}{2}})\, \frac{x^{2u} + 1}{(x^2 + z^2)^{\nu/2}}\, dx$$

$$= \frac{z^u \Gamma(u + 1)}{\alpha^{u+1}\, z^{\nu-u-1}}\, K_{\nu-u-1}(\alpha z) \qquad (\alpha > 0,\ Re(u) > -1)$$

(vi) $$K_\nu(z) = \frac{\pi^{\frac{1}{2}}(\frac{1}{2}z)^\nu}{\Gamma(\nu + \frac{1}{2})} \int_0^\infty e^{-zt}(t^2 - 1)^{\nu-\frac{1}{2}} dt$$

$(\nu > -\frac{1}{2})$

(vii) $$\int K_1(x)\, dx = -K_o(x)$$

APPENDIX 3

Propagation of a Wave Through a Series of Partially-Reflecting Interfaces

We shall consider the problem of a particle moving on a line, its distance from the origin being x. At $x = N$, where N is an integer, the particle either reverses direction, with probability p_2, or proceeds straight ahead, with probability $p_1 = 1 - p_2$. Initially, the particle is assumed to have been at $x = 0$, moving in the positive or negative direction with equal probability. We then wish to find $f(x,n)$, the probability that the particle is between the points $x = N$, where $N = [x]$ and $x = N + 1$, after having moved a total distance n. This may be related to the problem of sound propagation described in section 2·2 by writing $x = r/d$, $n = ct/d$, $p_2 = R$ and $p_1 = 1 - R$, and dividing f by d, to give the probability per unit distance.

Let $f_1(x,n)$ be the probability that the particle is moving in the positive direction, and $f_2(x,n)$ be the probability that it is moving in the negative direction. Then

$$f_1(x,n+1) = p_1 f_1(x-1,n) + p_2 f_2(x,n) \qquad \text{(A3·1)}$$

and $$f_2(x,n+1) = p_1 f_2(x+1,n) + p_2 f_1(x,n) \qquad \text{(A3·2)}.$$

Substituting in (A3·1) from (A3·2) for f_1 gives

$$\frac{1}{p_2} f_2(x-1,n+2) - \frac{p_1}{p_2} f_2(x,n+1)$$

$$= \frac{p_1}{p_2} f_2(x-2,n+1) - \frac{p_1^2}{p_2} f_2(x-1,n) + p_2 f_2(x-1,n)$$

or $$f_2(x,n+1) = p_1\{f_2(x+1,n) + f_2(x-1,n)\} + (p_2-p_1) f_2(x,n-1) \qquad (A3·3).$$

Similarly,

$$f_1(x,n+1) = p_1\{f_1(x+1,n) + f_1(x-1,n)\} + (p_2-p_1) f_1(x,n-1) \qquad (A3·4)$$

and thus, since $f(x,n) = f_1(x,n) + f_2(x,n)$,

$$f(x,n+1) = p_1\{f(x+1,n) + f(x-1,n)\} + (p_2-p_1) f(x,n-1) \qquad (A3·5).$$

We may take a continuous approximation to f, which satisfies (A3·5). (This will be equal to f at the points $x = N + \frac{1}{2}$.)

Then, $$\left.\frac{\partial f}{\partial x}\right|_x = f(x+1) - f(x),$$

where the variable n is omitted,

$$\text{i.e.} \quad f(x+1) = f(x) + \left.\frac{\partial f}{\partial x}\right|_x .$$

Also, $$\left.\frac{\partial^2 f}{\partial x^2}\right|_{x-1} = \left.\frac{\partial f}{\partial x}\right|_x - \left.\frac{\partial f}{\partial x}\right|_{x-1}$$

$$= \left.\frac{\partial f}{\partial x}\right|_x - f(x) + f(x-1)$$

$$\text{i.e.} \quad f(x-1) = f(x) - \left.\frac{\partial f}{\partial x}\right|_x + \left.\frac{\partial^2 f}{\partial x^2}\right|_{x-1}$$

and similarly for the variable n.

Thus, from (A3·5),

$$2p_2 \left.\frac{\partial f}{\partial n}\right|_n = p_1 \left.\frac{\partial^2 f}{\partial x^2}\right|_{x-1} + (p_2 - p_1) \left.\frac{\partial^2 f}{\partial n^2}\right|_{n-1}$$

and using $\left.\frac{\partial f}{\partial n}\right|_n = \left.\frac{\partial f}{\partial n}\right|_{n-1} + \left.\frac{\partial^2 f}{\partial n^2}\right|_{n-1}$,

we obtain

$$p_1 \frac{\partial^2 f}{\partial x^2} = \frac{\partial^2 f}{\partial n^2} + 2p_2 \frac{\partial f}{\partial n} \qquad \text{(A3·6)}.$$

In order to solve this differential equation, we put

$$f(x,n) = \int_{-\infty}^{\infty} g(q,n) e^{iqx}\, dq \qquad \text{(A3·7)}$$

so that $\frac{\partial^2 f}{\partial x^2} = -\int_{-\infty}^{\infty} q^2 g(q,n) e^{iqx}\, dq$ (A3·8).

Thus, (A3·6) becomes

$$-p_1 q^2 g = \frac{\partial^2 g}{\partial n^2} + 2p_2 \frac{\partial g}{\partial n} \qquad \text{(A3·9)}.$$

The characteristic equation of (A3·9) is

$$D^2 + 2p_2 D + p_1 q^2 = 0 \qquad \text{(A3·10)}$$

and its roots are

$$R_1 = -p_2\{1 + (1 - \frac{p_1}{p_2^2} q^2)^{\frac{1}{2}}\} \qquad \text{(A3·11)}$$

and

$$R_2 = -p_2\{1 - (1 - \frac{p_1}{p_2^2} q^2)^{\frac{1}{2}}\} \qquad \text{(A3·12)}.$$

Thus, $g = c_1 e^{R_1 n} + c_2 e^{R_2 n}$ (A3·13)

where c_1 and c_2 are constant with respect to n.

Since

$$g(q,n) = \frac{1}{2\pi} \int_{-\infty}^{\infty} f(x,n) e^{-iqn} \, dq,$$

the condition $f(x,0) = \delta(x)$

gives $g(q,0) = 1/2\pi$.

For $n = \Delta$, where Δ is small enough (i.e. less than the shortest distance from the origin to an interface), we have

$$f(x,\Delta) = \tfrac{1}{2}\{\delta(x - \Delta) + \delta(x + \Delta)\},$$

giving $g(q,\Delta) = \frac{1}{2\pi} \cos q\Delta$.

Thus, from (A3·13),

$$c_1 + c_2 = 1/2\pi$$

and $c_1 e^{R_1 \Delta} + c_2 e^{R_2 \Delta} = \frac{1}{2\pi} \cos q\Delta$,

giving $c_1 = \frac{1}{2\pi} \frac{\cos q\Delta - e^{R_2 \Delta}}{e^{R_1 \Delta} - e^{R_2 \Delta}}$ (A3·14)

and $c_2 = \frac{1}{2\pi} \frac{\cos q\Delta - e^{R_1 \Delta}}{e^{R_2 \Delta} - e^{R_1 \Delta}}$ (A3·15).

Now, for x large, q will be small, except in the area about the origin. If $x^2 \gg p_1/p_2^2$, we may put

$(p_1/p_2^2)q^2 \ll 1$, giving

$$R_1 \sim -2p_2 \qquad \text{(A3·16)}$$

and $$R_2 \sim -(p_1/2p_2)q^2 \qquad \text{(A3·17)}.$$

By the same approximation, we have $|R_2| \ll |R_1|$. Thus, for large n, (A3·13) becomes

$$g \sim c_2 e^{R_2 n} \qquad \text{(A3·18)}.$$

From (A3·15), by a suitably small choice of Δ, we can put $c_2 \sim 1/2\pi$ and thus, by (A3·7), we have

$$\begin{aligned} f(x,n) &= \frac{1}{2\pi} \int_{-\infty}^{\infty} e^{-(p_1/2p_2)q^2 n} \; e^{iqx} \; dq \\ &= \left(\frac{p_2}{2\pi p_1 n}\right)^{\frac{1}{2}} \; e^{-\left(\frac{p_2}{2p_1}\right)\frac{x^2}{n}} \end{aligned} \qquad \text{(A3·19)}.$$

Replacing $x = r/d$, $n = ct/d$, $p_2 = R$ and $p_1 = 1-R$, and dividing by d, gives

$$f(r,t) = \left(\frac{R}{2\pi(1-R)ctd}\right)^{\frac{1}{2}} \; e^{-\frac{Rr^2}{2(1-R)dct}} \qquad \text{(A3·20)}.$$

APPENDIX 4

Scattering and Absorption in Ducts

The theory of scattering in ducts is very similar to that in streets, with the exception that in a duct, there is no cylindrical spreading. Thus, in finding the total intensity due to all scattered components, equation (2·1) must be replaced by

$$I = \int_0^\infty f(r,t)\ d(ct) \qquad \text{(A4·1)}.$$

If f is taken as in equation (2·2), this integral does not converge, emphasising the unphysical nature of the assumptions that the duct is infinitely long and has no absorption.

If absorption is included, the integral becomes

$$I = \int_0^\infty f(r,t)\ e^{-\gamma ct/d}\ d(ct)$$

$$= \left(\frac{R}{2\gamma(1-R)}\right)^{\frac{1}{2}}\ e^{-\left(\frac{2R\gamma}{1-R}\right)^{\frac{1}{2}}\frac{r}{d}} \qquad \text{(A4·2)}$$

where γ has the same meaning as in Chapter 2.

This formula implies that in situations dominated by scattering, i.e., where $\gamma < 2R/1\text{-}R$, attenuation rates may be most easily increased by increasing γ (as is the case for streets). However, in situations dominated by absorption, attenuation rates will be changed more easily by increasing R.

APPENDIX 5

SCATTERING FROM SMALL PROTRUSIONS

A5·1 The Effect of a Large Number of Scatterers

If a protrusion from a street wall is small compared to the wavelength of the propagating sound, the incoming wave may be regarded as a plane wave travelling in the x-direction, with its pressure field given by

$$p = p_{in} e^{ikx} \qquad (A5\cdot1).$$

In cylindrical polar co-ordinates centred on the scatterer (figure A5·1), the pressure field of the outgoing wave will consist of a scattered and an unscattered component [21] –

$$p_{out} = p_{in} \{e^{ikx} + f\, e^{ikr}/r^{\frac{1}{2}}\} \qquad (A5\cdot2)$$

where f is a parameter representing the degree of scattering and will in general be a function of θ. The intensity of the scattered wave will be

$$I_{sc}(\theta) = I_{in}|f|^2/r \qquad (A5\cdot3)$$

where I_{in} is the incident intensity.

The energy scattered through a line segment $dl = rd\theta$ will thus be

$$I_{sc}dl = I_{in}|f|^2 d\theta \qquad (A5\cdot4).$$

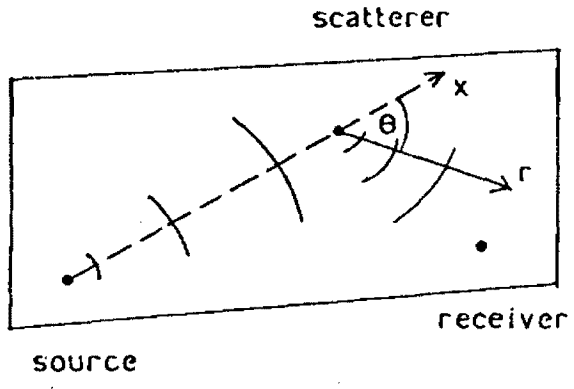

Figure A5·1: Scattering from a small protrusion on a street wall.

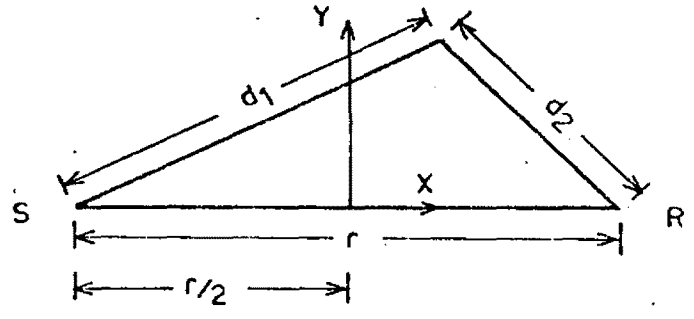

Figure A5·2: Distances used in calculations of scattering intensity.

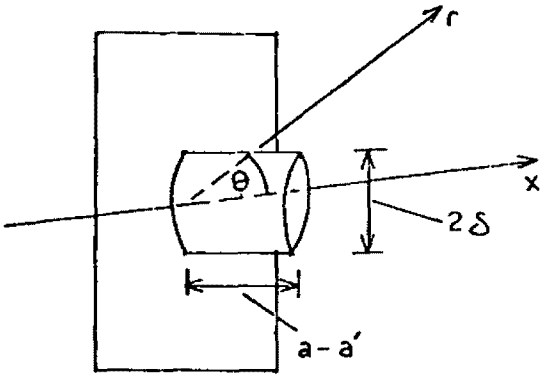

Figure A5·3: Assumed geometry of a small scatterer.

The total energy scattered will be

$$\int_0^{2\pi} I_{sc} r d\theta = I_{in} \int_0^{2\pi} |f|^2 d\theta$$

$$= I_{in}\sigma \qquad \text{(A5·5)}$$

where σ, the scattering cross-section, is defined to be $\int_0^{2\pi} |f|^2 d\theta$.

The total energy scattered by all scatterers in an element of area $dxdy$ will be $n\sigma I_{in} dxdy$, where n is the number of scatterers per unit area on the street walls. It is assumed here that secondary scattering may be neglected and this assumption limits the range of validity of the final expression (see below).

We now change to cylindrical polar co-ordinates centred on the source. The total energy lost from a previously unscattered wave in moving a distance dr outward will be

$$\int_0^{2\pi} n\sigma I_{in} r \, dr \, d\theta = 2\pi r I_{in} n\sigma dr \ .$$

Thus, the energy in this wave front at $r + dr$ will be

$$E(r + dr) = E(r)(1 - n\sigma dr) \qquad \text{(A5·6)},$$

from which it follows that

$$E(r) = E_o e^{-n\sigma r} \qquad \text{(A5·7)},$$

where E_o is a constant and the intensity at r will be

$$I(r) = \frac{I_o R}{r} e^{-n\sigma r} \qquad \text{(A5·8)},$$

where I_o is the intensity at a distance R, in the absence of scattering.

Now consider an element $dx\,dy$ of the street wall, at a distance d_1 from the source. For this element we will have

$$I_{in} = \frac{I_o R}{d_1} \; e^{-n\sigma d_1} \; .$$

Changing again to cylindrical polar co-ordinates centred on this element of area, we see that the energy scattered from the element through a line segment $dl = d_2 d\theta$ (see figure A5·2) will be

$$\frac{I_o R}{d_1} \; e^{-n\sigma d_1} \; |f|^2 d\theta \; n\,dx\,dy \; ,$$

neglecting attenuation of the scattered wave due to further scattering. If this effect is included, the energy passing through dl after being scattered from $dx\,dy$ is

$$\frac{I_o R}{d_1} \; e^{-n\sigma d_1} \; |f|^2 d\theta \; n\,dx\,dy \; e^{-n\sigma d_2} \; .$$

The intensity at R (figure 5·2) due to scattering from $dx\,dy$ will be

$$dI_1 = \frac{I_o R}{d_1 d_2} \; |f|^2 \; e^{-n\sigma(d_1+d_2)} \; n\,dx\,dy \qquad \text{(A5.9)}$$

and the total intensity due to scattered waves is

$$I_1 = I_o R n \iint_{-\infty}^{\infty} \frac{|f|^2}{d_1 d_2} \; e^{-n\sigma(d_1+d_2)} \; dx\,dy \qquad \text{(A5·10)}.$$

If f is assumed to be independent of θ, then $\sigma = 2\pi|f|^2$, and we have

$$I_1 = \frac{I_O R n\sigma}{2\pi} \iint_{-\infty}^{\infty} \frac{1}{d_1 d_2} e^{-n\sigma(d_1+d_2)} dx\, dy \qquad \text{(A5·11)}.$$

Including the intensity of the unscattered wave reaching the point R in figure A5·2, the total intensity at this point will be

$$I = \frac{I_O R}{r} e^{-n\sigma r} + I_1$$

$$= I_O R \{\frac{1}{r} e^{-r/d} + \frac{1}{2\pi d} \iint_{-\infty}^{\infty} \frac{1}{d_1 d_2} e^{-(d_1+d_2)/d} dx\, dy \} \qquad \text{(A5·12)},$$

where $d = 1/n\sigma$.

This expression, of course, neglects the possibility of multiple scattering. Taking absorption into account will simply have the effect of altering the effective value of d.

A5·2 Evaluation of the Integral Appearing Above

Co-ordinates may be set up as in figure A5·2. If we put

$$\mu = d_1 + d_2$$
$$\xi = d_1 - d_2 \qquad \text{(A5·13)}$$

then $d_1 d_2 = \frac{1}{4}(\mu^2 - \xi^2)$ (A5·14).

Also,

$$x = \frac{1}{2r}\,\mu\xi \quad \text{and}$$

$$y = \pm\frac{r}{2}\left\{\left(\frac{\mu^2}{r^2} - 1\right)\left(1 - \frac{\xi^2}{r}\right)\right\}^{\frac{1}{2}} \qquad \text{(A5·15)}$$

giving $$\frac{\partial(x,y)}{\partial(\mu,\xi)} = \frac{1}{4r^2}\,\frac{\mu^2 - \xi^2}{\left\{\left(\frac{\mu^2}{r^2} - 1\right)\left(1 - \frac{\xi^2}{r^2}\right)\right\}^{\frac{1}{2}}} \qquad \text{(A5·16)}.$$

Thus,

$$\iint_{-\infty}^{\infty} \frac{1}{d_1 d_2}\, e^{-(d_1+d_2)/d}\, dx\, dy$$

$$= 2\int_r^{\infty} \frac{e^{-\mu/d}}{(\mu^2 - r^2)^{\frac{1}{2}}}\, d\mu \int_{-r}^{r} \frac{d\xi}{(r^2 - \xi^2)^{\frac{1}{2}}}$$

$$= 2\pi K_o(r/d) \qquad \text{(A5·17)}.$$

Then, from (A5·12), we have

$$I = \frac{I_o R}{r}\, e^{-r/d}\left\{1 + \frac{r}{d}\, e^{r/d}\, K_o(r/d)\right\} \qquad \text{(A5·18)}.$$

This expression will be valid only when multiple scattering is not important. A rough guide to its range of validity is given by the point where the intensity due to first-order scattering is equal to that due to direct radiation, i.e. $r/d \sim 0.8$. Beyond that point, second and higher order scattering will clearly be important.

A5·3 Determination of the Scattering Cross-Section

Since, in determining the scattering cross-section of a protrusion, some assumption must be made about its shape, protrusions were assumed to be cylinders jutting abruptly from the street wall, having a radius δ, and changing the street width from a to a'(figure A5·3). As in section 2·5, one component of the scattered wave will result from direct scattering from the surface, giving rise to a cross-section σ_r, while another component will result from scattering of the portion of the wave between the scatterer and the other wall of the street, giving a cross-section σ_s. The total cross-section may then be written

$$\sigma = (1 - a'/a)\sigma_r + (a'/a)\sigma_s \qquad \text{(A5·19)}.$$

In calculating r, reference [21] gives (in cylindrical co-ordinates centred on the scatterer, with $\theta = 0$ along the direction of the incoming wave)

$$|f|^2 = \tfrac{1}{8}\,\pi\delta\,(k\delta)^3(1 - 2\cos\theta)d\theta \qquad \text{(A5·20)}$$

for small $k\delta$, where k is the wavenumber of the incident radiation.

Thus, $$\sigma_r = \tfrac{3}{4}\,\delta\pi^2\,(k\delta)^3 \qquad \text{(A5·21)}.$$

Equation (A5·20), of course, violates the assumption made in section A5·1 that f is independent of θ. However, it is assumed that real scatterers will not act as perfect cylinders,

but will have angular dependances significantly different from equation (A5·20) and that these dependances will be "averaged out" over a large number of scatterers, with equation (A5·21) giving an approximation to the resulting average value.

In order to calculate σ_s, we may express the acoustic pressure and velocity of the incoming wave (assumed to be a plane wave) in terms of Bessel functions.

$$p_{in} = p_o \{J_o(kr) + 2 \sum_{1}^{\infty} i^m \cos(m\theta) J_m(kr)\}$$
$$u_{in} = ikp_o \{J_1(kr) + \sum_{1}^{\infty} i^m (J_{m+1}(kr) - J_{m-1}(kr)) \cos m\theta\} \quad (A5\cdot22)$$

(see reference [21].

The wave which is scattered away from the protrusion may be represented as a series of Hankel functions of the first kind --

$$p_{out} = \sum_{o}^{\infty} A_m \cos m\theta \, H_m^{(1)}(kr)$$
$$u_{out} = ik\{A_o H_1^{(1)}(kr) + \tfrac{1}{2}\sum_{1}^{\infty} A_m (H_{m+1}(kr) - H_{m-1}(kr)) \cos m\theta\}. \quad (A5\cdot23)$$

The wave which will be present in the area of the protrusion will have a different wavenumber, k' (see section 2·5). This wave may be represented by --

$$p'_{in} = \sum_{o}^{\infty} B_m \cos m\theta \, J_m(k'r)$$
$$u'_{in} = ik' \{B_o J_1(k'r) + \tfrac{1}{2}\sum_{1}^{\infty} B_m (J_{m+1}(k'r) - J_{m-1}(k'r)) \cos m\theta\}. \quad (A5\cdot24)$$

Applying the boundary conditions

$$p_{in}(r=\delta) + p_{out}(r=\delta) = p'_{in}(r=\delta)$$

and $u_{in}(r=\delta) + u_{out}(r=\delta) = u'_{in}(r=\delta)$

gives

$$A_o \{k' H_o^{(1)}(k\delta) J_1(k'\delta) - k H_1^{(1)}(k\delta) J_o(k'\delta)\}$$

$$= -p_o\{k' J_o(k\delta) J_1(k'\delta) - k J_1(k\delta) J_o(k'\delta)\} \qquad (A5\cdot25)$$

and

$$A_m\{k' H_m^{(1)}(k\delta)(J_{m+1}(k'\delta) - J_{m-1}(k'\delta)) - k J_m(k'\delta)(H_{m+1}^{(1)}(k\delta) - H_{m-1}^{(1)}(k\delta))\}$$

$$= -2i^m p_o\{k' J_m(k\delta)(J_{m+1}(k'\delta) - J_{m-1}(k'\delta)) - k J_m(k'\delta)(J_{m+1}(k\delta) - J_{m-1}(k\delta))\}$$

$$(A5\cdot26)$$

for $m > 0$.

If $k\delta \ll 1$ (and $k'\delta << 1$),

$$A_o \sim \tfrac{1}{4} i\pi p_o((k'\delta)^2 - (k\delta)^2) \qquad (A5\cdot27)$$

and $A_m << A_o$ for $m > 0$.

Thus, we may write

$$p_{out} \sim \tfrac{1}{4} i\pi p_o((k'\delta)^2 - (k\delta)^2)\, H_o^{(1)}(kr) \qquad (A5\cdot28)$$

which for $kr >> 1$ becomes

$$p_{out} \sim \tfrac{1}{4} i\pi p_o((k'\delta)^2 - (k\delta)^2)\left(\frac{2}{\pi kr}\right)^{\frac{1}{2}} e^{i(kr - \pi/4)} \qquad (A5\cdot29)$$

giving

$$\sigma_s \sim \tfrac{1}{4}\delta\pi^2(k\delta)^3((k'/k)^2 - 1)^2 \qquad (A5\cdot30).$$

Thus, the total cross-section, from (A5·18), (A5·21) and (A5·30), is

$$\sigma = \tfrac{1}{4}\delta\pi^2(k\delta)^3\{3(1-a/a') + (a/a')((k'/k)^2 - 1)^2\} \qquad (A5\cdot31)$$

APPENDIX 6

PROPAGATION IN A STREET WITH ABSORBING WALLS

The wave-equation for the acoustic pressure p,

$$\nabla^2 p + k_o^2 p = 0 \qquad \text{(A6·1)}$$

where k_o is the free-space wavenumber, becomes in cylindrical polar co-ordinates,

$$\frac{\partial^2 p}{\partial r^2} + \frac{1}{r}\frac{\partial p}{\partial r} + \frac{\partial^2 p}{\partial z^2} + k_o^2 p = 0 \qquad \text{(A6·2)},$$

if propagation is assumed to be radially symmetric.

Writing $p = R(r)Z(z)$ leads, on separation of variables, to

$$\frac{\partial^2 R}{\partial r^2} + \frac{1}{r}\frac{\partial R}{\partial r} + (k_o^2 - c^2)R = 0 \qquad \text{(A6·3)}$$

and $$\frac{\partial^2 Z}{\partial z^2} + c^2 Z = 0 \qquad \text{(A6·4)}$$

where c is a constant.

If a co-ordinate system is set up as in figure (A6·1) and if the street walls have specific acoustic admittance β, the resulting boundary condition will be

$$\frac{\partial Z}{\partial z} = \pm ik_o \beta Z$$

at $z = \pm a/2$.

The linearly independent solutions of (A6·4) are

(i) $Z = \cos cz$

(ii) $Z = \sin cz$,

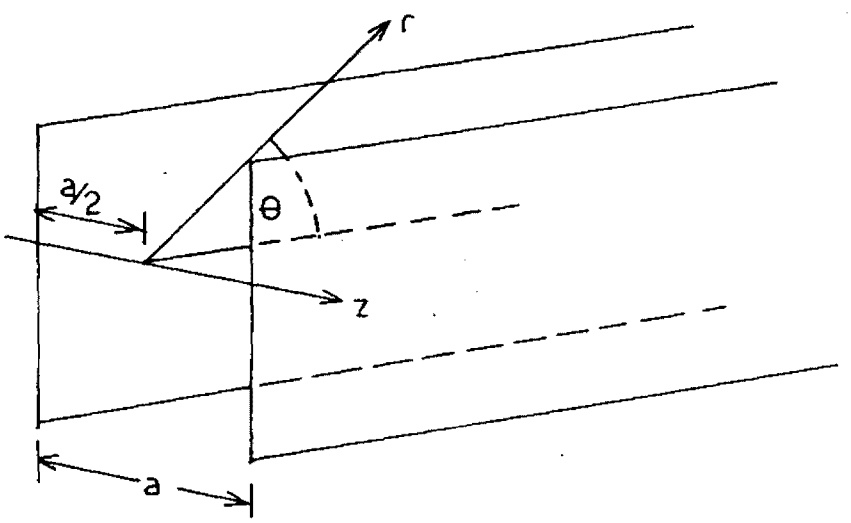

Figure A6•1: Co-ordinates in a street.

APPENDIX 7

TRANSMISSION AND REFLECTION OF A WAVE AT AN INTERFACE

A7·1 Normal Incidence

Let the incident wave in region I of figure 2·4 be represented by

$$p = P_n (k_n r)^{-\frac{1}{2}} e^{ik_n r} \cos \varepsilon_n z \qquad (A7\cdot1).$$

The reflected wave may be written

$$p = \sum_{i=1}^{\infty} P_n R_i (k_i r)^{-\frac{1}{2}} e^{-ik_i r} \cos \varepsilon_i z + \tfrac{1}{2} P_n R_o e^{-ik_o r} \qquad (A7\cdot2)$$

and the transmitted wave

$$p = \sum_{i=1}^{\infty} P_n T_i (k'_i r)^{-\frac{1}{2}} e^{ik'_i r} \cos \varepsilon'_i r + \tfrac{1}{2} P_n T_o e^{ik_o r} \qquad (A7\cdot3)$$

in region II, where $\varepsilon'_i = \pi i/a'$, *etc.*

From conservation of energy at the interface ($r=R$), integrating the intensity from $z=0$ to a', we have

$$1 - \mathrm{sinc}\,(\varepsilon_n a') = \tfrac{1}{2} \sum_{\substack{i,j,\ \text{not} \\ \text{both } 0}} (k_j/k_i)^{\frac{1}{2}} (R_i R_j^* + R_i^* R_j)\, e^{-i(k_i - k_j)R}$$

$$\times \{\mathrm{sinc}(\tfrac{1}{2}(\varepsilon_i + \varepsilon_j)a') + \mathrm{sinc}(\tfrac{1}{2}(\varepsilon_i - \varepsilon_j)a')\} + |R_o|^2 + \sum_i |T_i|^2 \qquad (A7\cdot4)$$

where $\mathrm{sinc}(x) = \sin(x)/x$.

Since $|sinc(x)| < 1/x$, and the arguments of the function here are generally relatively large, we shall approximate

$$sinc(x) = \begin{cases} 1 & x = 0 \\ 0 & \text{otherwise} . \end{cases}$$

Thus, we have $$1 = \sum_i |R_i|^2 + \sum_i |T_i|^2 \qquad (A7\cdot5).$$

From (A7·1), (A7·2) and (A7·3), by continuity of acoustic pressure at $r=R$,

$$k_n^{-\frac{1}{2}} e^{ik_nR} \cos \varepsilon_n z + \sum_{i=1}^{\infty} R_i k_i^{-\frac{1}{2}} e^{-k_nR} \cos \varepsilon_i z + \tfrac{1}{2} R_o e^{-k_oR}$$
$$= \sum_{i=1}^{\infty} T_i k'^{-\frac{1}{2}}_i e^{ik'_iR} \cos \varepsilon'_i z + \tfrac{1}{2} T_o e^{ik_oR} \qquad (A7\cdot6).$$

Multiplying by $\cos \varepsilon'_i z$ and integrating from $z=0$ to a' gives

$$k_n^{-\frac{1}{2}} \{sinc(\tfrac{1}{2}(\varepsilon_n+\varepsilon'_j)a') + sinc(\tfrac{1}{2}(\varepsilon_n-\varepsilon'_j)a')\} e^{ik_nR}$$
$$+ \sum_i R_i k_i^{-\frac{1}{2}} \{sinc(\tfrac{1}{2}(\varepsilon_i+\varepsilon'_j)a') + sinc(\tfrac{1}{2}(\varepsilon_i-\varepsilon'_j)a')\} e^{-ik_iR}$$
$$= T_j k_j^{-\frac{1}{2}} e^{ik'_jR} \qquad (A7\cdot7).$$

We put $sinc(\frac{1}{2}(\varepsilon_i-\varepsilon_j)a') = 1$ when ε_i and ε_j are as close as possible, i.e. $j = [ia'/a + \frac{1}{2}]$. Otherwise, it is taken to be zero.

Then, putting $j = m = [na'/a + \frac{1}{2}]$,

$$k_n^{-\frac{1}{2}} e^{ik_nR} + R_n k_n^{-\frac{1}{2}} e^{-ik_nR} = T_m k'^{-\frac{1}{2}}_m e^{ik'_mR} \qquad (A7\cdot8).$$

Similarly, from continuity of particle velocity (i.e. of $\frac{\partial p}{\partial r}$) at $r = R$,

$$k_n^{\frac{1}{2}} e^{ik_n R} - k_n^{\frac{1}{2}} R_n e^{-ik_n R} = T_m k_m'^{\frac{1}{2}} e^{ik_m' R} \qquad \text{(A7·9)}.$$

(A7·8) and (A7·9) lead to

$$|R_n|^2 = \left(\frac{k_n - k_m'}{k_n + k_m'}\right)^2 \qquad \text{(A7·10)}$$

$$|T_m|^2 = \frac{4k_n k_m}{(k_n + k_m)^2} \qquad \text{(A7·11)}.$$

Since $|R_n|^2 + |T_m|^2 = 1$, by (A7·5), $R_i = 0$ for $i \neq n$, and $T_i = 0$ for $i \neq m$.

A7·2 Reflection at an Angle to an Interface

If the incident wave is in the nth mode, we may assume, as above, that the reflected wave is in the nth mode, and the transmitted wave in the mth mode, where $m = [na'/a + \frac{1}{2}]$.

From the continuity of acoustic pressure at $y = 0$ (figure A7·1), we have

$$k_n^{-\frac{1}{2}} e^{ik_n x \sin\theta} + R_n k_n^{-\frac{1}{2}} e^{ik_n x \sin\theta'} = T_m k_m'^{-\frac{1}{2}} e^{ik_m' x \sin\phi} \qquad \text{(A7·12)}.$$

Since this is true for all x, the exponents must be equal, i.e. $\theta = \theta'$ and $k_n \sin\theta = k_m' \sin\phi$.

From continuity of particle velocity in the y-direction,

$$k_n^{\frac{1}{2}} \cos\theta e^{ik_n x \sin\theta} - R_n k_n^{\frac{1}{2}} \cos\theta e^{ik_n \sin\theta} = T_m k_m'^{\frac{1}{2}} \cos\phi e^{ik_m' x \sin\theta} \qquad \text{(A7·13)}.$$

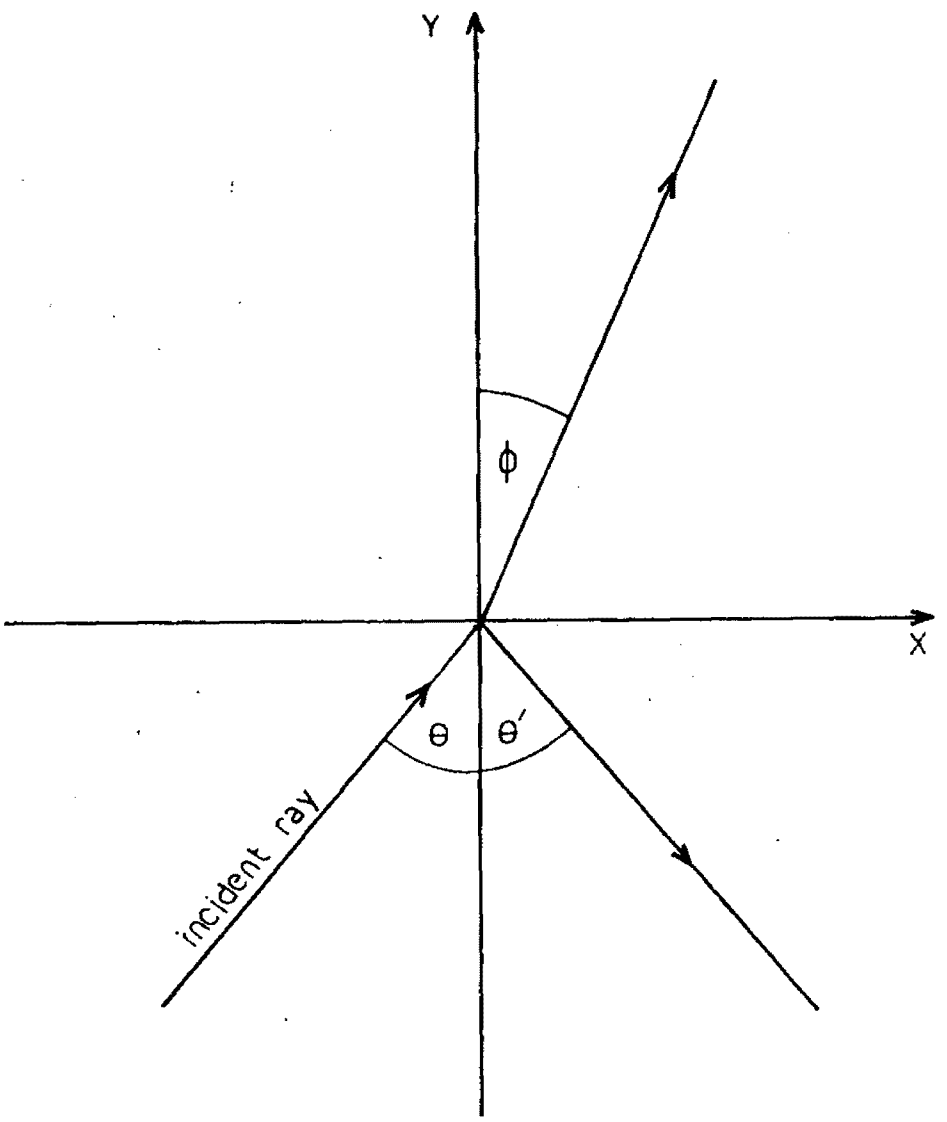

Figure A7•1: Reflection and transmission of a wave approaching at an angle θ to an interface.

(A7·12) and (A7·13) lead to

$$|R_n|^2 = \left(\frac{k'_m \cos\phi - k_n \cos\theta}{k'_m \cos\phi + k_n \cos\theta} \right)^2$$

$$= \{ \frac{\cos\theta - ((k'_m/k_n)^2 - \sin^2\theta)^{\frac{1}{2}}}{\cos\theta + ((k'_m/k_n)^2 - \sin^2\theta)^{\frac{1}{2}}} \}^2 \qquad \text{(A7·14)}.$$

For $\sin\theta > k'_m/k_n$, we have "total internal reflection", and $|R_n|^2 = 1$.

APPENDIX 8

Attenuation in Lined Ducts

The rate of sound attenuation in a lined duct will depend on the size and shape of the duct, and on the absorption co-efficient of the lining material at the relevant frequency. It will also depend on the modal structure of the sound field, since higher-order modes are attenuated faster than lower-order modes. If the duct is rectangular with sides of length l_1 and l_2, and $2\pi|\beta|l_i\lambda \ll 1$, where $\beta = \xi - i\sigma$ is the specific acoustic admittance of the lining, the attenuation per metre of the (m,n) mode will be

$$\Gamma_{mn} = 8.686\ \xi d k_o / k_{mn} \qquad \text{(A8·1)},$$

where $d = 1/l_1 + 1/l_2$ is the "characteristic distance" of the duct, and $k_{mn}^2 = k_o^2 - (2\pi m/l_1)^2 - (2\pi n/l_2)^2$. The effect of the presence of higher-order modes is shown in figure A8·1*, where the same lining is used in rectangular ducts of different sizes.

If high-order modes are present, these are quickly absorbed, after which the overall rate of attenuation is that of the remaining low-order modes. This effect is shown in figure A8·2.

*All values of insertion loss used here were supplied by ACI Fibreglass.

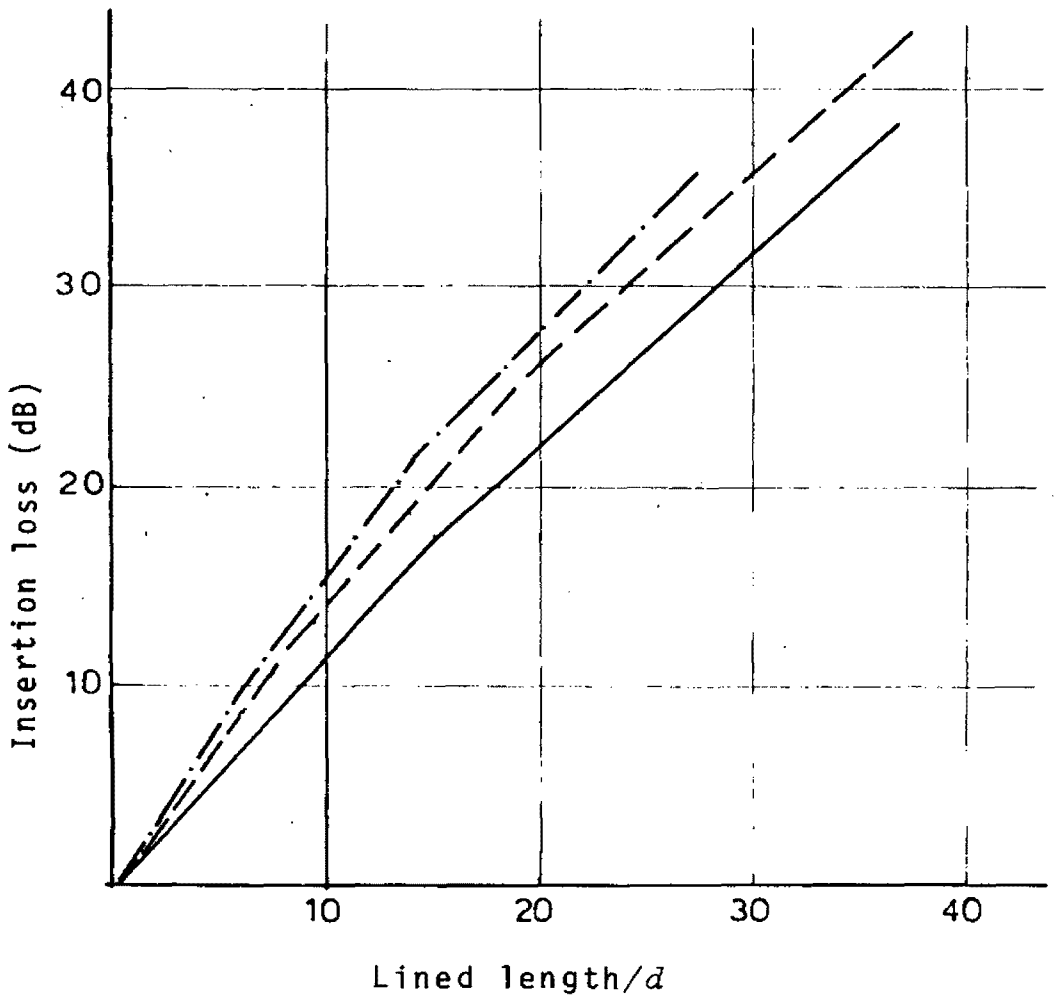

Figure A8-1: Insertion losses in ducts lined with 25 mm-thick, 50 kg/m^3, fibreglass, at 500 Hz.

—— - 300 x 250 mm duct (1 propagating mode);

--- - 800 x 400 mm duct (6 propagating modes);

—•— - 900 x 600 mm duct (6 propagating modes).

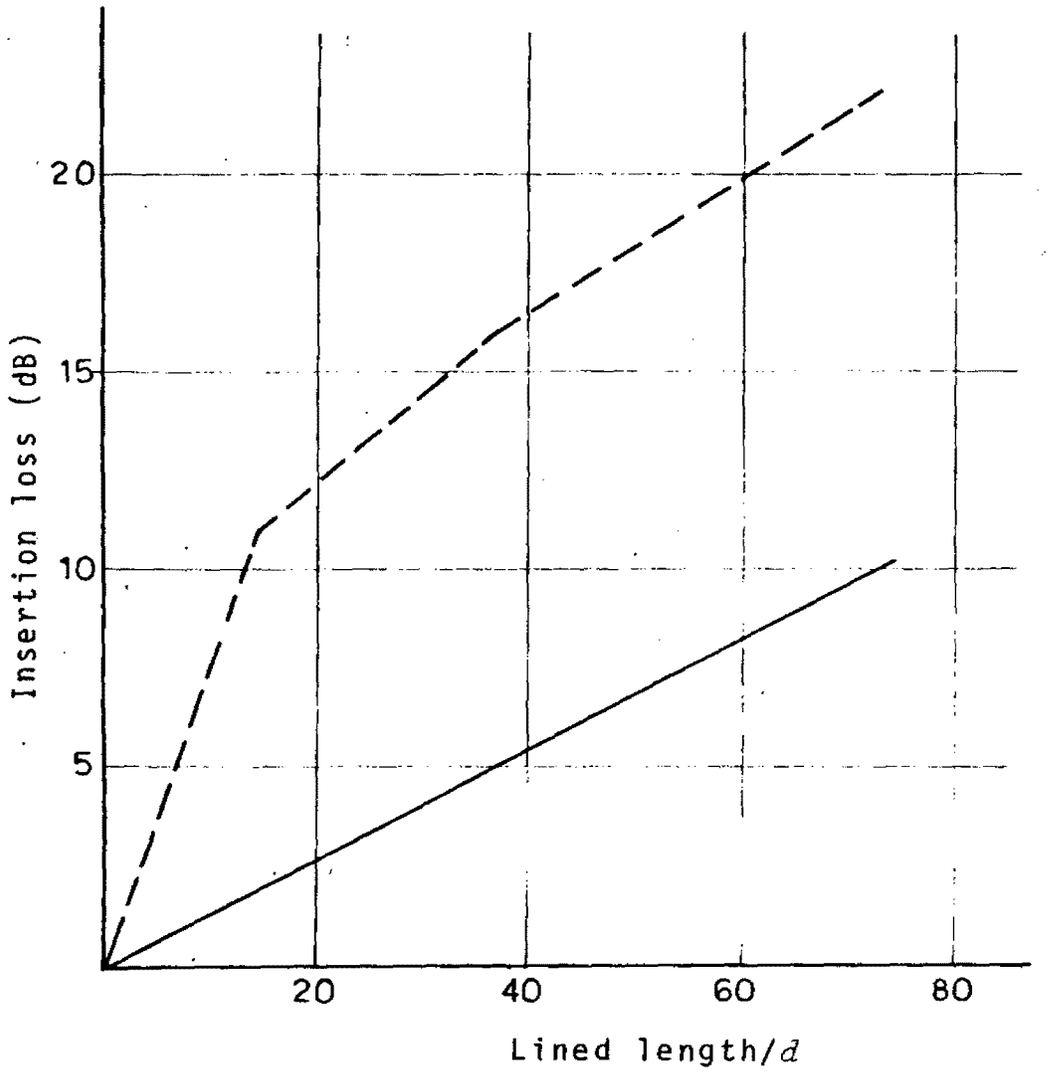

Figure A8•2: Insertion losses in a 300 x 250 mm duct, lined with 25 mm-thick, 50 kg/m³, fibreglass.

——— - 250 Hz (1 propagating mode);
---- - 8 kHz (42 propagating modes).

APPENDIX 9

Sound Level For Sources Distributed On a Plane

A large city may be approximately represented by an infinite plane containing n sound sources per unit area, the sound intensity resulting from each source being given by equation (6·4).

The total intensity at one point could be written as

$$\bar{I} = nI_r(R_r/l)^2 \int_0^\infty 2\pi r I(r)\, dr \qquad \text{(A9·1)}.$$

However, if the expression in equation (6·4) is used for $I(r)$, this integral diverges. Shaw and Olsen [19] explain similar behaviour of their expression for $I(r)$ by pointing out that sources close to the receiver have intensities which vary greatly with time. Thus, they integrate their expression down to a radius $R_o = (1/n\pi)^{\frac{1}{2}}$, which includes all sources except the one closest to $r=0$, and then they add $I(R_o/2^{\frac{1}{2}})$, which is the intensity which will be exceeded by the "local" source for 50% of the time. (The expression should thus predict L_{50}, and not L_{eq} .)

Using the expression in equation (6·4), the integral becomes

$$nI_r(R_r/l)^2 \int_{R_o}^\infty 8\pi\gamma^{\frac{1}{2}} l K_1(2r\gamma^{\frac{1}{2}}/l)\, dr$$

$$= 4\pi n I_r R^2 K_o(2R_o\gamma^{\frac{1}{2}}/l) \qquad \text{(A9·2)},$$

and thus we have

$$\bar{I} = 4\pi n I_r R_r^2 \{K_o(2^{\frac{1}{2}}s) + sK_1(s)\} \qquad (A9\cdot3)$$

where $s = (2\gamma/\pi n l^2)^{\frac{1}{2}}$.

APPENDIX 10

TRAFFIC NOISE MEASUREMENTS — COPENHAGEN

Site 21

The two major roads nearest to this site are Vejlands Allé and Englandsvej. Although detailed traffic counts for Englandsvej are not given, the total daily traffic, percentage of heavy vehicles and mean speed (60 km/h) are the same as for Vejlands Allé. It was assumed that half-hourly variations would also be similar. For both roads, k = 180 m, giving k/l = 2.9.

n is shown for Vejlands Allé, in units of vehicles/km. $n(c)$ is the density of cars, and $n(h)$ that of heavy vehicles.

Beginning of time period	$n(c)$	$n(h)$	L_{eq}, dB(A)'s (predicted)	L_{eq}, dB(A)'s (measured)
0000	6.40	0.27	47	45
0030	3.20	0.17	44	44
0100	1.60	0.12	42	45
0130	0.98	0.02	37	44
0200	0.94	0.06	39	41
0230	0.65	0.02	36	41
0300	0.97	0.03	38	40
0330	0.94	0.06	39	48
0400	0.63	0.37	45	53
0430	2.50	0.80	49	50

Beginning of time period	$n(c)$	$n(h)$	L_{eq}, dB(A)'s (predicted)	L_{eq}, dB(A)'s (measured)
0500	5.4	1.3	51	52
0530	12	1.3	52	54
0600	23	2.3	54	59
0630	36	1.9	55	55
0700	29	3.2	56	57
0730	40	3.5	56	58
0800	29	4.3	57	56
0830	23	3.2	55	58
0900	22	5.1	57	57
0930	21	4.3	56	58
1000	20	4.1	56	55
1030	18	4.6	56	56
1100	19	4.2	56	54
1130	19	4.0	56	57
1200	18	4.3	56	56
1230	21	4.3	56	55
1300	20	4.4	56	55
1330	24	4.3	56	53
1400	23	3.7	56	56
1430	24	4.5	57	55
1500	26	4.6	57	54
1530	35	2.6	55	55
1600	43	2.3	56	57
1630	46	1.9	55	55
1700	35	1.4	54	56

Beginning of time period	$n(c)$	$n(h)$	L_{eq}, dB(A)'s (predicted)	L_{eq}, dB(A)'s (measured)
1730	32	1.30	54	52
1800	25	1.30	53	53
1830	27	0.85	52	54
1900	24	0.75	52	54
1930	24	0.49	51	56
2000	16	0.51	50	49
2030	16	0.50	50	50
2100	16	0.50	50	45
2130	15	0.30	49	49
2200	15	0.31	49	46
2230	15	0.31	49	45
2300	16	0.48	50	53
2330	10	0.31	48	45

Site 23

The two nearest major roads are Lyngbyvej (k = 240m, k/l = 3.5) and Vangedvej (k = 210 m, k/l = 3.1). Mean speeds are 70 km/h, on Lyngbyvej and 60 km/h on Vangedvej.

The units of n are vehicles/km. $n(c)$ is the density of cars, and $n(h)$ that of heavy vehicles.

Beginning of time period	Lyngbyvej		Vangedvej		L_{eq}, dB(A)'s (predicted)	L_{eq}, dB(A)'s (measured)
	$n(c)$	$n(h)$	$n(c)$	$n(h)$		
0000	7	0.2	3.2	0.1	41	39
0030	6	0.3	1.7	-	40	38
0100	4	0.1	0.6	-	37	54
0130	1.4	0.1	0.6	-	34	39
0200	2	0.2	0.6	-	35	36
0230	1.4	0.2	0.6	-	35	37
0300	1.4	0.3	0.6	-	35	36
0330	1.1	0.01	0.6	-	33	47
0400	1.3	0.1	0.5	0.1	35	38
0430	2	0.3	0.5	0.1	36	39
0500	2.5	0.5	0.5	0.1	38	38
0530	6	0.7	4	0.4	42	41
0600	16	1.4	11	1.0	46	43
0630	21	3	14	1.1	48	45
0700	35	2	13	0.9	48	52
0730	53	3	27	0.8	50	50
0800	42	4	21	1.7	50	53

Beginning of time period	Lyngbyvej		Vangedvej		L_{eq}, dB(A)'s (predicted)	L_{eq}, dB(A)'s (measured)
	n(c)	*n(h)*	*n(c)*	*n(h)*		
0830	40	3	17	1.2	49	48
0900	30	3	11	0.9	48	47
0930	27	3	10	1.5	48	45
1000	25	3	9	1.7	48	45
1030	25	3	7	1.5	47	45
1100	23	3	10	1.8	48	46
1130	21	2	9	1.2	47	43
1200	21	3	9	1.8	48	38
1230	23	2	10	1.4	47	55
1300	23	2	11	1.7	48	46
1330	24	3	11	2.0	49	40
1400	28	3	14	1.6	49	46
1430	29	4	13	1.4	49	41
1500	31	3	15	1.4	49	47
1530	38	2	20	1.5	49	48
1600	51	1.6	27	1.7	49	49
1630	53	1.6	22	0.9	48	46
1700	40	1.2	21	0.6	48	45
1730	39	0.8	20	0.4	48	47
1800	32	1.0	15	0.3	47	51
1830	29	0.9	14	0.3	47	46
1900	27	0.8	12	0.2	46	44
1930	21	0.6	12	0.3	46	47
2000	18	0.6	9	0.3	45	42

Beginning of time period	Lyngbyvej		Vangedvej		L_{eq}, dB(A)'s (predicted)	L_{eq}, dB(A)'s (measured)
	n(c)	*n(h)*	*n(c)*	*n(h)*		
2030	15	0.5	8	0.2	44	40
2100	15	0.5	5	0.1	43	46
2130	14	0.4	5	0.1	43	37
2200	13	0.3	7	0.1	43	40
2230	12	0.4	8	0.2	44	43
2300	15	0.3	6	0.1	43	46
2330	12	0.4	5	0.1	43	39

APPENDIX 11

TRAFFIC NOISE MEASUREMENTS — SYDNEY

Measurements were taken over 6 minutes at some time during one of the periods below.

1. 1 a.m. - 5 a.m. Monday through Sunday
2. 7 a.m. - 9 a.m. Monday through Friday
3. 10 a.m. - 12 noon Monday through Friday
4. 9 a.m. - 12 noon Saturday
5. 7.30 p.m. - 10.30 p.m. Monday through Wednesday
6. 7 p.m. - 9 p.m. Thursday
7. 7.30 p.m. - 10.30 p.m. Friday and Saturday
8. 7 p.m. - 10 p.m. Sunday
9. 1 p.m. - 5 p.m. Saturday
10. 9 a.m. - 11 a.m. Sunday
11. 1 p.m. - 5 p.m. Sunday.

When measurements were taken in period 9 on King Street, the measurers described the situation as a traffic jam, with cars having an average speed of 3 km/h. In this situation, densities and emission levels are not easily predictable, and thus these measurements were discarded.

Measurements at sites 3 and 4 during period 4 were also discarded, since it was noted that overhead planes caused significant noise.

Figures were not available for periods 1 and 2 at site 9.

In period 5, no average speed is given for vehicles on either King Street or Missenden Road. A speed of 30 km/h was assumed.

In period 1, predictions based on equation (7·3) were not calculated, since the vehicle flow rate is far lower than the limit which is set on the validity of this expression.

Vehicle densities and speeds in King Street and Missenden Road are shown below. The units of n are vehicles/km. $n(c)$ is the density of cars, and $n(h)$ that of heavy vehicles. Average speeds are in km/h.

Period	King Street			Missenden Road		
	$n(c)$	$n(h)$	speed	$n(c)$	$n(h)$	speed
1	4.9	0.69	55	0.21	-	50
2	35	4.90	40	23	2.90	40
3	67	9.50	25	36	6.60	30
4	34	1.90	30	17	0.98	40
5	29	1.40	30	12	0.49	30
6	30	1.60	30	50	0.50	20
7	35	0.75	40	54	1.50	20
8	27	0.20	50	17	0.31	30
10	31	1.30	30	14	-	30
11	25	0.95	30	15	-	30

Values of k and k/l are shown below for each site.

Site	King Street		Missenden Road	
	$k(m)$	k/l	$k(m)$	k/l
3	60	1.4	160	3.8
4	96	2.3	160	3.8
9	220	5.3	130	3.1

Predicted and measured values of L_{eq}, in dB(A), are shown below. "A" refers to predictions made on the basis of equation (7·3).

Period	Site 3			Site 4			Site 9		
	L_{eq} (pred.)	L_{eq} (meas.)	L_{eq} (A)	L_{eq} (pred.)	L_{eq} (meas.)	L_{eq} (A)	L_{eq} (pred.)	L_{eq} (meas.)	L_{eq} (A)
1	57	46	-	52	43	-	---	---	---
2	64	59	57	57	54	52	---	---	---
3	61	60	52	56	59	54	50	50	48
4	---	---	---	---	---	---	47	51	48
5	57	52	50	52	52	49	45	42	44
6	57	53	50	53	60	57	49	51	46
7	58	54	52	55	56	51	52	56	51
8	58	55	54	54	54	51	49	50	49
10	57	58	49	52	57	49	44	42	40
11	56	54	49	51	54	47	44	54	47

APPENDIX 12

TRAFFIC NOISE MEASUREMENTS — BRISBANE

Results for all suitable measurement sites not on a major road were analysed, with the exception of one where the experimenters comment that there was very significant shielding due to depression of the site below road level. Details of the major roads nearest to each site are given below.

The units of n are vehicles/km. $n(c)$ is the density of cars, and $n(h)$ that of heavy vehicles.

Site no.	Road	$k(m)$	k/l	$n(c)$	$n(h)$
9	O'Keefe	120	2.2	24	1.3
	Carl	50	0.9	6.2	-
	Ipswitch	175	3.1	60	2.5
18	Cornwall	42	0.75	18	0.7
20	Juliette	107	1.9	13	0.7
	Cornwall	150	2.6	18	0.7
27	Juliette	100	1.8	13	0.7
57	O'Keefe	50	0.88	24	1.3
	Junction	42	0.75	10	1.1
70	Victoria	63	1.1	3.0	0.15
	Juliette	230	4.1	13	0.7
	Earl	43	0.75	9.2	-

Predicted and measured values of L_{eq}, together with those predicted by equation (7·3), are shown below.

Site no.	L_{eq}, dB(A)'s predicted	L_{eq}, dB(A)'s equation(7·3)	L_{eq}, dB(A)'s measured
9	56	56	50
18	60	57	50
20	53	53	45
27	51	48	43
57	60	57	55
70	55	51	47